IUCr 2014. XAFS Tutorial for Crystallographers. Montreal August 5

XAFS Theory: XANES and EXAFS Spectra. Recent advances in synchrotron techniques, new opportunities in organometallic materials, complex phase systems and cluster studies.

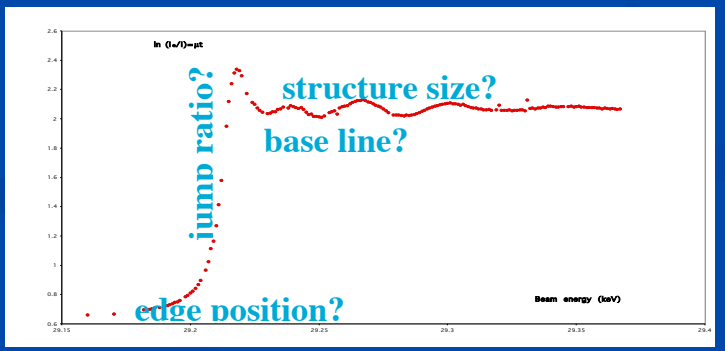

Chris. Chantler

Prof., FAIP, Chair CXAFS

University of Melbourne

Victoria 3010, Australia

chantler@unimelb.edu.au

http://optics.ph.unimelb.edu.au/~chantler/home.html

XAFS Theory: XANES and EXAFS Spectra

SESSION 1. Chair: Farideh Jalilevand (Canada)

9:00 – X-ray absorption spectroscopy for beginners - Chris Chantler (Australia)

9:45 - 10:15 Experimental approaches to XAS, XANES and related techniques: synchrotron radiation, beamlines, detectors, measurement modes, geometry – Bruce Bunker (USA)

SESSION 2.Chair: Bruce Bunker (USA)

10:30 - 11:00 Physics and materials Science – Federico Boscherini (Italy)

11:00 – 11:20 EXAFS Spectroscopy and Its Applications in Chemical Speciation in Solution - Farideh Jalilehvand (Canada)

11:20 - 11:40 Applications of XAS in Biosciences - Ritimukta Sarangi (Stanford)

SESSION 3.Chair: Christopher Chantler (Australia)

13:20 – 14:00 Multiple Scattering EXAFS Analysis - Anatoly Frenkel (US)

14:00 – 14:40 IFEFFIT / Analysis - Applications - Shelly Kelly (USA)

15:00 – 15:30 Hands-on tutorial on FDMNES and FDMX. – Jay Bourke (Australia)

15:30 - 16:00 EXCURVE code – Martin Feiters (Radboud Nijmegen, Netherlands)

16:00 – 16:30 GNXAS and applications – Keisuke Hatada (Japan, Italy)

16:30 - 17:00 XANES: MXAN and FPMS codes - Keisuke Hatada (Japan, Italy)

XAFS Theory: XANES and EXAFS Spectra

The Workshop

165 registrants from 28 countries

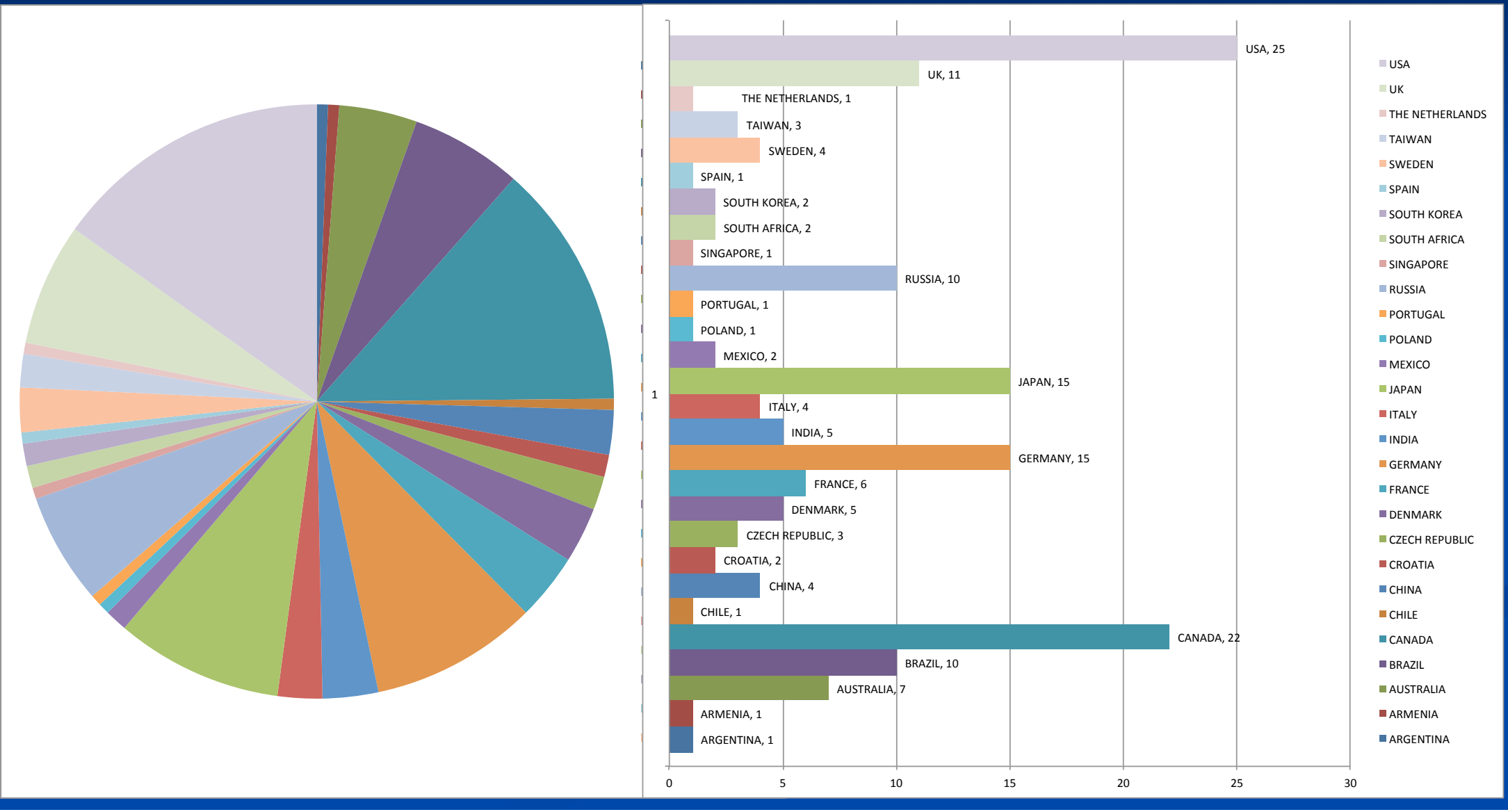

XAFS Theory: XANES and EXAFS Spectra

Thanks for this initiative:

IUCr Commission on XAFS

International X-ray Absorption Society

IUCr Local Organising Committee

Isabella Ascone, Hiroyuki Oyanagi

All organisers, execs, etc.

Session leaders and presenters at IUCr Congress

Continuing engagement and collegial development

The World of Synchrotron Radiation

Synchrotron Sources – 1st generation
(particle accelerators) General Electric 1947

Tantalus - The 2nd Generation Synchrotron
(purpose- built)
University of Wisconsin 10 beam lines 1968

Insertion Devices – The 3rd generation 1980

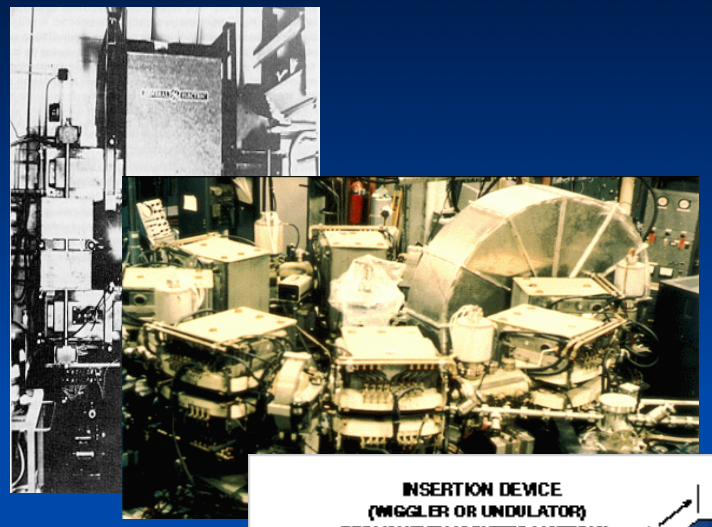

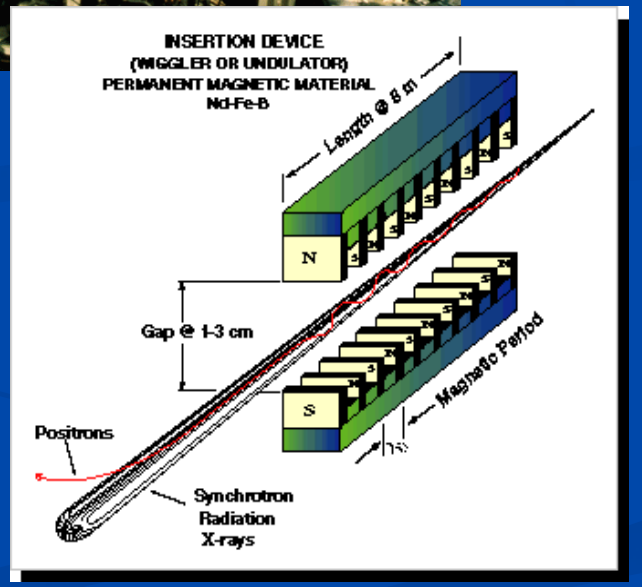

Wavelength and object size

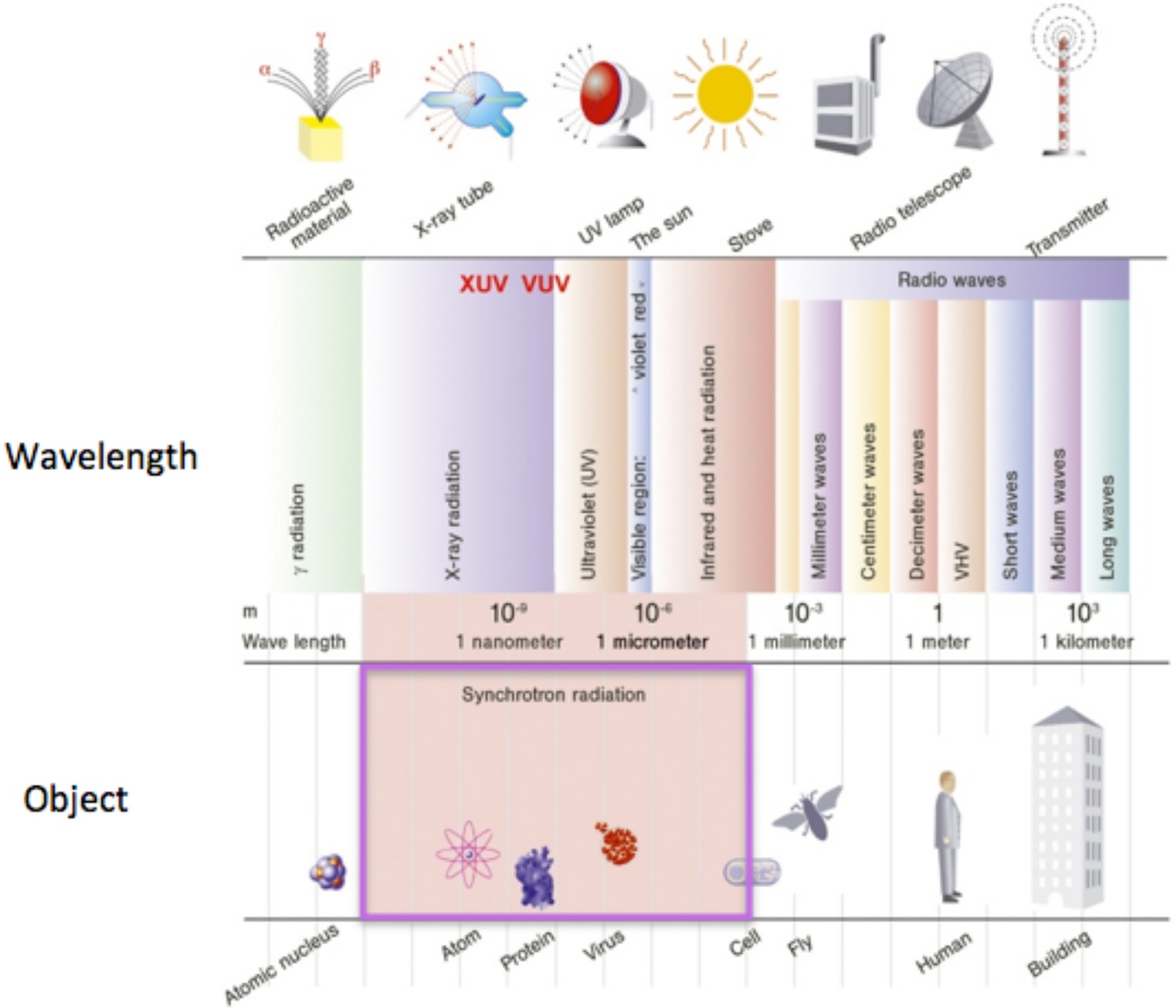

DESY Hamburg

Brilliance

Brilliance

10^{23}

Phtons/s
/mrad²
/mm²
/0.1% bandwidth

Flux

10^{12}

Phtons/s

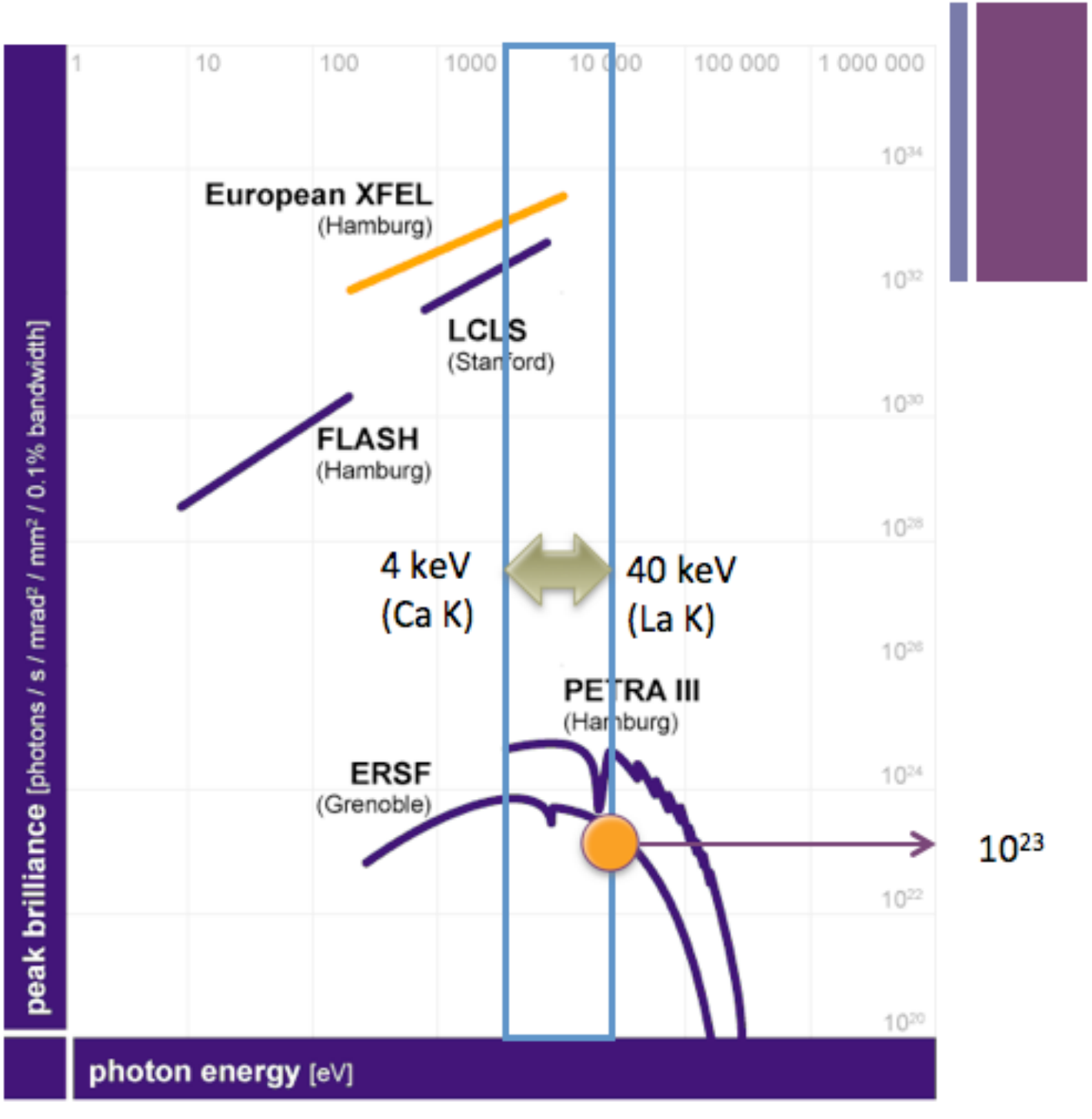

Moore's law in Synchrotron Radiation

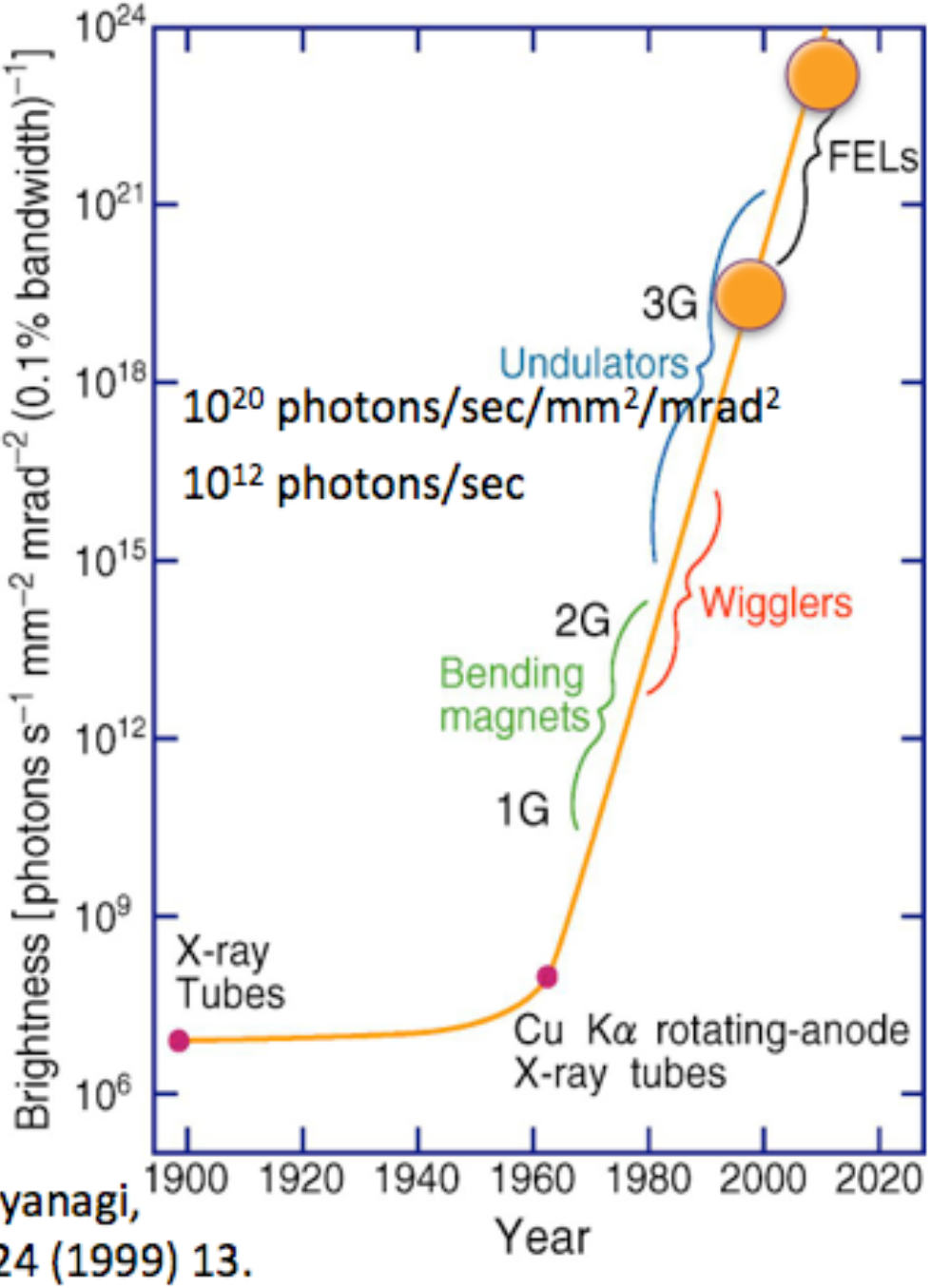

We are here!

Note that exponential growth is due to successive inventions of different devices

10^7 times brighter beam in 30 years

Montano and Oyanagi, MRS BULLETIN 24 (1999) 13.

XAFS Theory: XANES and EXAFS Spectra

Oxford Instruments PLC
E=700Mev i=600mA

Big 3: ESRF (Grenoble), SPRING8 (Tokyo), Advanced Photon Source (Chicago) [1997]

Synchrotron Radiation Sources

http://www.iucr.org/resources/commissions/xafs/
http://en.wikipedia.org/wiki/List_of_synchrotron_radiation_facilities
http://www.lightsources.org/light-source-facility-information
http://www.esrf.eu/UsersAndScience/Links/Synchrotrons/
http://www.ixasportal.net/ixas/index.php?option=com_content&view=article&id=102&Itemid=145

X-ray and photon interaction processes

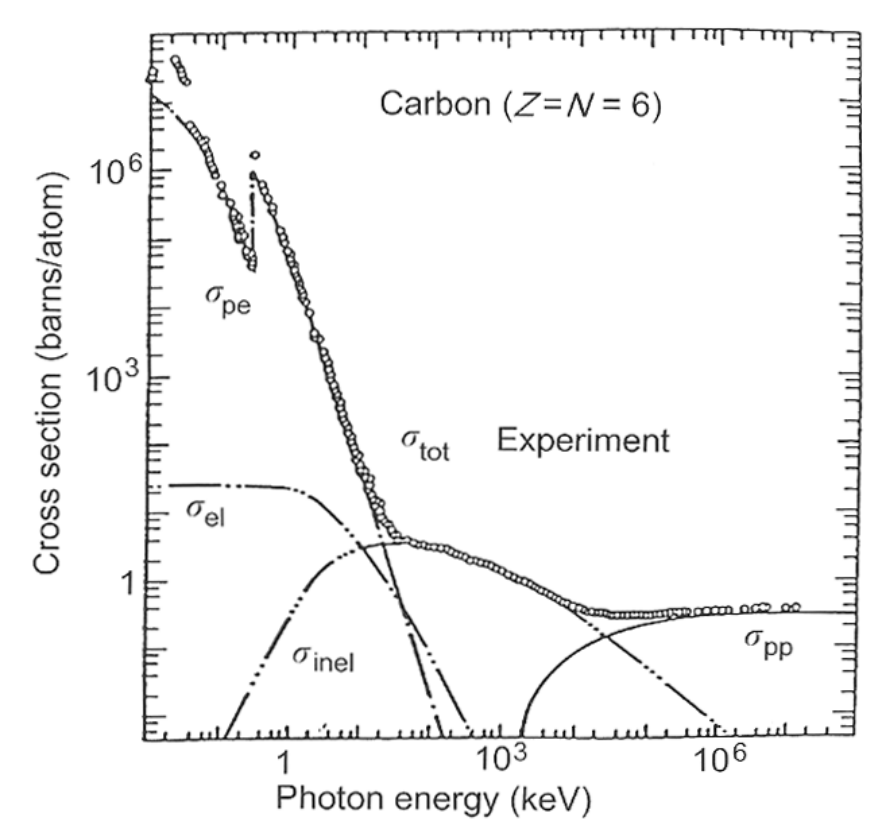

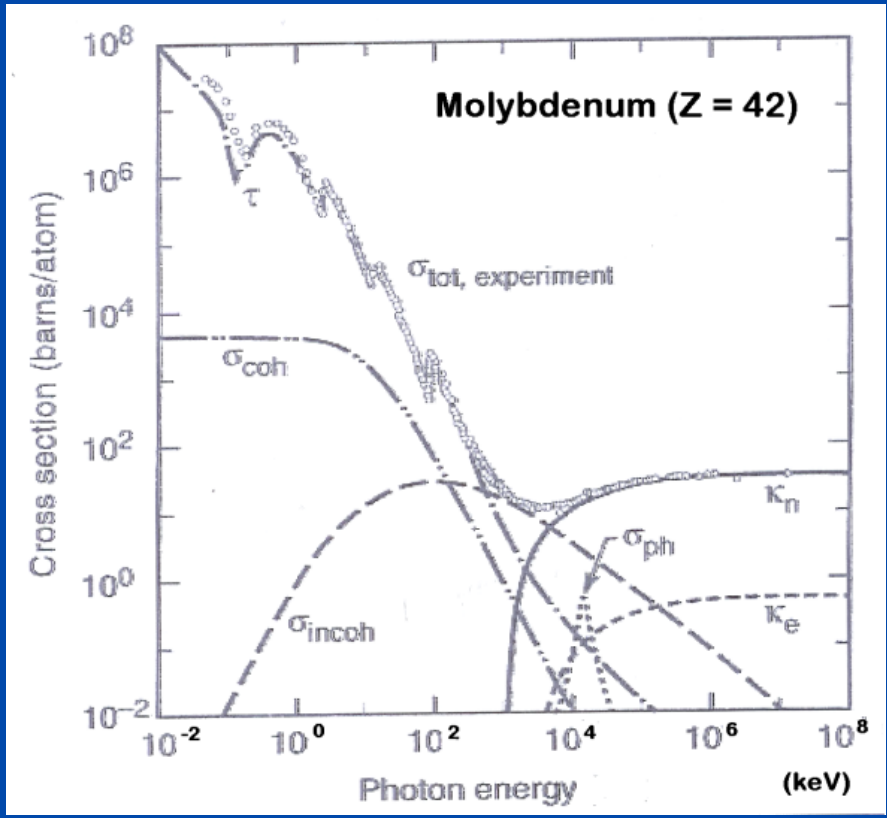

Interactions include:

photoelectric absorption **σ_pe, τ**

inelastic scattering (Compton Effect) σ_inel (coh)

including *X-ray fluorescence*

elastic scattering (Rayleigh) σ_el (incoh)

pair production σ_pp (κ)

Links: X-ray Absorption Fine Structure and Crystallography *ATTENUATION & THE (X-RAY) ATOMIC FORM FACTOR*: One Example of usage: FFAST:

$$\mu_{PE}(E) = f_2(E)2hcr_0 / E$$

$$[\mu_{PE} / \rho](E) = \sigma_{PE} / (uA)$$

$$\mathrm{Im}(f) = f''(E) = f_2(E) = \frac{E\mu_{PE}(E)}{2hcr_e}$$

$$\mathrm{Re}(f) = f_0 + f' + f_{NT}, f' = f_1 + f_{rel} - Z$$

$$f_0(q,Z) = 4\pi \int_0^\infty \frac{\rho(r)\sin(qr)r^2 dr}{qr}$$

http://physics.nist.gov/PhysRefData/FFast/Text/cover.html

Chantler, CT, Olsen, K, et al. (2005) X-Ray Form Factor, Attenuation & Scattering Tables (v2.1) [Online]; Chantler, CT, JPhysChemRefData 29(4), 597-1048 (2000); Chantler, CT, JPhysChemRefData 24, 71-643 (1995).

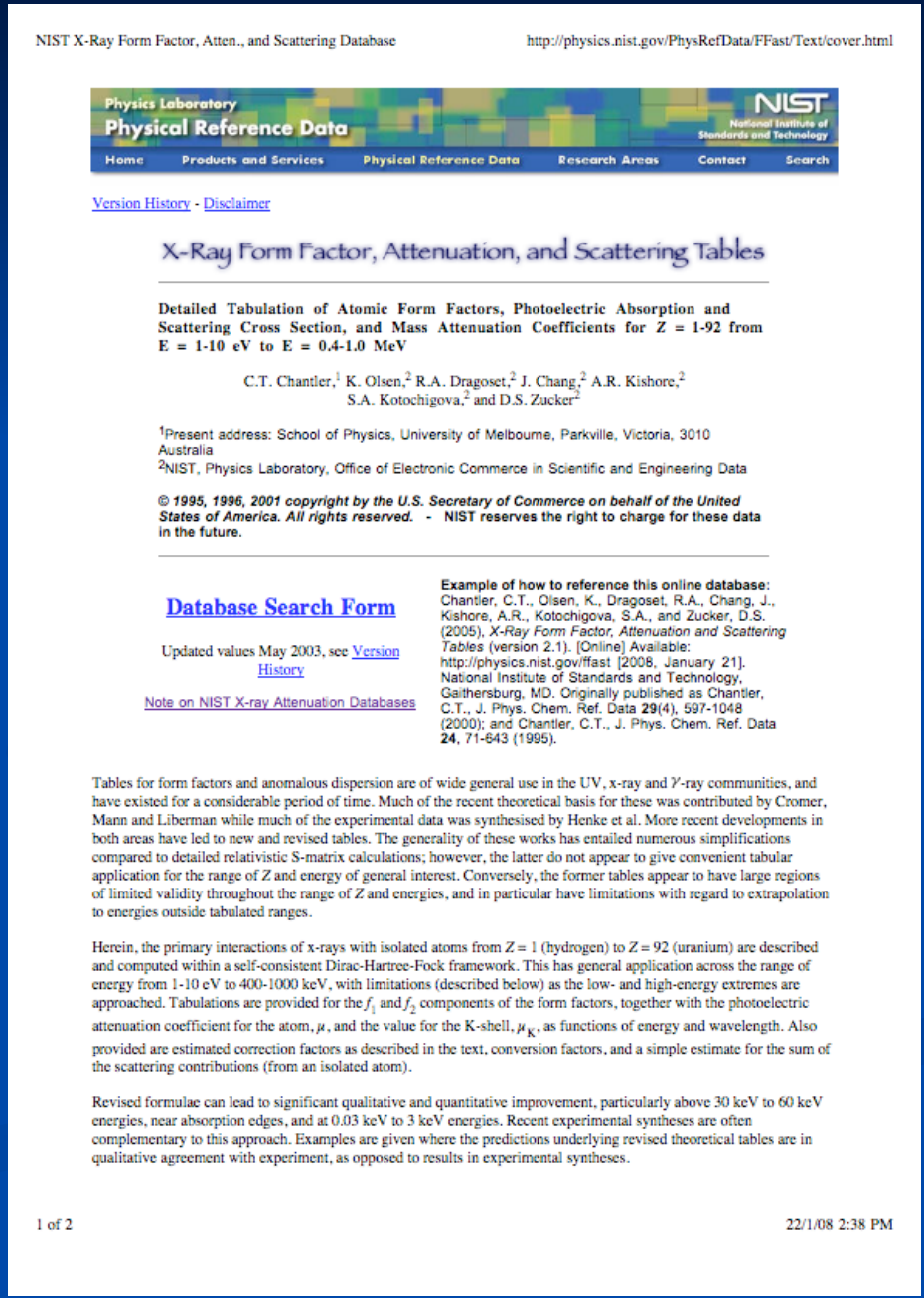

NIST X-Ray Form Factor, Atten., and Scattering Database http://physics.nist.gov/PhysRefData/FFast/Text/cover.html

Physics Laboratory Physical Reference Data — NIST National Institute of Standards and Technology

Home | Products and Services | Physical Reference Data | Research Areas | Contact | Search

Version History - Disclaimer

X-Ray Form Factor, Attenuation, and Scattering Tables

Detailed Tabulation of Atomic Form Factors, Photoelectric Absorption and Scattering Cross Section, and Mass Attenuation Coefficients for Z = 1-92 from E = 1-10 eV to E = 0.4-1.0 MeV

C.T. Chantler,[1] K. Olsen,[2] R.A. Dragoset,[2] J. Chang,[2] A.R. Kishore,[2] S.A. Kotochigova,[2] and D.S. Zucker[2]

[1]Present address: School of Physics, University of Melbourne, Parkville, Victoria, 3010 Australia
[2]NIST, Physics Laboratory, Office of Electronic Commerce in Scientific and Engineering Data

Database Search Form

Updated values May 2003, see Version History

Note on NIST X-ray Attenuation Databases

Example of how to reference this online database: Chantler, C.T., Olsen, K., Dragoset, R.A., Chang, J., Kishore, A.R., Kotochigova, S.A., and Zucker, D.S. (2005), *X-Ray Form Factor, Attenuation and Scattering Tables* (version 2.1). [Online] Available: http://physics.nist.gov/ffast [2008, January 21]. National Institute of Standards and Technology, Gaithersburg, MD. Originally published as Chantler, C.T., J. Phys. Chem. Ref. Data **29**(4), 597-1048 (2000); and Chantler, C.T., J. Phys. Chem. Ref. Data **24**, 71-643 (1995).

Tables for form factors and anomalous dispersion are of wide general use in the UV, x-ray and γ-ray communities, and have existed for a considerable period of time. Much of the recent theoretical basis for these was contributed by Cromer, Mann and Liberman while much of the experimental data was synthesised by Henke et al. More recent developments in both areas have led to new and revised tables. The generality of these works has entailed numerous simplifications compared to detailed relativistic S-matrix calculations; however, the latter do not appear to give convenient tabular application for the range of Z and energy of general interest. Conversely, the former tables appear to have large regions of limited validity throughout the range of Z and energies, and in particular have limitations with regard to extrapolation to energies outside tabulated ranges.

Herein, the primary interactions of x-rays with isolated atoms from Z = 1 (hydrogen) to Z = 92 (uranium) are described and computed within a self-consistent Dirac-Hartree-Fock framework. This has general application across the range of energy from 1-10 eV to 400-1000 keV, with limitations (described below) as the low- and high-energy extremes are approached. Tabulations are provided for the f_1 and f_2 components of the form factors, together with the photoelectric attenuation coefficient for the atom, μ, and the value for the K-shell, μ_K, as functions of energy and wavelength. Also provided are estimated correction factors as described in the text, conversion factors, and a simple estimate for the sum of the scattering contributions (from an isolated atom).

Revised formulae can lead to significant qualitative and quantitative improvement, particularly above 30 keV to 60 keV energies, near absorption edges, and at 0.03 keV to 3 keV energies. Recent experimental syntheses are often complementary to this approach. Examples are given where the predictions underlying revised theoretical tables are in qualitative agreement with experiment, as opposed to results in experimental syntheses.

XAFS Theory: XANES and EXAFS Spectra

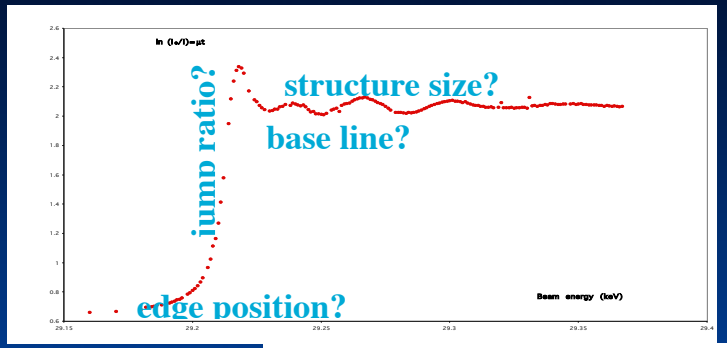

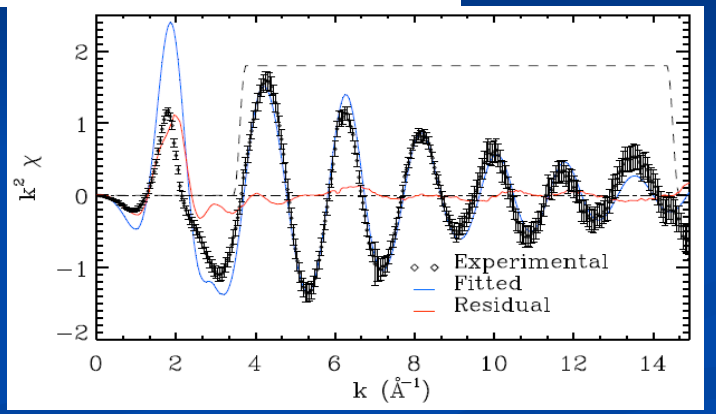

1. Why XAFS?
2. What is XAFS?
3. How does XAFS work?
   - Difficulties
   - Links with Crystallography
   - Realisation: A: Absorption
   - Realisation: B:Fluorescence
4. Past, present and future...

Recent advances in synchrotron techniques, new opportunities in organometallic materials, complex phase systems and cluster studies.

XAFS Theory: XANES and EXAFS Spectra

1. Why XAFS?

- Crystallography - periodicity, symmetry and mean structure of perfect crystals [X-ray; Electron Diffraction; Neutron Diffraction]
- Nanocrystallites in advanced synchrotron beams; or [X-ray] Powder Diffraction
- TEM etc. of surfaces or slices [destructive].
- Great difficulties for disordered systems; solutions; dilute systems; local order; dynamic bond lengths; active centres.
- X-ray Absorption Fine Structure [XAFS] deals directly with these questions and more.
- Complementary for complex systems, organometallics, bioactive systems, ideal crystals or metals

XAFS Theory: XANES and EXAFS Spectra

1. Why XAFS?

- Recent advances in synchrotron techniques,
- new opportunities in organometallic materials,
- dynamic bond investigation,
- thermal dependence of structure [especially disordered],
- complex phase systems
- cluster studies
- >12000 papers in the last 5 years.

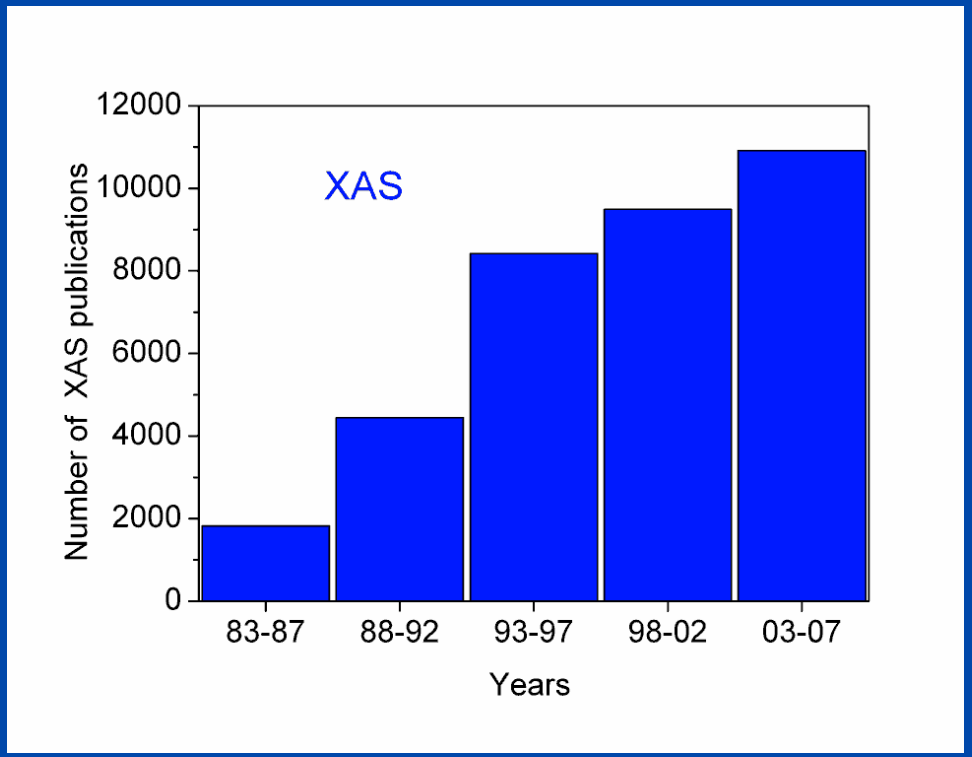

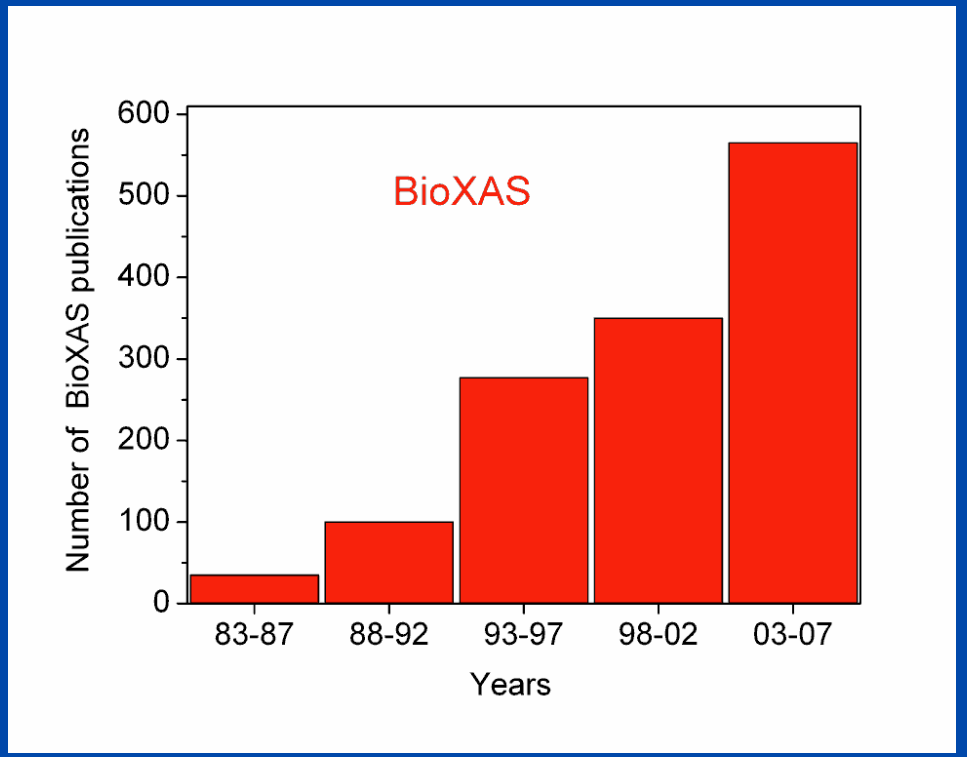

Application to physics, earth science, chemistry and biology

Ascone et al. (2009). Journal of Synchrotron Radiation 16, 413-42

XAFS Theory: XANES and EXAFS Spectra

2. What is XAFS?

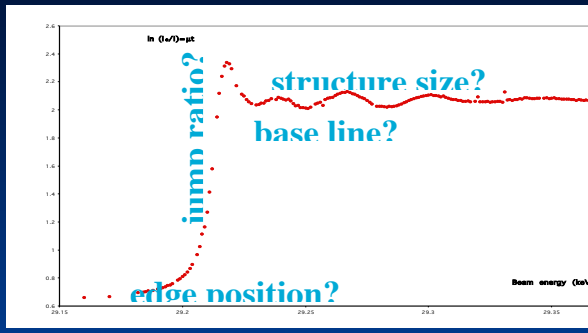

X-ray Absorption Fine Structure [XAFS] is the sequence of sharp oscillations in the Absorption coefficient just above the absorption edge for a particular sub-shell [K, LI, LII, LIII, M...] of an element [Fe, Cu, Ni, C, Mo, Au, ...] in a material, corresponding to the creation of electron holes in the 1s, 2s, 2p1/2, 2p3/2 etc. atomic subshells.The material may be an ideal crystal or metal, a nanocrystal or powder, or a non-ideal mixture or dilute solution.

For detailed background, see IUCr Commission on XAFS Definitions: http://www.iucr.org/resources/commissions/xafs/xafs-related-definitions-for-the-iucr-dictionary See also: http://www.iucr.org/

THIS CONGRESS: *MS-06 Time Resolved Spectroscopic Studies with Synchrotron Radiation and Free Electron Laser Sources*

MS-14 Electronic Structure and Chemical Bond Information by High Energy Resolution X-ray Spectroscopy

MS-38 X-Rays Techniques for Innovation in Industry

MS-46 XAS of Hydrated Metal Ions and Protein Active Centres in Aqueous Solutions

MS-64 EXAFS Analysis at the Nanoscale and in Highly Disordered Materials

MS-103 Spectroscopic Approaches (XAFS, XANES, NMR, ...) in Crystallography

Also note: MS-25 Electron Density and Optical Properties of Materials

XAFS Theory: XANES and EXAFS Spectra

2. What is XAFS?

•X-ray Absorption Fine Structure (XAFS): modulation of the absorption coefficient above an Absorption Edge of an element due to chemical state & structure of immediate surroundings. Commonly divided into 'near edge' region (XANES or NEXAFS) to ~50 eV above the absorption edge & 'extended' region (EXAFS) giving oscillations in the absorption coefficient from ~50 eV.

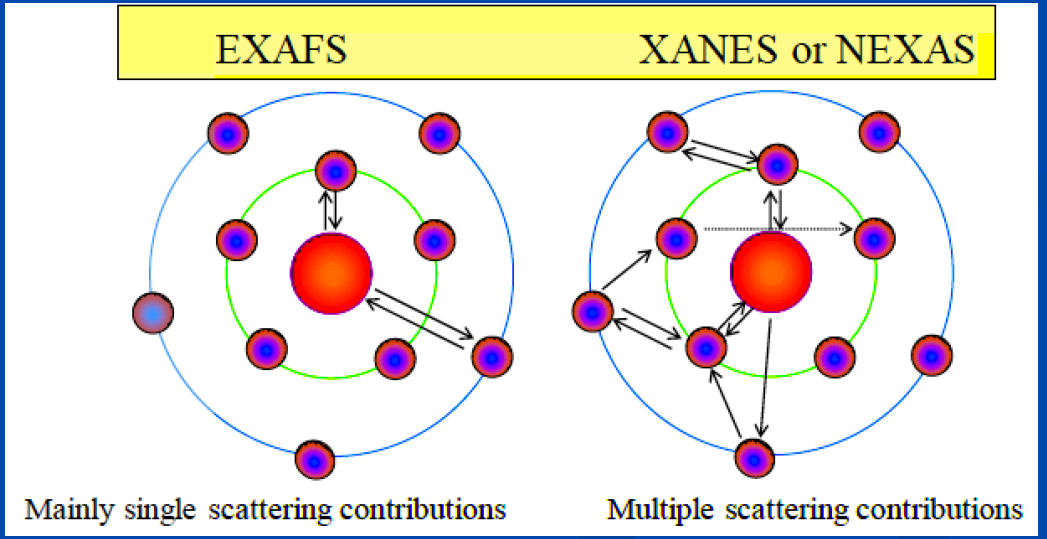

•XANES (X-ray Absorption Near Edge Spectroscopy) for X-ray edges (~1 keV and above); NEXAFS (Near-edge X-ray Absorption Fine Structure) for soft X-ray edges.

•Spectral features before the main absorption edge - 'pre-edge' features - are associated with transitions to bound states.

2. What is XAFS?

X-ray Absorption Spectroscopy (XAS) measures the linear absorption coefficient $\mu(E)$ of a substance as a function of the incident photon energy *E* in the X-ray regime:

Element & orbital-specific & determines the local atomic & electronic structure of matter. XAS conventionally includes techniques of XAFS, which in turn includes both XANES & EXAFS. An XAS spectrum may also be obtained using fluorescence, electron yield & scattering processes indirectly (i.e. without directly measuring the absorption of X-rays).

XAFS Theory: XANES and EXAFS Spectra

2. What is XAFS?

XANES (X-ray Absorption Near-Edge Structure) is represented by pre-edge features from bound-bound transitions in the molecular structure around the target element, which is a reflection of the Fermi level & Fermi surface. If the region of the target atom is depleted of electrons, representing ionic bonding & positive cations, then additional pre-edge spectral lines are likely to ensue. Conversely, if the target atom is negatively charged, the Fermi level will rise and pre-edge features may disappear. Discrete transitions often have a particular symmetry & polarity, so that pre-edge features may appear or disappear in particular polarisations of the incident X-ray field; or for particular coordination of the nearest neighbours of the target atom (two-fold, linear or bent; square planar or tetrahedral; etc.)

XAFS Theory: XANES and EXAFS Spectra

2. What is XAFS?

XANES is often used qualitatively to evaluate charge state, bonding symmetry & coordination of a central atom; or by comparison to a series of empirical standards to evaluate the likely molecular species & surroundings of a target ion.

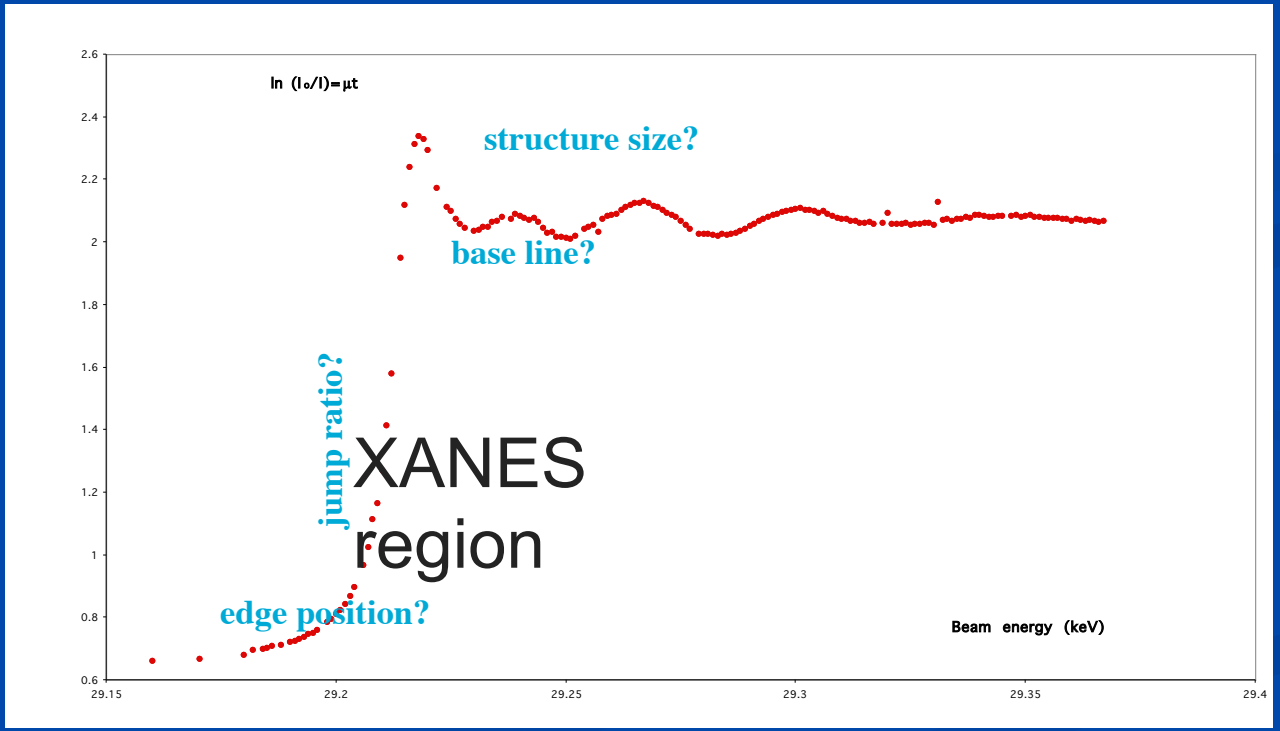

X-ray Absorption Spectroscopy -how to measure

XANES, EXAFS, …

Most fundamental technique is a transmission mode

Transmission

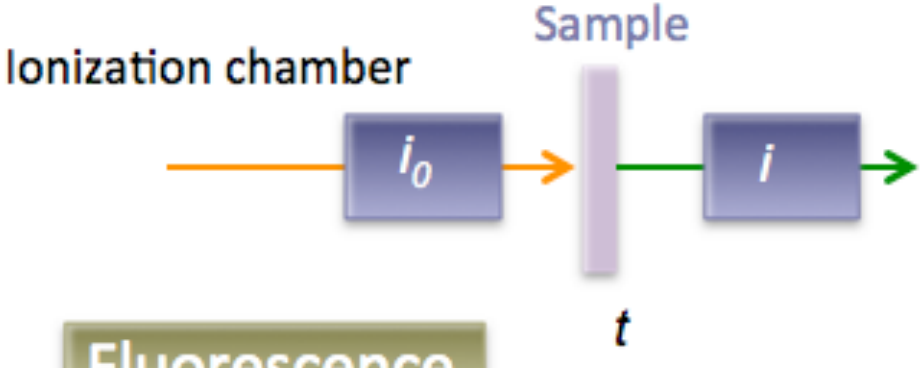

$$\mu t\,(E) = \ln\,(i_0 / i)$$

You measure attenuated beam intensity, that" exponentially" decreases

Fluorescence

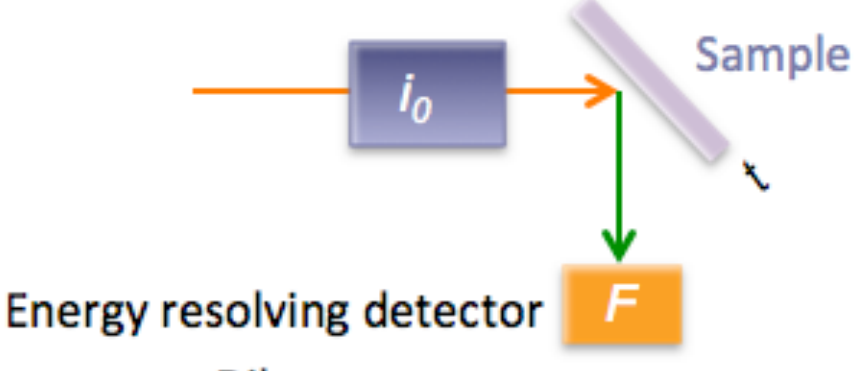

$$\mu t\,(E) = F / i_0$$

You measure emitted beam intensity
Which "linearly" proportional to conc.

Dilute system
Impurities, surfaces, thin films

Power of Synchrotron radiation

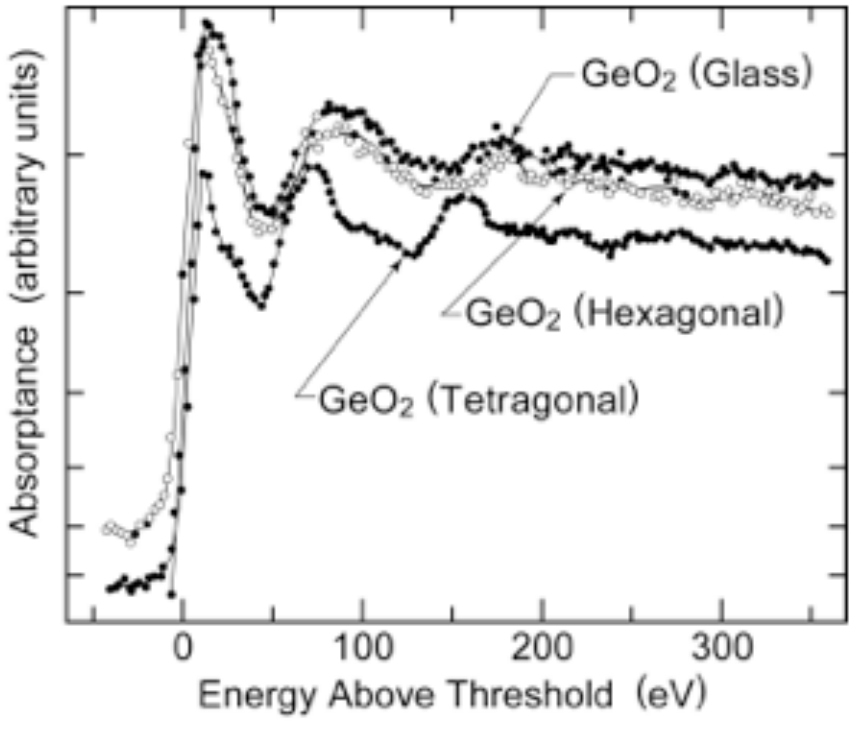

Nelson et al., Phys. Rev. 127, 2025 (1962).
1 week for one spectrum, tube x-ray source + diffractometer

Synchrotron radiation changed Quality of XAS

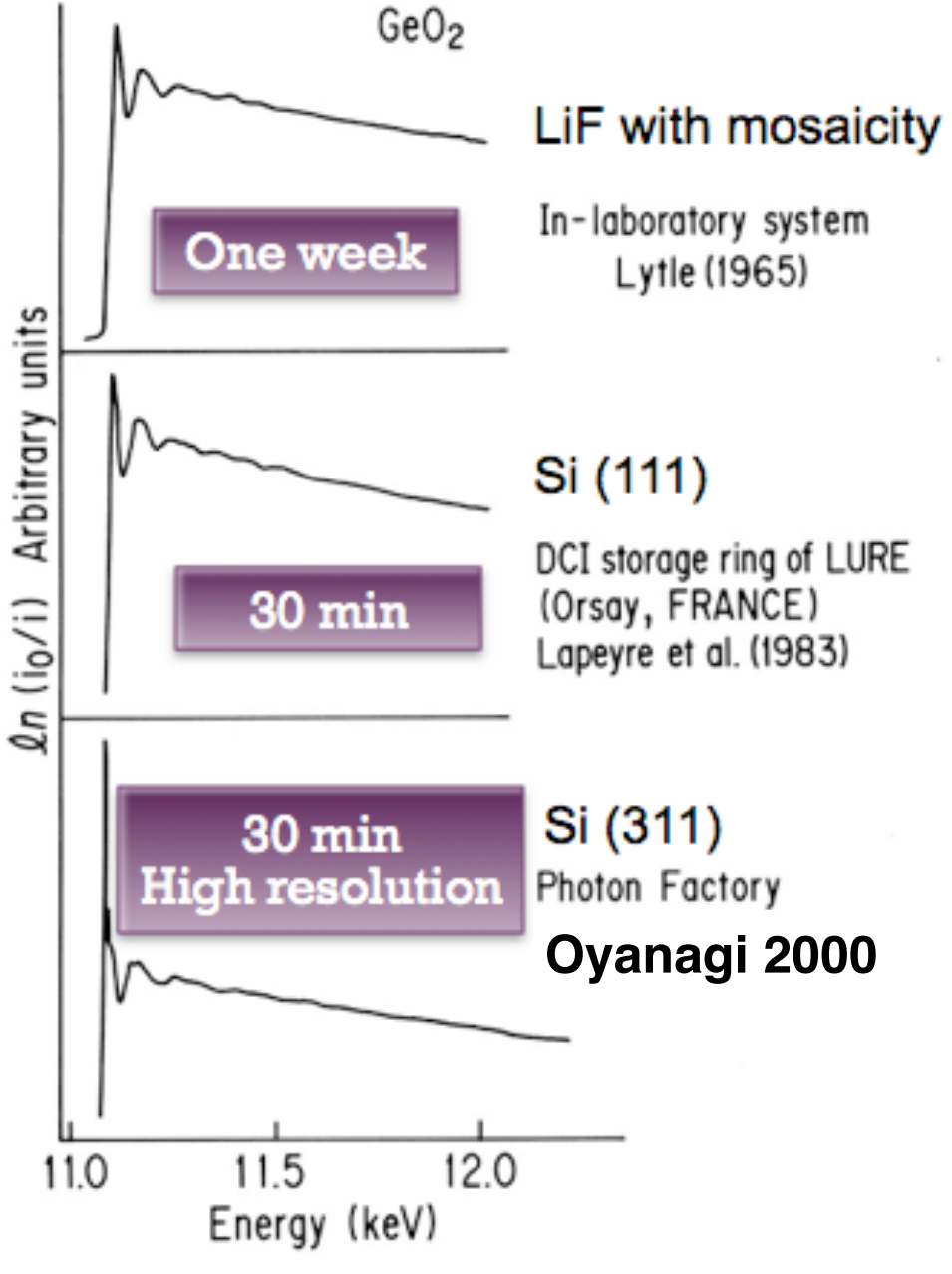

Fourier Transform -example

FT magnitude function for crystalline and glass GeO_2 Okuno et al.

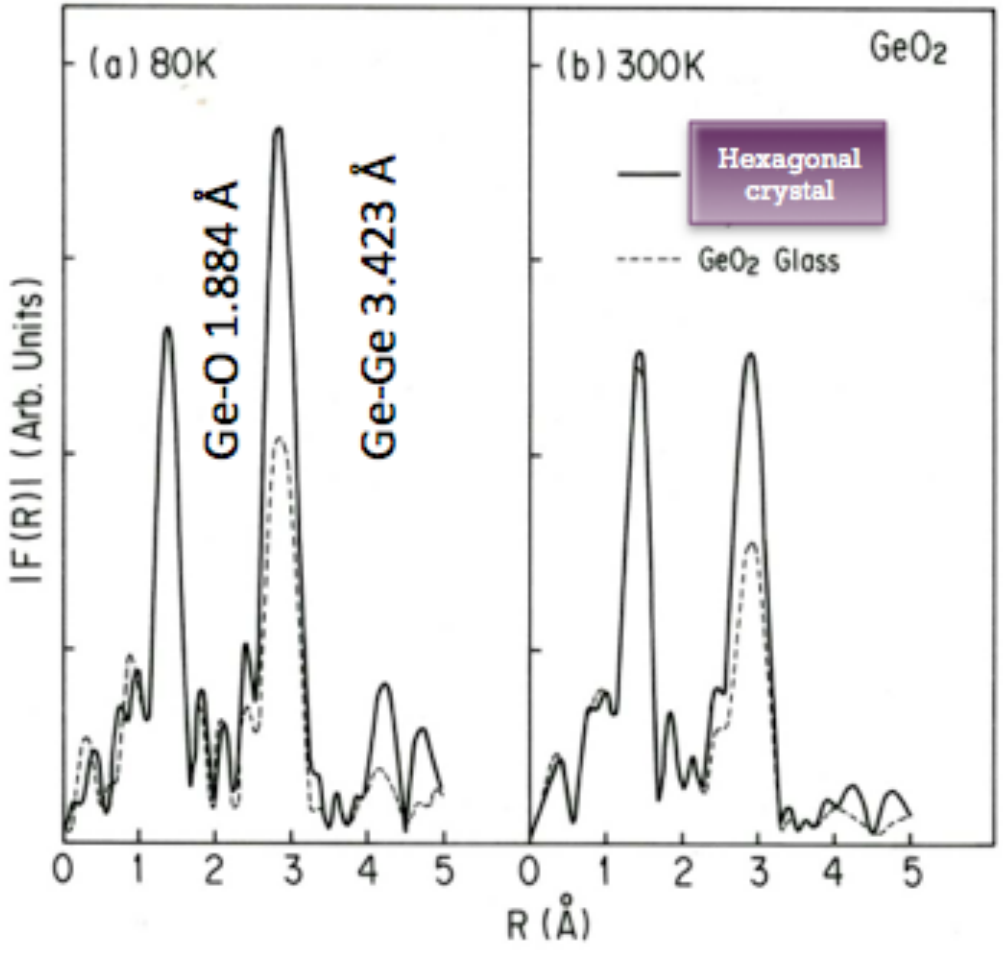

Crystal structure (hexagonal)

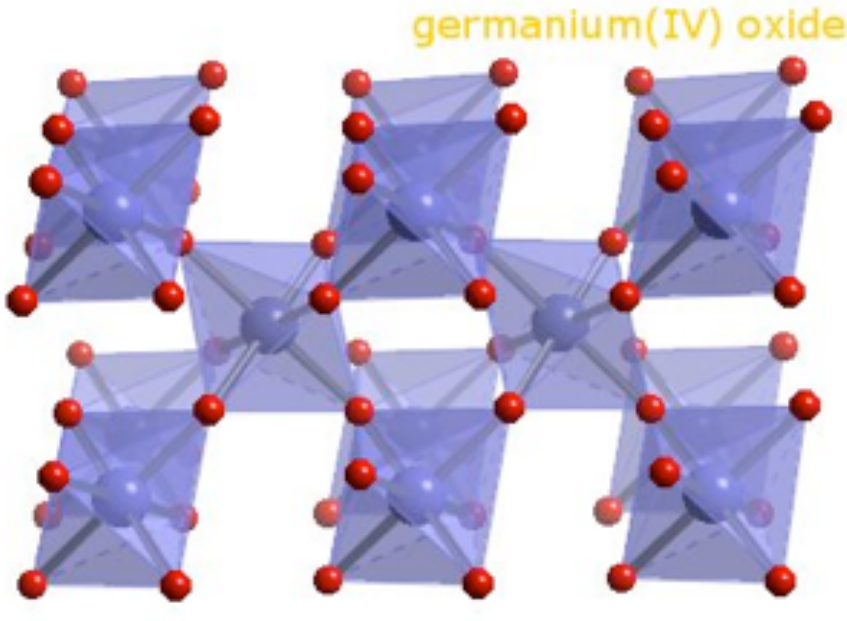

Acta Cryst. 17, 842 (1964)
Acta Cryst. B27, 2133 (1971)

Glass structure

Short range order is close to the hexagonal crystal
Disorder in arrangement of GeO_4 units (connectivity)

Fluorescence intensity estimation

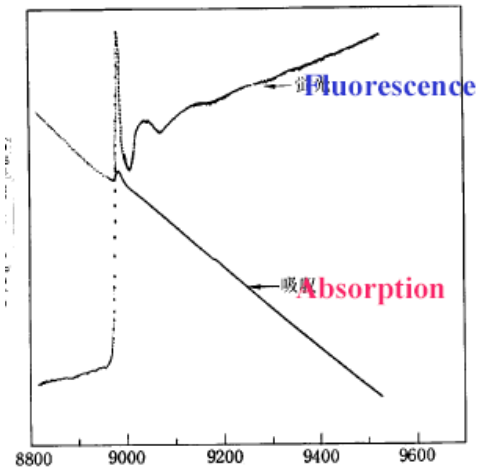

For x-rays incident on a slab of sample with thickness of x:

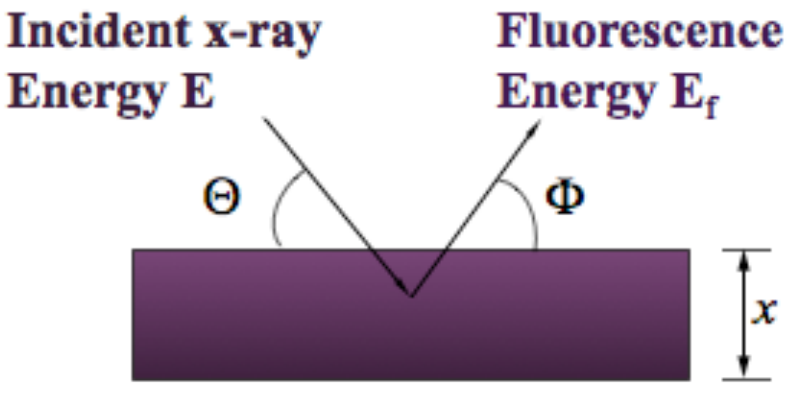

The fluorescence intensity $I_f(E)$ accepted by a detector with a solid angle of $\Omega/4\pi$ is:

$$I_f = \frac{\dfrac{f I_0 \Omega [\mu/\rho]^*_{pe}}{4\pi \cos\theta_{inc}}}{\dfrac{[\mu/\rho]}{\cos\theta_{inc}} + \dfrac{[\mu_f/\rho]}{\cos\theta_{out}}} \left(A - \exp\left(-\frac{\left[\frac{\mu}{\rho}\right][\rho t]}{\cos\theta_{inc}} - \frac{\left[\frac{\mu_f}{\rho}\right][\rho t]}{\cos\theta_{out}} \right) \right)$$

$I_f(E) \approx I_0 \times 8.8\times10^{-4}\times0.012 \approx 1\times10^{-5} I_0$, lower than I_0 by 5 orders.

XAFS Theory: XANES and EXAFS Spectra

2. What is XAFS?

XANES: Ideal examples and archetypes:
charge state, bonding symmetry and coordination of a central atom; or by comparison to a series of empirical standards to evaluate the likely molecular species and surrounding of a target atom or ion.

Metal Transport

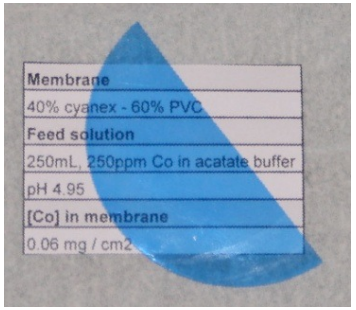

Feed stream
Impure Co^{2+}

Extract stream
Pure Co^{2+}

Polymer: CTA
Extractant: cyanex

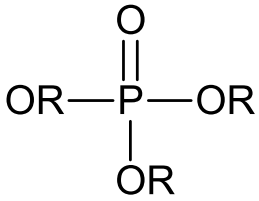

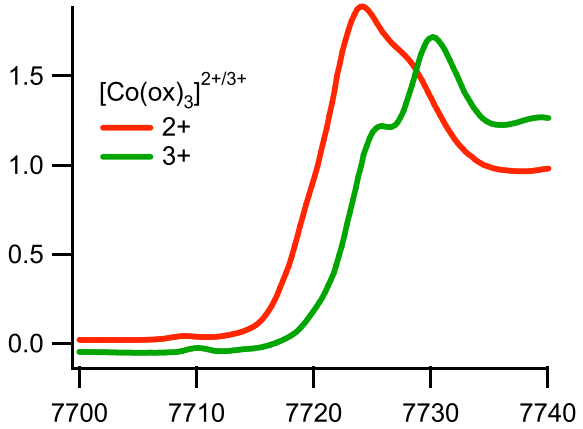

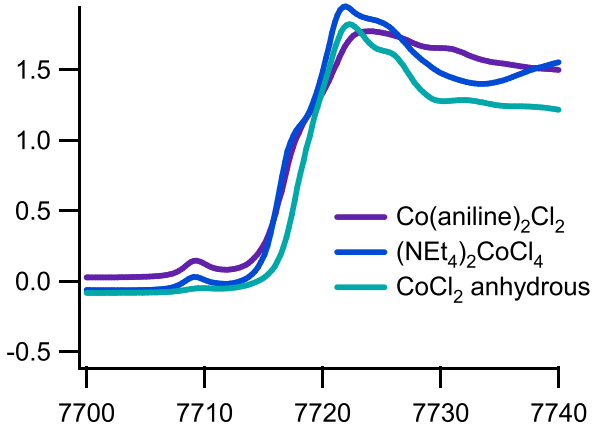

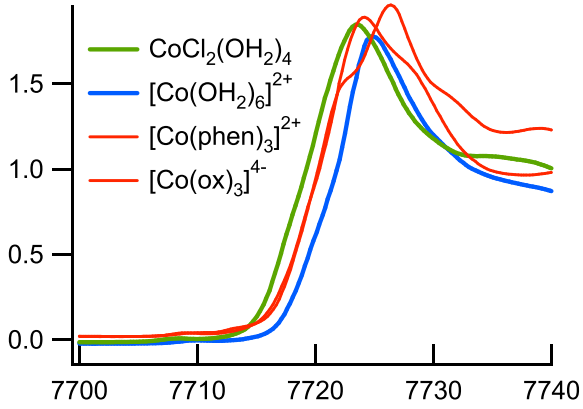

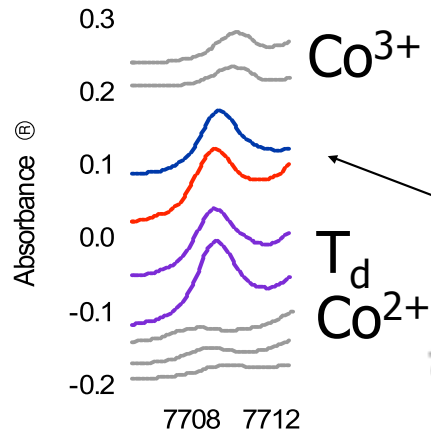

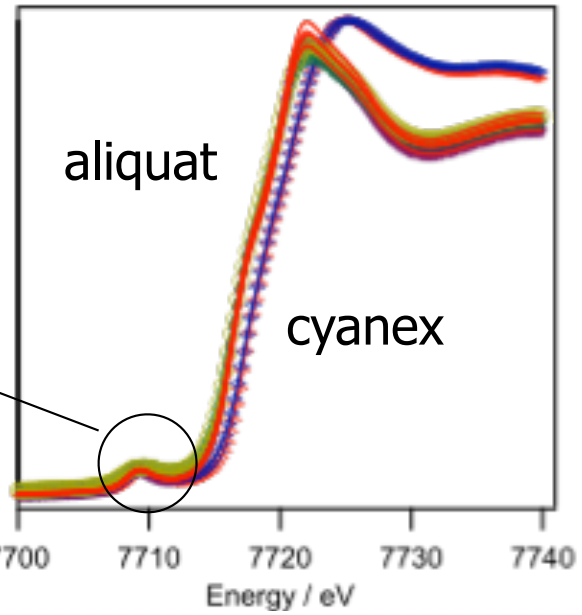

Example of XANES – why resolution?

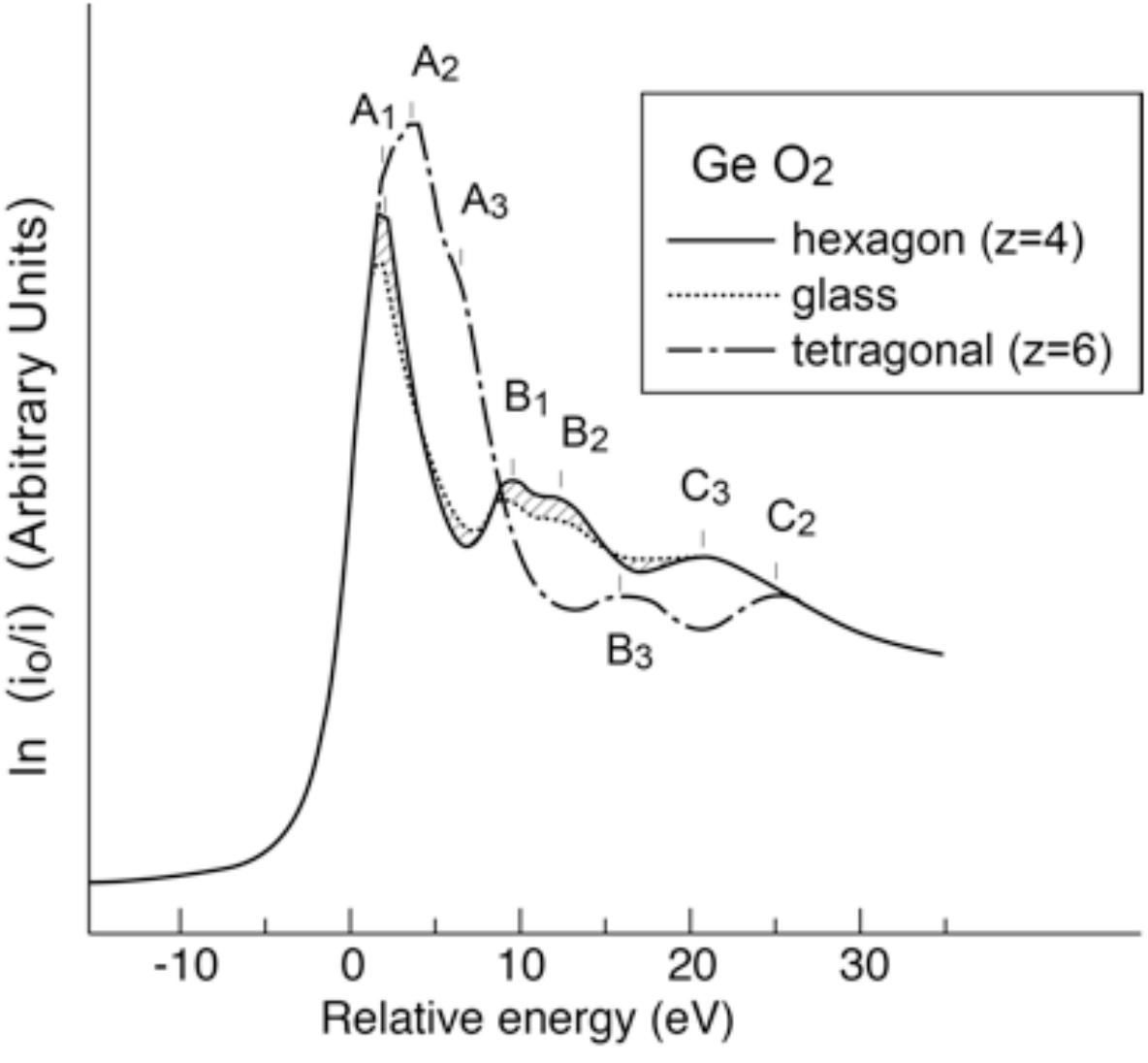

Si (311) monochromator Okuno et al.

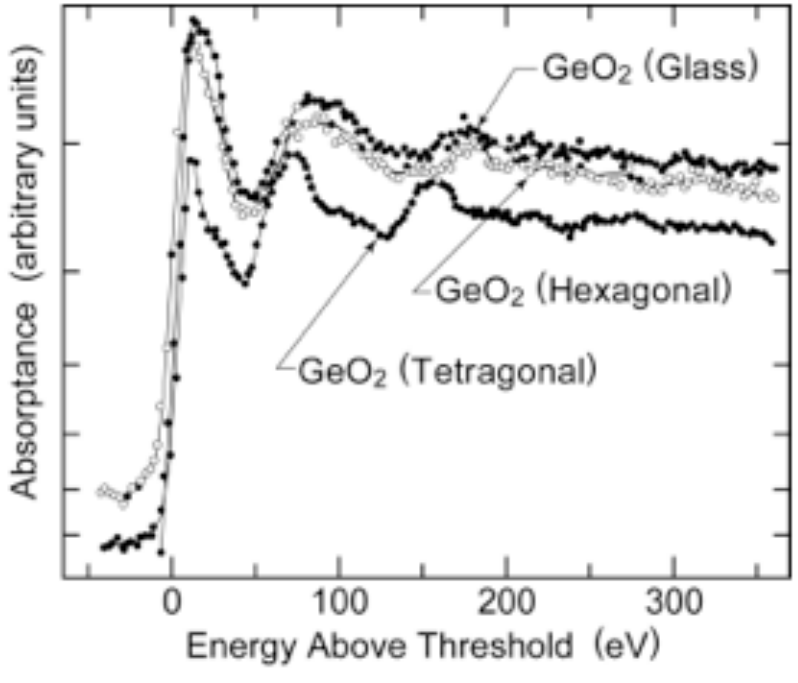

Nelson et al., Phys. Rev. 127, 2025 (1962).
1 week for one spectrum, tube x-ray source + diffractometer

Short range in glass sample is close to that of hexagonal crystal

XAFS Theory: XANES and EXAFS Spectra

XAFS, XANES, XERT

- Quantitative X-ray Absorption in non-crystalline systems
- XANES: Oxidation state. Pre-edge bound features.Valence interactions. Chemical shifts. Site symmetry.
- XAFS: Nearest-neighbour radii. Types of ligands. Coordination number. Element (ionization state) of nearest neighbour. Phase offsets and amplitudes. *Active Centres. Reactive Intermediates*. Bonding, correlated motion.
- Scattering. Radiation safety, Medical imaging.
- Fundamental parameters: Atomic & condensed matter theory & quantum chemistry. Complex form factor.
- Applications: Chemistry, Biology, Biomedicine, Earth Sciences, Spectroscopy, Mineralogy, Engineering, Physics

XAFS Theory: XANES and EXAFS Spectra

2. What is XAFS?

The Extended X-ray Absorption Fine Structure (EXAFS) (q.v.) region contains modulation of the absorption coefficient that can be interpreted in terms of photo-electron scattering.

In relation to the (linear) absorption coefficient, the XAFS is defined as

$$\chi = \frac{\mu(E) - \mu_{free}(E)}{\mu_{free}(E)}$$

where μ_{free} is the (linear) absorption coefficient of the free atom, that is in the absence of any immediate surroundings and chemical modifications. The XAFS is often practically defined as

$$\chi = \frac{\mu_{measured}(E) - \mu_{ref}(E)}{\mu_{ref}(E)} \quad \text{or} \quad \chi = \frac{\mu_{measured}(E) - \mu_0(E)}{\Delta\mu} \quad \text{instead.}$$

where $\mu_{measured}$ is the measured linear absorption (typically from the ratio of ion chamber intensities, possibly normalised for some experimental errors), and μ_{ref} is a reference background spectrum simulating aspects of both the edge and a pseudo-atomic state. In the third approach, μ_0 is a smooth mathematical background function through $\mu_{measured}$ (e.g. a spline fit) and the XAFS is normalized by $\Delta\mu$ the 'edge jump' at the Absorption edge in $\mu_{measured}$. Naturally, these different definitions can give variations in μ where the normalisations might differ significantly, especially if their differences vary with energy.

XAFS Theory: XANES and EXAFS Spectra

XAFS, XANES, XERT

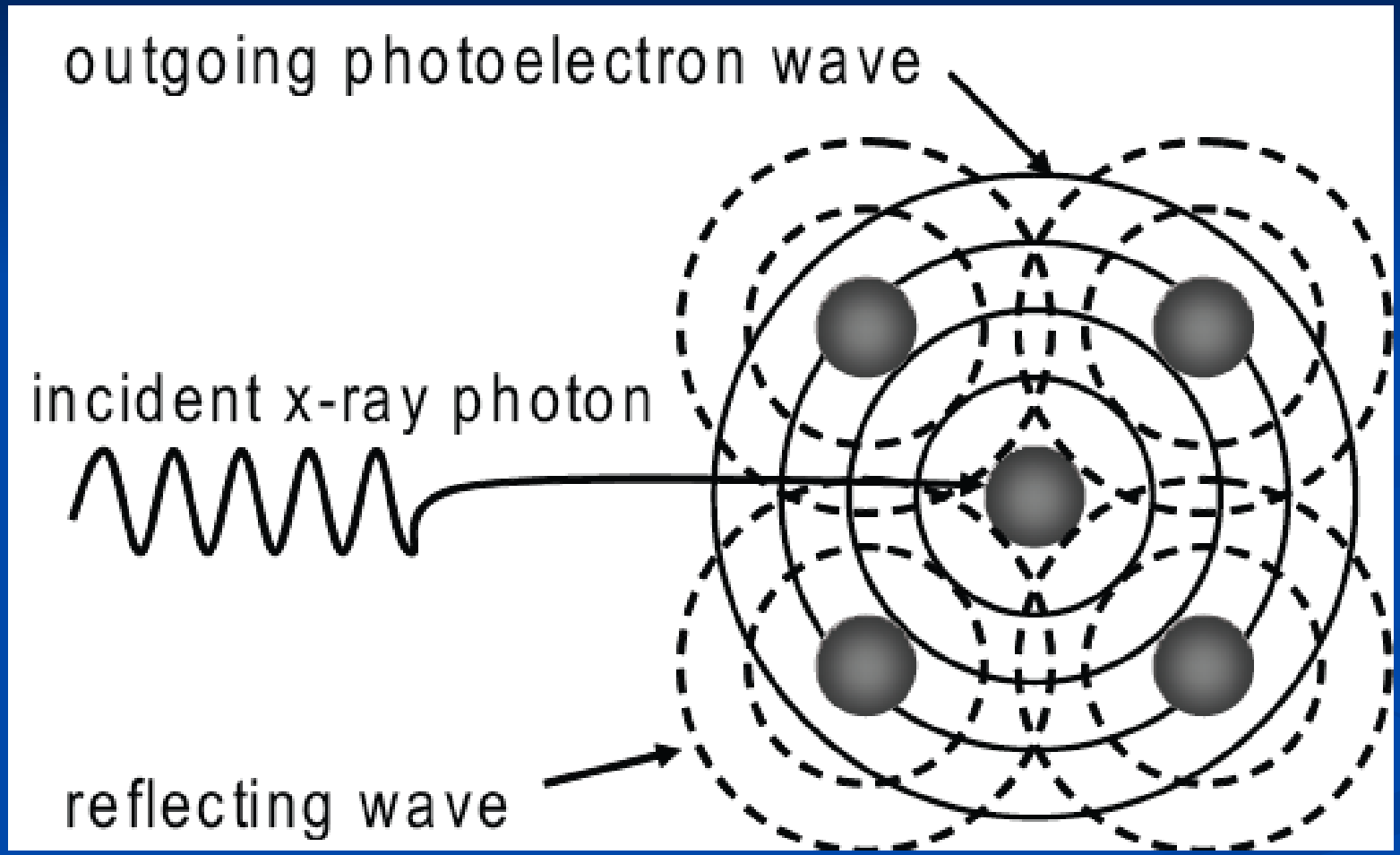

$$\chi(k) = \frac{[\mu/\rho](E) - [\mu_0/\rho](E)}{[\mu_0/\rho](E)}$$

$$k = \frac{2\pi}{h}\sqrt{2m_e(E - E_0)}$$

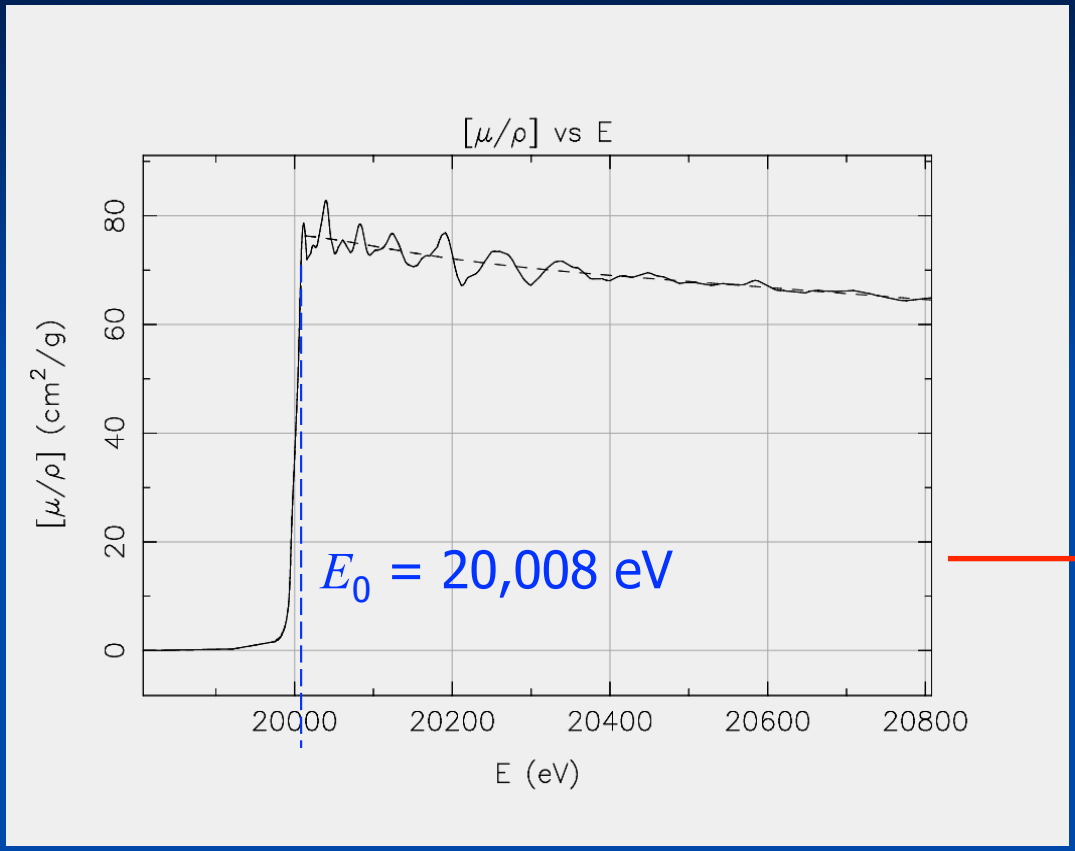

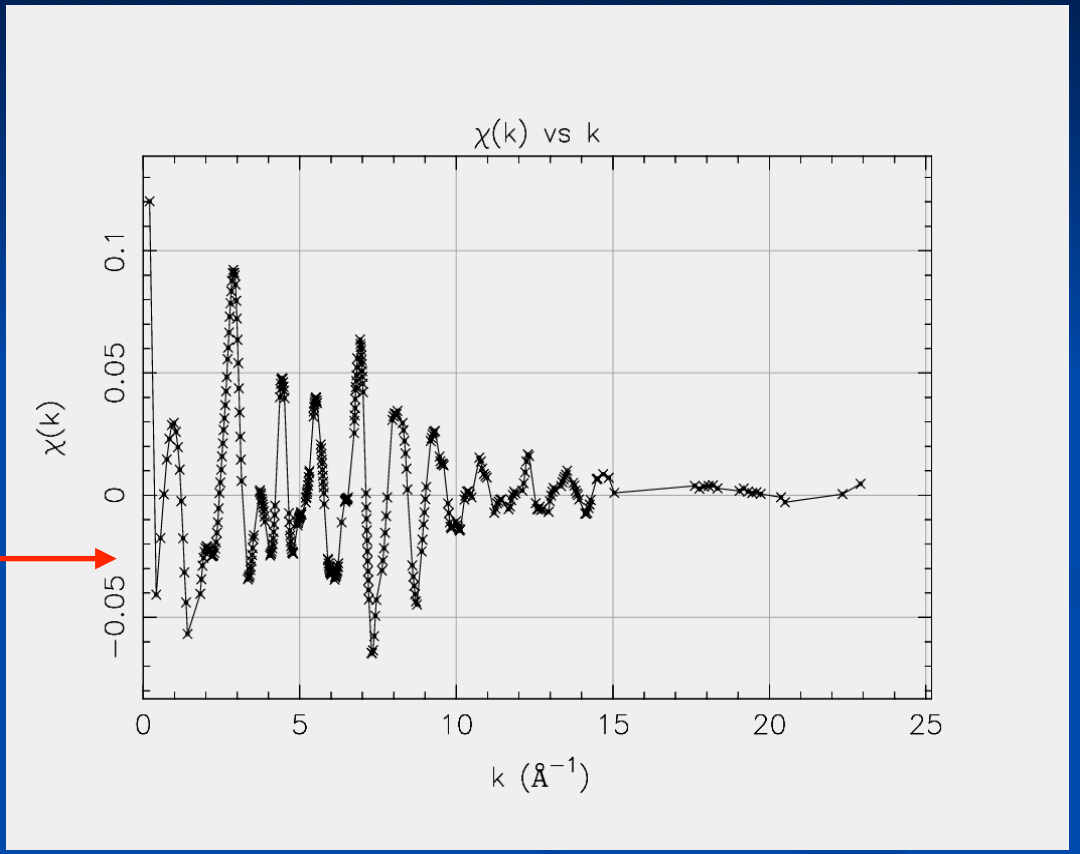

Mass Attenuation Coefficients (solid) Background Atom-Like Mass Attenuation (dashed)

M. D. de Jonge, C. Q. Tran, C. T. Chantler, Z. Barnea, B. B. Dhal, D. J. Cookson, W.-K. Lee, A. Mashayekhi, Phys. Rev. A 71, 032702 (2005) 032702-1-16

Isolated XAFS Spectrum (Error bars smaller than width of line)

L. F. Smale, C. T. Chantler, M. D. de Jonge, Z. Barnea, C.Q. Tran, Radiation Physics & Chemistry 75 (2006) 1559-1563

XAFS Theory: XANES and EXAFS Spectra

XAFS, XANES [vs Crystallography / Diffraction]

- Fine Structure observed 1920s (Fricke, Hertz, Lindh). LRO/SRO theory Kronig (1931/1932)
- Imaginary component & function needed for dynamical diffraction theory (Zachariasen 1945)
- Bijvoet ratios, absolute configurations & phasing (1949)
- Fourier Transform approach to EXAFS (Sayers Stern Lytle 1971)
- Spherical wavelets Lee, Pendry (1975), D Shirley (1985), Excurve, McKale (1986), Natoli, Rehr (1986… 2000), Muffin-tin
- Recent techniques e.g. Joly, Benfatto, Soldatov, Chantler, Shirley, Bourke

Data reduction

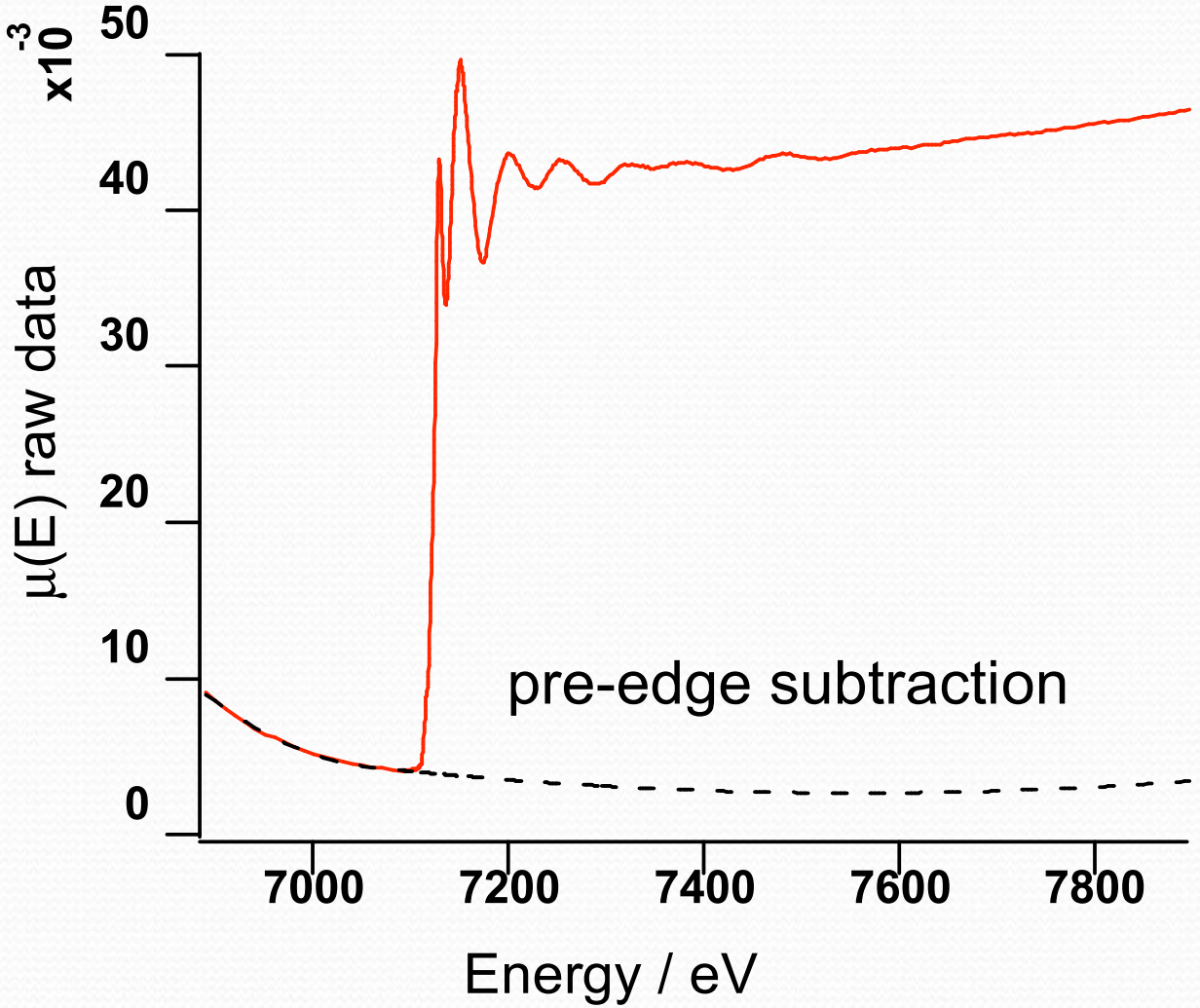

Data reduction

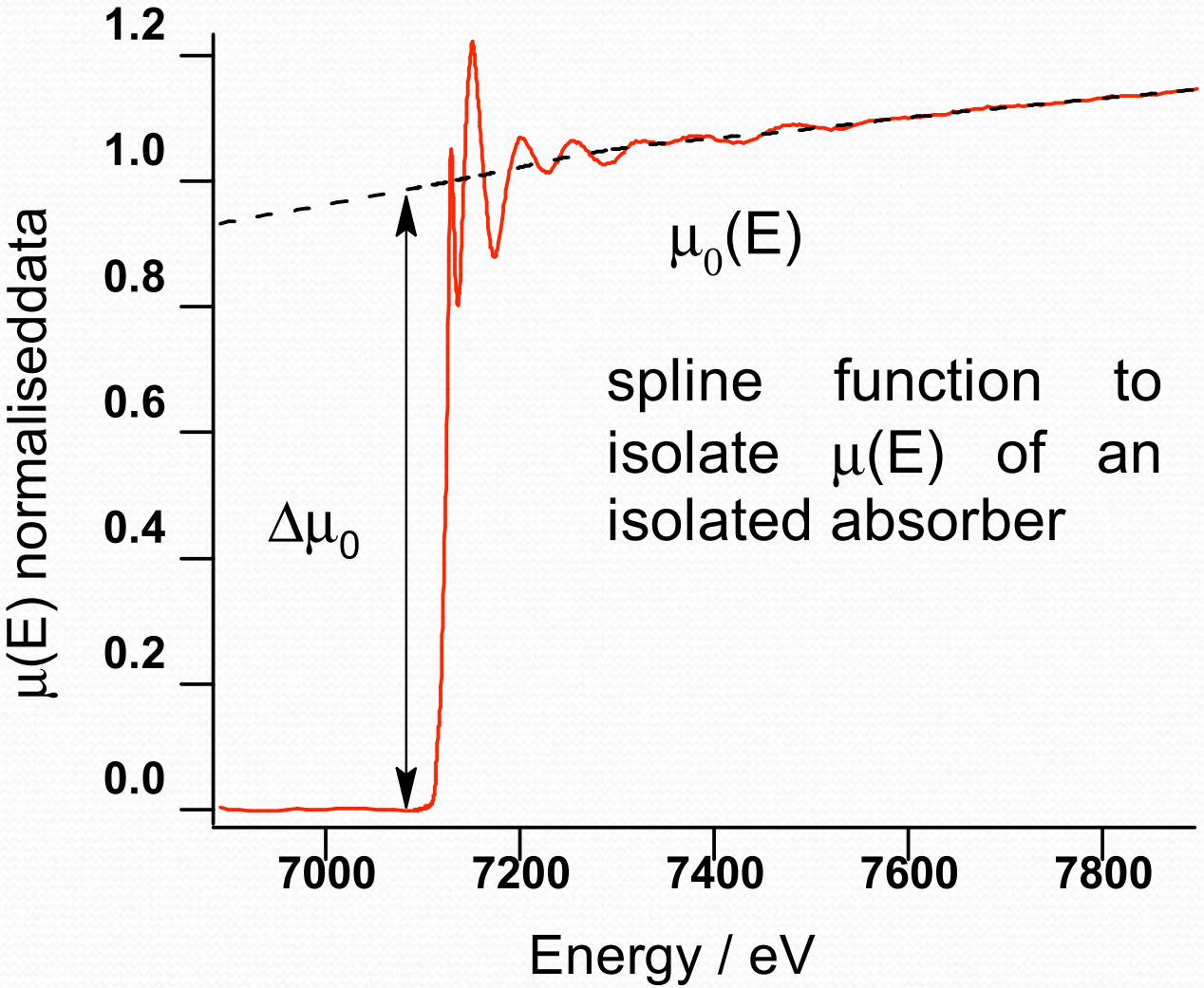

Data reduction

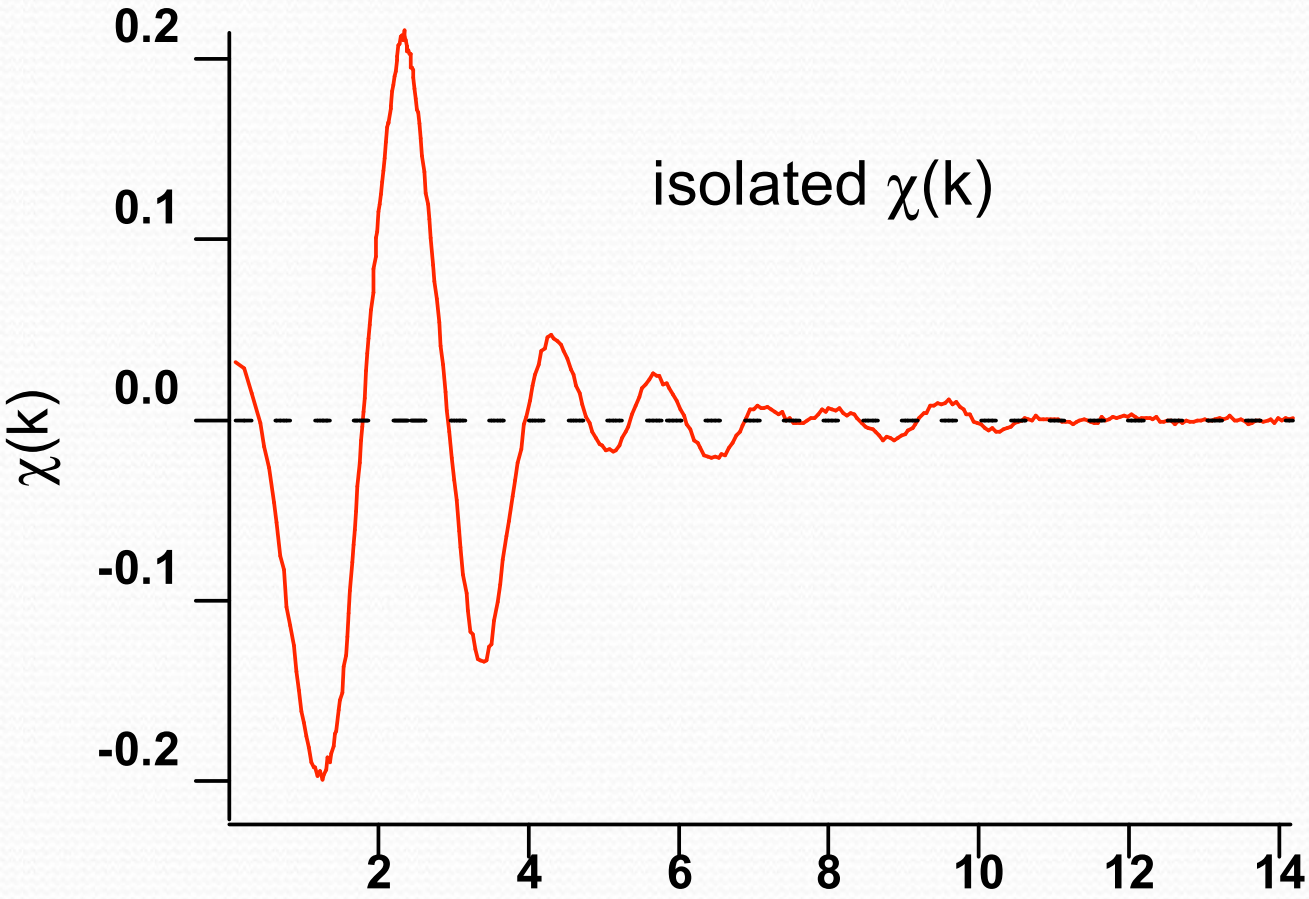

Data reduction

What are the uncertainties?
How much information content remains?
How much has been lost for hypothesis testing?

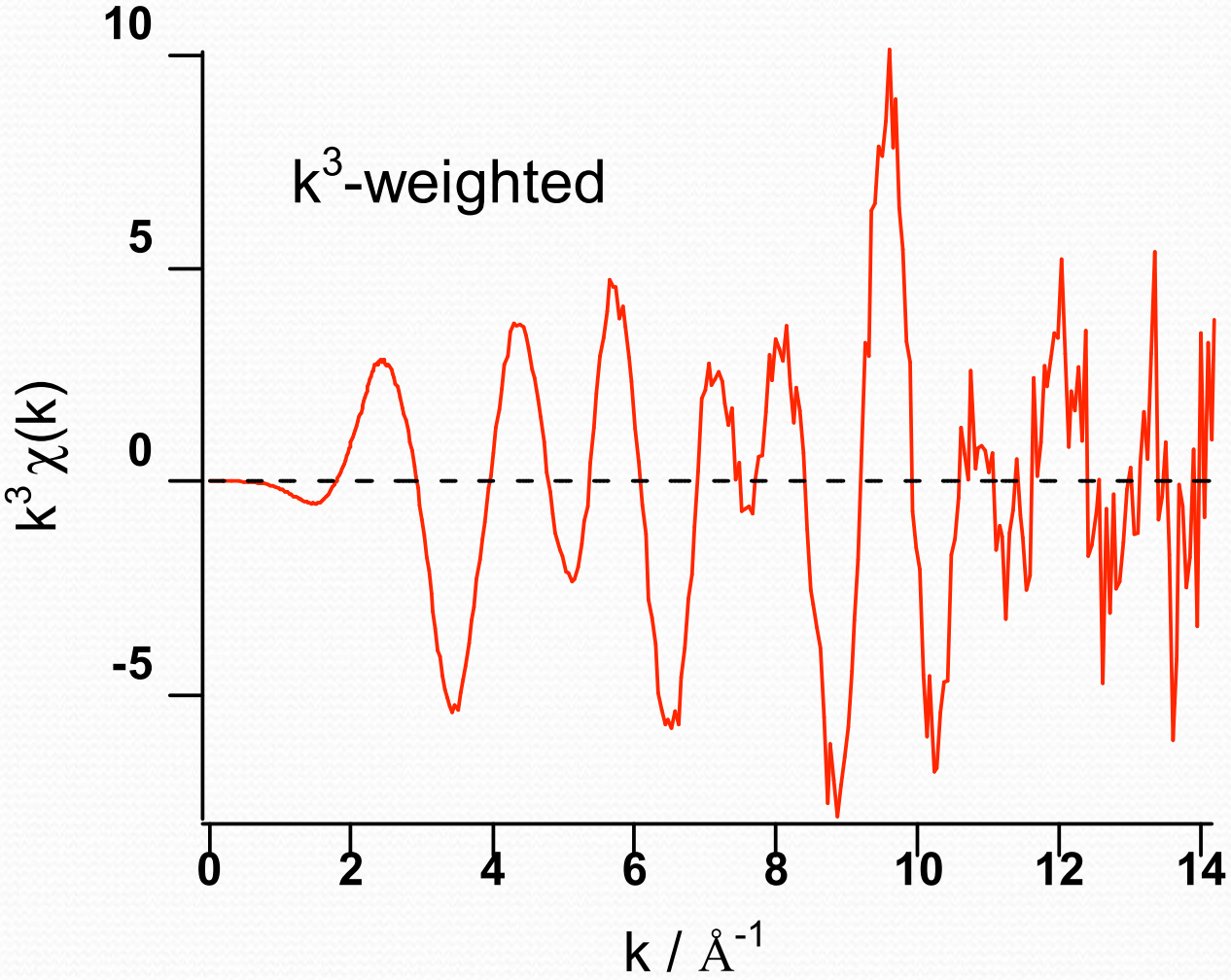

Data reduction

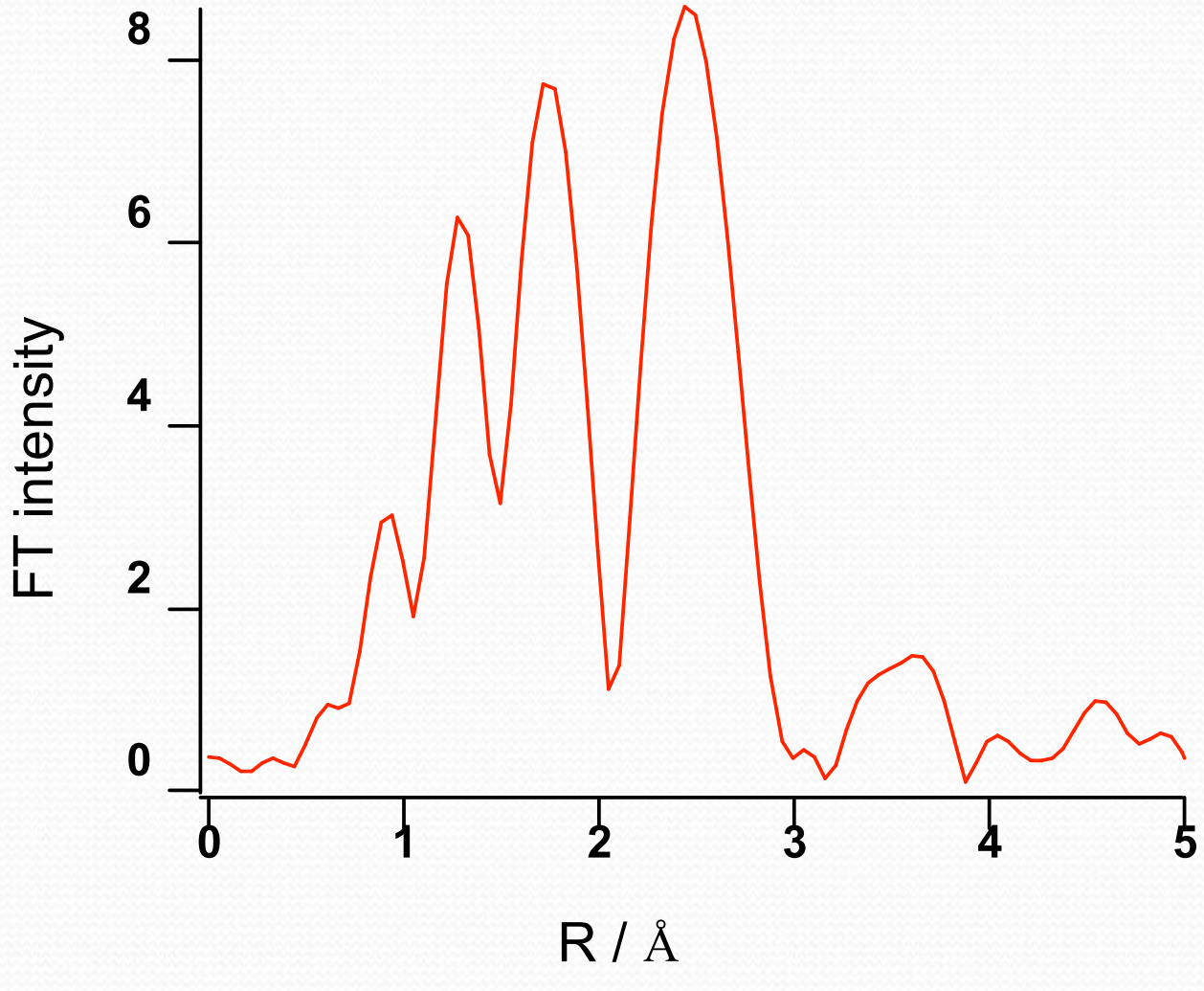

3. How does XAFS work?

Lots of structure (even at room temperature)

Lots of spectral features

If a theory can predict these, it can fit for unknown coordination, bond lengths, etc...

$Fe_2(\mu\text{-}PPh_2)_2(CO)_6$

Stephen P Best, Michael Cheah

Phosphido-Bridged Diiron Compounds

- Reduction product highly air sensitive

SP Best et al., Inorg. Chem., **2004**, 43, 5635.

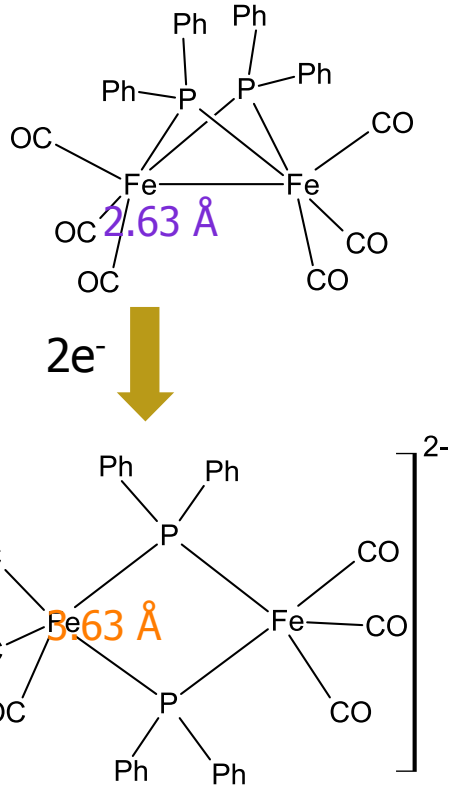

Fe-Fe / Å	Fe-P / Å	R(%) {χ
2.61 [2.63] (0.0007)	2.21 [2.21] (0.0009)	11.35 {2.80}
3.58 [3.63] (0.0060)	2.26 [2.29] (0.0034)	9.22 {1.48}

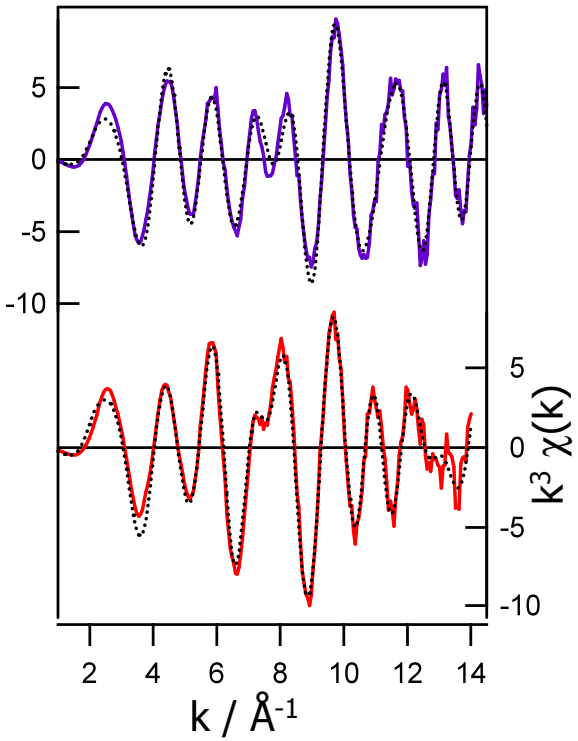

BL 20 B, Photon Factory
Data analysis: XFit
$N_{refined}$ = 16, N_{idp} = 26

Ginsburg *et. al. JACS*, **1979,** 101, 6550.

3. How does XAFS work?

Local Structure Guess

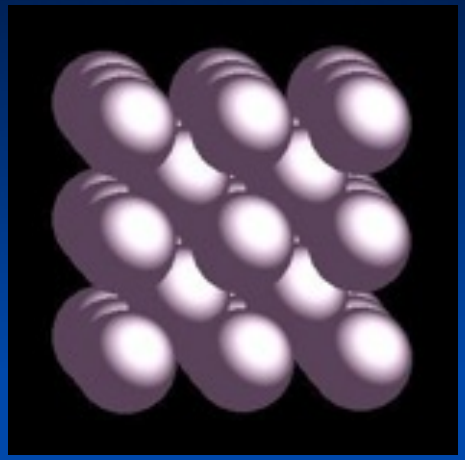

Metallic Molybdenum:
BCC Crystal

Program?

Model of XAFS Spectrum (XAFS Equation)

$$\chi_{th}(k) = \sum_j N_j S_0^2 F_j(k) \frac{\sin\left(2kr_j + \phi_j(k)\right)}{kr_j^2} e^{-2\sigma_j^2 k^2} e^{-2r_j/\lambda_j(k)}$$

$$r_j = (1+\alpha) r_{0,j}$$

Expansion Coefficient

Distance To Coordination Shell Based On Input

Backscattering Amplitude and Phase

Many Body Reduction Factor

Coordination Numbers

Debye-Waller Factor

Mean Free Path

k 'photoelectron momentum index' cf physical momentum.
χ(k) is dimensionless: F in units of 1/k (i.e. length)
Other definitions for F being dimensionless (as a form factor or scattering amplitude) have $(kR)^2$ in the denominator to maintain consistency of units.

XAFS Theory: XANES and EXAFS Spectra

3. How does XAFS work?

$$\chi_{th}(k) = \sum_j N_j S_0^2 F_j(k) \frac{\sin\left(2kr_j + \phi_j(k)\right)}{kr_j^2} e^{-2\sigma_j^2 k^2} e^{-2r_j/\lambda_j(k)}$$

$$r_j = (1+\alpha) r_{0,j}$$

Sum over *shells* of a particular atom type *j* & distances from the origin of the initial photoelectron.

N_j : coordination number, r_j : interatomic distance, σ^2_j : mean-square disorder in distance for j^{th} shell.

F_j : photoelectron (back-)scattering amplitude, $\varphi_j(k)$: (back-)scattering phase for the j^{th} atomic shell.

S_0^2: amplitude reduction factor (relaxation of the absorbing atom due to the presence of the empty core level and Multi-Electron Excitations).

$\lambda_j(k)$: photoelectron inelastic mean free path - strong dependence upon *k*, range 1 - 100 Å over XAFS

XAFS Theory: XANES and EXAFS Spectra

3. How does XAFS work?

$$\chi_{th}(k) = \sum_j N_j S_0^2 F_j(k) \frac{\sin\left(2kr_j + \phi_j(k)\right)}{kr_j^2} e^{-2\sigma_j^2 k^2} e^{-2r_j/\lambda_j(k)}$$

$$r_j = (1+\alpha) r_{0,j}$$

Crude approximation of $F_j(k) \approx -2\, a_0 k$ (a_0 : Bohr radius) works for many systems: peaks for a particular shell in Fourier transform of $\chi(k)$ shifted ~ 0.5 Å below actual interatomic distance.

$F_j(k)$ depend upon Z of scattering atom, with non-linear dependence on k.

$\exp(-2k^2 \sigma_j^2)$: EXAFS isotropic or effective Debye-Waller Factor, including thermal vibration & static disorder. Sum over shells and σ_j^2 in the standard EXAFS equation can be generalized to an integral over the partial pair distribution function $\gamma(R)$ in which one atom is always the absorbing atom.

XAFS Theory: XANES and EXAFS Spectra

3. How does XAFS work?

$$\chi_{th}(k) = \sum_j N_j S_0^2 F_j(k) \frac{\sin\left(2kr_j + \phi_j(k)\right)}{kr_j^2} e^{-2\sigma_j^2 k^2} e^{-2r_j/\lambda_j(k)}$$

$$r_j = (1+\alpha) r_{0,j}$$

Sum can be generalized to be over photo-electron *scattering paths* instead of *shells of atoms*. This allows inclusion of multiple scattering paths for the photo-electron, giving important contributions. The interpretation of the EXAFS Equation is then slightly modified: r_j is then half the path length; $F_j(k)$ and $\phi_j(k)$ become (multiple) scattering amplitudes and phase-shifts for the entire path.

The EXAFS Equation allows the numerical determination of the local structural parameters N_j, r_j, σ_j^2 knowing the scattering amplitude $F_j(k)$ for a small number (typically 1 to 10) of shells or paths. Theory normally breaks down at low k (the XANES region) as the $1/k$ term increases, $\lambda_j(k)$ increases, the disorder terms do not strongly dampen the EXAFS, and the EXAFS picture of single particle scattering is no longer a good approximation.

XAFS Theory: XANES and EXAFS Spectra

3. How does XAFS work? Difficulties

$$\chi_{th}(k) = \sum_j N_j S_0^2 F_j(k) \frac{\sin\left(2kr_j + \phi_j(k)\right)}{kr_j^2} e^{-2\sigma_j^2 k^2} e^{-2r_j/\lambda_j(k)}$$

$$r_j = (1+\alpha) r_{0,j}$$

Fermi level / Fermi Energy.

1) the energy of 50% probability of occupation, lying between the highest occupied level and the lowest unoccupied level, often defined as their average. If the energy level spectrum is a continuum (or almost a continuum) the three levels coincide. In a many-body approach, the Fermi level is the energy necessary for adding or subtracting a particle from the system. In XAS the Fermi level is below or at the first allowed transition.

2) In XAS, the **Fermi energy** dictates possible pre-edge features and explains the possibility or impossibility of open scattering channels adding to near-edge structure. When theoretical formalisms compute the Fermi energy, crucial for the XANES region, the quantum mechanical convergence is essential, whether atomic, cluster, or periodic boundary conditions are used. The lack of convergence for theoretical formalisms can at this time lead to systematic errors in the determination of the Fermi energy and corresponding pre-edge structure of order 1- 10 eV in the X-ray regime and should be considered carefully as this affects the interpretation of XAFS and XANES.

XAFS Theory: XANES and EXAFS Spectra

3. How does XAFS work?

Difficulties

$$k = \frac{2\pi}{h}\sqrt{2m_e(E - E_0)}$$

$$\chi_{th}(k) = \sum_j N_j S_0^2 F_j(k) \frac{\sin\left(2kr_j + \phi_j(k)\right)}{kr_j^2} e^{-2\sigma_j^2 k^2} e^{-2r_j/\lambda_j(k)}$$

$$r_j = (1+\alpha) r_{0,j}$$

Absorption threshold. The absorption threshold should indicate the first allowed transition in an absorption spectrum. Many definitions are used in common parlance. They yield very different values in analysis.

1. The energy at which the open continuum channel for photo-electric absorption becomes available, producing a continuum photo-electron. This has an exact value from theory, subject to convergence issues.
2. An (higher) energy at which a secondary (two-step) photo-ionization channel becomes energetically possible; more challenging to compute theoretically, and less easily separable in XAS;
3. Experimentally, the **absorption threshold** is sometimes defined as the inflection point in the first derivative of the experimental edge spectrum (the point of maximum slope on the rising edge for a particular sub-shell); this is a convenient marker but – a. it is source, beam-line, and band-width dependent; b. it is affected by pre-edge structure and the **Fermi level** due to contributions from bound-bound channels ; c. the experimental edge often contains two inflection points, and d. the determination depends upon instrumental resolution.
4. Experimentally, the **absorption threshold** is sometimes defined as the point exactly 50% of the jump ratio from the background absorption (from other shells, including scattering) to the peak absorption coefficient of the XAS spectrum, defined either by the clear maximum or by the smooth line representing the background to be subtracted in the determination of $\chi(k)$; this is problematic, since it depends upon beam-line dependent effects (3 above), and a wide variety of different predictions of the 'true background level' m_0 above the edge.
5. Computationally, an **absorption threshold** is defined for XAFS fitting as E_0 which is either an arbitrary fitting coefficient or the starting point of the *k* transform, which in turn generates the Fourier transform for the XAFS structure $\chi(k)$; as the latter, it should be defined as per 1 above; as the former, this will often yield a function of *r* and errors in E_0 of order 10 eV or more which can result in bond length errors of order 0.02 Å or more. Computationally and experimentally, the energy axis is often not defined, so inconsistencies between these definitions are relatively common.

XAFS Theory: XANES and EXAFS Spectra

3. How does XAFS work? Difficulties

$$k = \frac{2\pi}{h}\sqrt{2m_e(E - E_0)}$$

$$\chi_{th}(k) = \sum_j N_j S_0^2 F_j(k) \frac{\sin\left(2kr_j + \phi_j(k)\right)}{kr_j^2} e^{-2\sigma_j^2 k^2} e^{-2r_j/\lambda_j(k)}$$

$$r_j = (1+\alpha) r_{0,j}$$

Most theoretical approaches have great difficulty in experimental modelling at low k, which is one of the key reasons for standard analysis [fitting] to use both a window function (i.e. to fit over a restricted *k*-range) and a k^2 or k^3 weighting (to emphasise higher-*k* oscillations). Also, experimental uncertainties are not propagated.

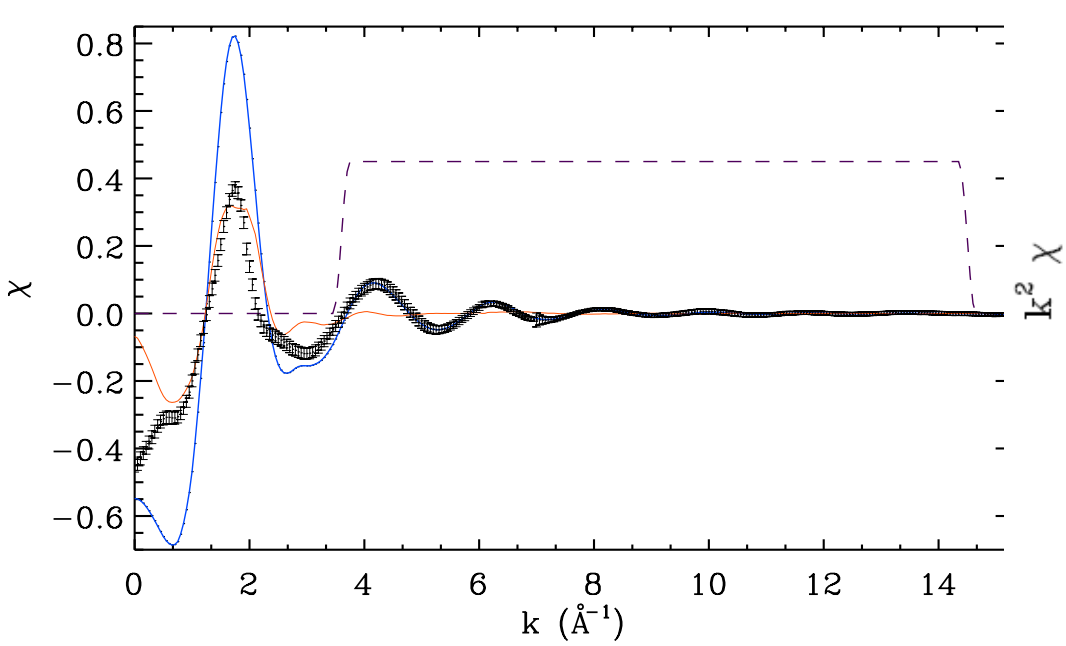

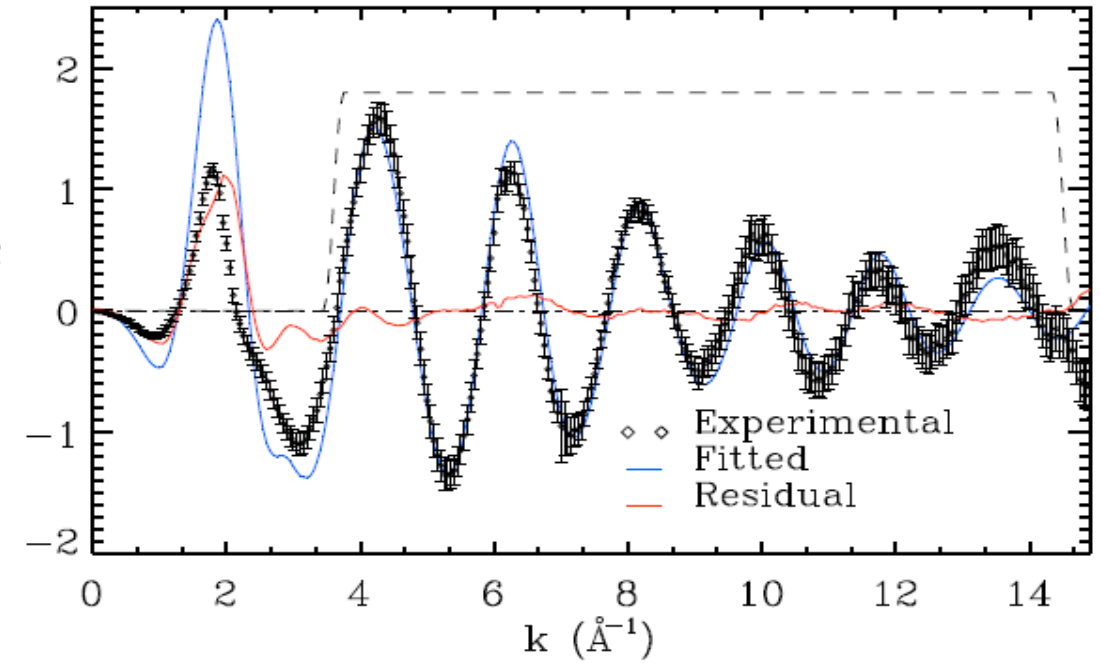

XAFS Theory: XANES and EXAFS Spectra

3. How does XAFS work?

$$\chi_{th}(k) = \sum_j N_j S_0^2 F_j(k) \frac{\sin\left(2kr_j + \phi_j(k)\right)}{kr_j^2} e^{-2\sigma_j^2 k^2} e^{-2r_j/\lambda_j(k)}$$

$$r_j = (1+\alpha) r_{0,j}$$

- Lytle, F. W., 1999, J. Synchrotron Radiat. 6, 123
- Stumm von Bordwehr, R., 1989, Ann. Phys. (Paris) 14, 377.
- EXAFS Scattering Theory: Sayers, Stern, Lytle, Phys. Rev. Lett. 27 (1971) 1204
- Rehr, Albers, Rev. Mod. Phys. 72 (2000) 621-654
- Newville, M. (2004). *Fundamentals of XAFS. CARS, University of Chicago, Chicago IL*, pp. 23–24
- Bunker, G. (2010). In *Introduction to XAFS: A practical guide to X-ray Absorption Fine Structure Spectroscopy*, pp. 92–95. CUP
- Chantler et al., J Synch. Rad.19 (2012) 145-158; J Synch Rad 19 (2012) 851-862

Different Approaches to Analysis

FEFF and related codes: Spherically symmetric potentials (Muffin-tin (MT) approximation). Simulation of XANES spectra and fitting of EXAFS region. (developed in US) **IFEFFIT** (US, Australia) **Athena, Artemis etc.** (US)
EXCURVE : Potentials and corresponding phase shifts are calculated for each constituent atom of the examined material sample from a superposition of neutral atomic solutions or potential files produced by *ab initio* codes are used. Simulation of XANES spectra and fitting of EXAFS region. (developed in UK)
MXAN: Full multiple scattering calculations with MT approximation and **FPMS** (Non MT approximation). Structural and electronic properties are fitted in XANES region (developed in Italy)
FDMNES: Finite Difference Method (FDM) to solve the Schrödinger equation (non MT approximation) and MT approximation. Pre-edge and XANES spectra are simulated (developed in France)
Fit-it: Use FEFF and FDMNES to fit XANES (developed in Russian Federation)
FDMX: Finite Difference Method (FDM) with full XAFS analysis. Pre-edge, XANES and XAFS spectra fitted, Inelastic mean free paths simulated and fitted, thermal broadening fitted or measured (developed in Australia from France)
Others - Shirley et al.

XAFS Theory: XANES and EXAFS Spectra

3. How XAFS works - Realisation

A: Absorption

Absorption is conventionally given by the Beer-Lambert equation:

$$I = I_0 \exp\{-[\mu/\varrho]\,[\varrho t]\}$$

I_0 is the incident X-ray beam intensity, I is the transmitted intensity, $[\mu/\varrho]$ is the X-ray mass absorption coefficient of the material for the energy of the X-ray beam, and t is the thickness of the foil. The beauty of this is that the negative values of the natural logarithms of the measured ratios of I/I_0,

$$-ln\{I/I_0\} = [\mu/\rho]\,[\rho t] = \mu t$$

plotted against t (or $[\varrho t]$), fall on a straight line with slope μ (linear absorption coefficient) (or $[\mu/\varrho]$). Hence the mass absorption coefficient, the photoelectric coefficients, the scattering components and the form factors of the material can be directly evaluated from the logarithm of the normalised ratio. This then gives the input spectrum for the extraction of the XAFS, XANES or EXAFS signal.

This requires careful correction for **detector efficiencies and air path** (Tran, CQ, Chantler, CT & Barnea, Z (2003). *Phys. Rev. Letts*, **90**, 257401–1–4), **scattering** (Tran, CQ, et al. (2004). *Rev.* Sci. Instrum. **75**, 2943–2949), **harmonics** (Tran, C. Q., et al. (2003). *X-ray Spectrometry*, **32**, 69–74), **detector linearity** (Barnea, Z., et al. (2011). *J. Appl. Cryst.* **44**, 281–6), **energy calibration** (Rae, N. A., et al. (2010). Nucl. Instr. Meth. A, **619**, 147–149), **thickness calibration, bandwidth** (de Jonge, M. D., Barnea, Z. & Chantler, C. T. (2004). Phys. Rev. A, **69**, 022717–1 –12), but yields a highly accurate measurement of the coefficients with the correct scaling and relative amplitudes for processing using, for example, XERT for XAFS analysis (*Chantler, C. T. (2009). European Physical Journal ST*, **169**, 147–153; Chantler, C. T. (2010). *Rad. Phys. Chem.* **79**, 117–123).

XAFS Theory: XANES and EXAFS Spectra

Normalisation of signals for dark current and common paths: Absorption!

$$\ln\left(\frac{\left(\frac{I_2-dc_2}{I_1-dc_1}\right)_{sample+air}}{\left(\frac{I_2-dc_2}{I_1-dc_1}\right)_{air}}\right)$$

$$= \ln\left(\frac{\frac{A_2Y_2E_2e^{-(\mu t)_{IC1}}e^{-(\mu t)_{sample}}e^{-(\mu t)_{air}}}{A_1Y_1E_1}}{\frac{A_2Y_2E_2e^{-(\mu t)_{IC1}}e^{-(\mu t)_{air}}}{A_1Y_1E_1}}\right)$$

$$= -(\mu t)_{sample}$$

with: A = amplification

Y = electron yield per x-ray absorbed

E = Ion Chamber efficiency

dc = dark current measurement

I = Ion Chamber measured current

1, 2 = upstream / downstream ion chamber

Statistical precision on monitor does not imply same precision on the logarithm and μt or [μ/ρ][ρt]
Precision will be reduced significantly more than just the sum of precisions in quadrature

$\sigma(\ln x)=\sigma(x)/x$

[% uncertainty in detector count => absolute uncertainty in logarithm]

C. T. Chantler, Optical & Quantum Electronics 31 (1999) 495-505
C. T. Chantler, Phys. Rev. A64 (2001) 062506

XAFS Theory: XANES and EXAFS Spectra

Harmonic Components

3-foil measurement & signature for harmonic contamination

With a fraction x of harmonic photons in the beam

$$\ln(I/I_0) = \ln\left([1-x]e^{-[\mu/\rho]_F [\rho t]} + x e^{-[\mu/\rho]_H [\rho t]} \right)$$

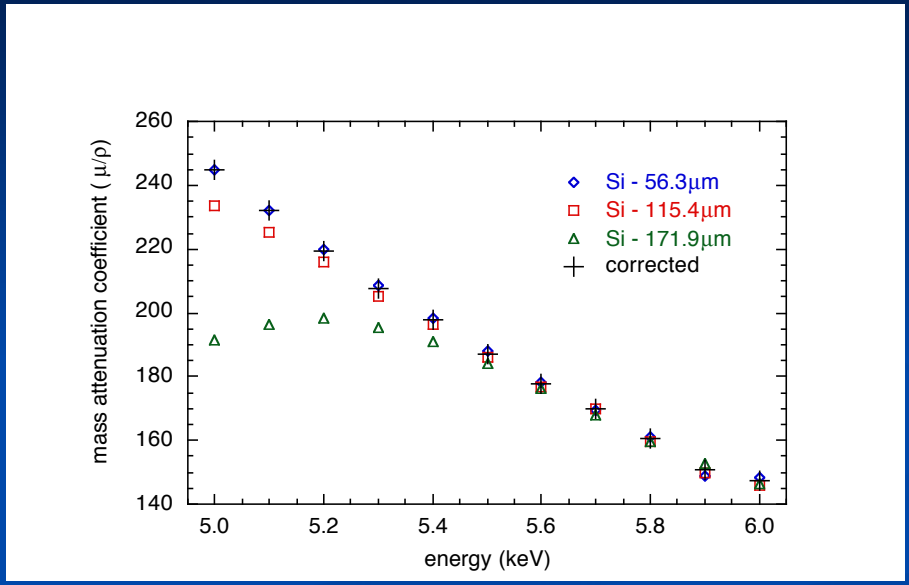

APS, 1-ID 5th order undulator radiation, monochromated by a double-bounce silicon (311) monochromator, detuned to suppress higher order harmonics

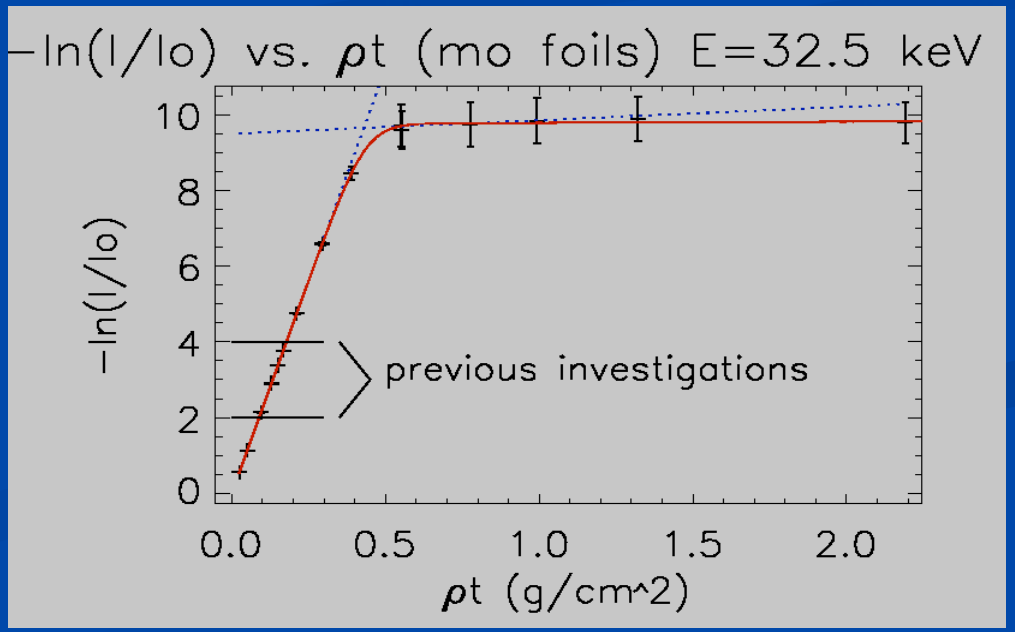

Tran, CQ, Barnea, Z, de Jonge, MD, Dhal, BB, Paterson, D, Cookson, D & Chantler, CT (2003). *X-ray Spectr*, **32**, 69–74

Harmonic Component ≤ $e^{-9.5}$ ≤ 1 in 10^4 photons

XAFS Theory: XANES and EXAFS Spectra

Multiple-Foil Measurement & Effect of Tuning/Detuning

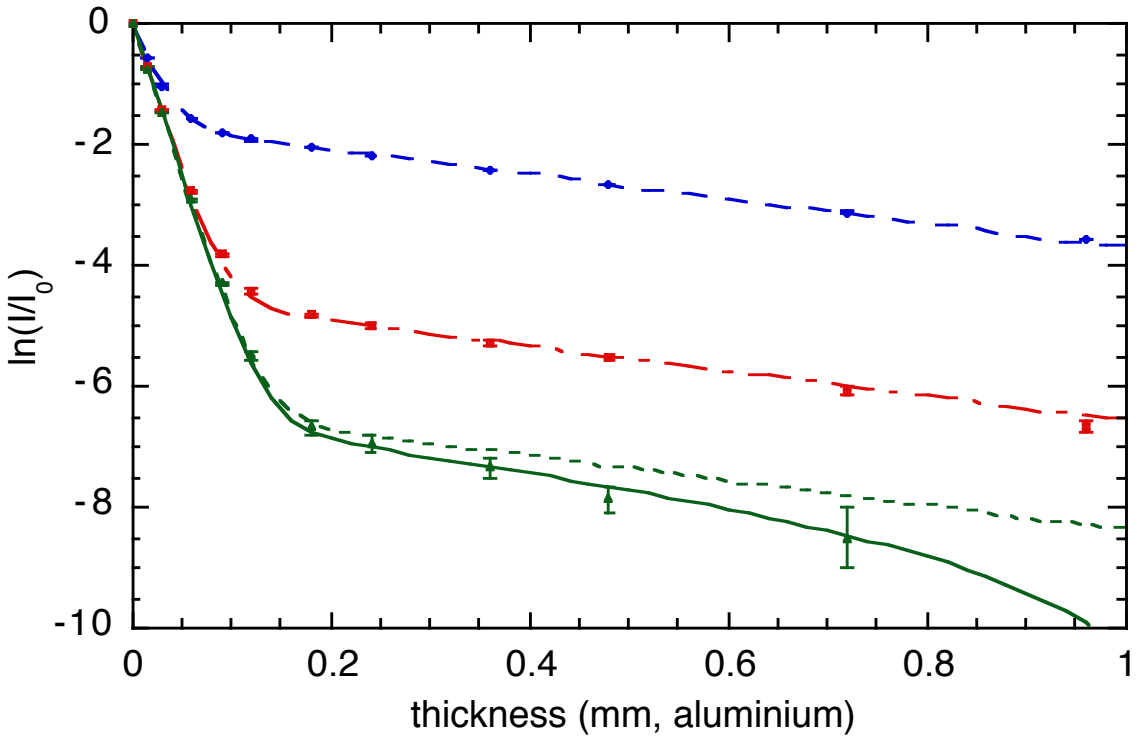

Detuning:

decrease harmonic component

decrease total incident flux

Tuning:

increase harmonic component

increase total incident flux

Optimisation:

minimise harmonic component without cutting too much flux

Multiple-foil measurement:

effective tool to quantitative investigation of harmonic component

XAFS Theory: XANES and EXAFS Spectra

Optimal range!

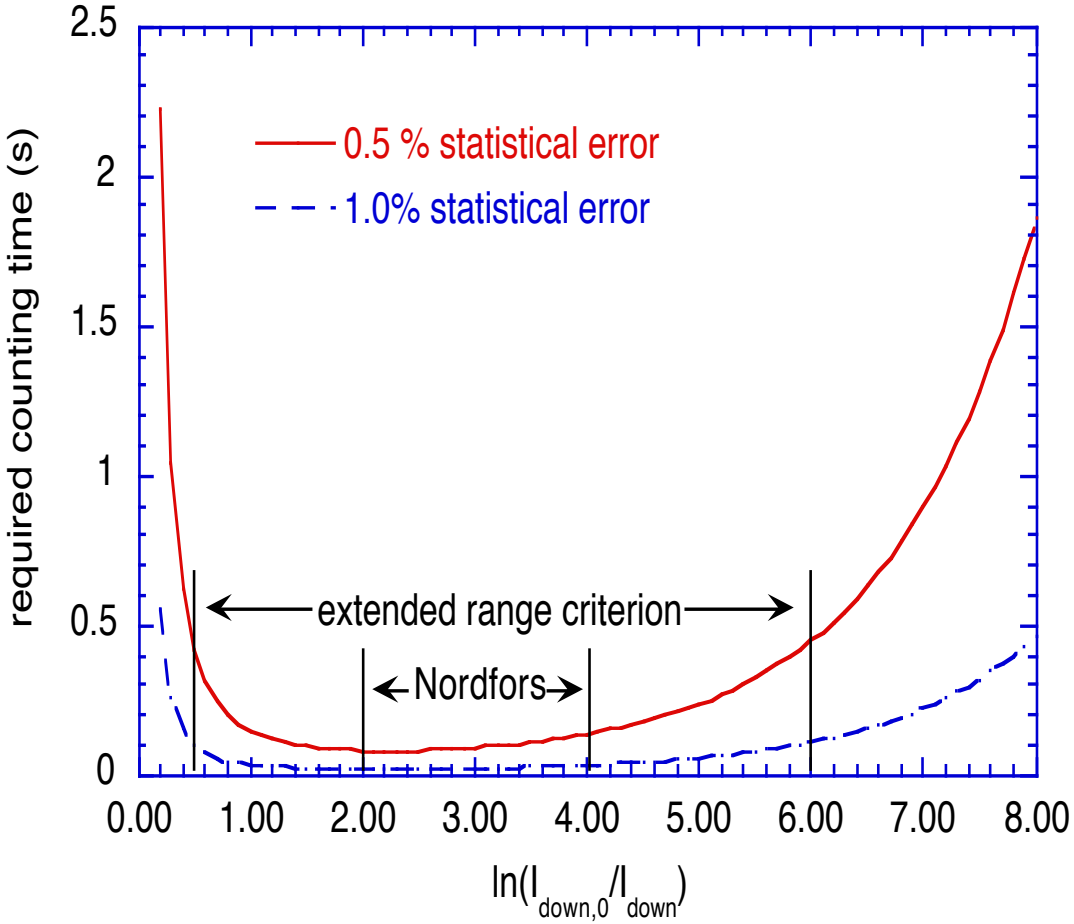

If monitor/flux set to 10^6 cps [counts in photons absorbed, not counts in reading]; detector ion chamber matched; negligible dark current (electronic baseline noise)

We can still get a statistical precision on the log ratio of <0.1%

XAFS Theory: XANES and EXAFS Spectra

Bandwidth

Effective beam monochromation:

Synchrotron beam characterised:

1.57 eV ± 0.03 eV @ 20 keV

[μ/ρ] corrected by 0.35%- 1.4%

de Jonge, M. D., Barnea, Z. & Chantler, C. T. (2004). Phys. Rev. A, 69, 022717–1 –12

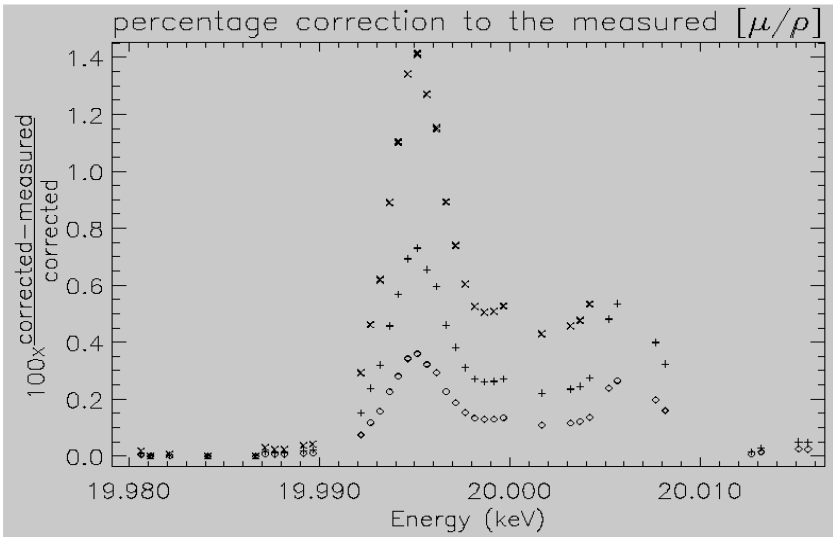

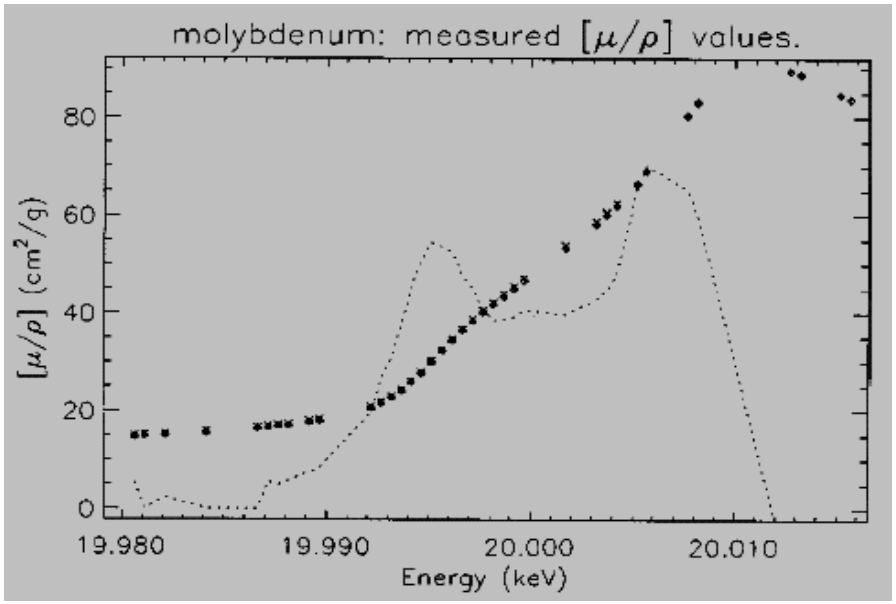

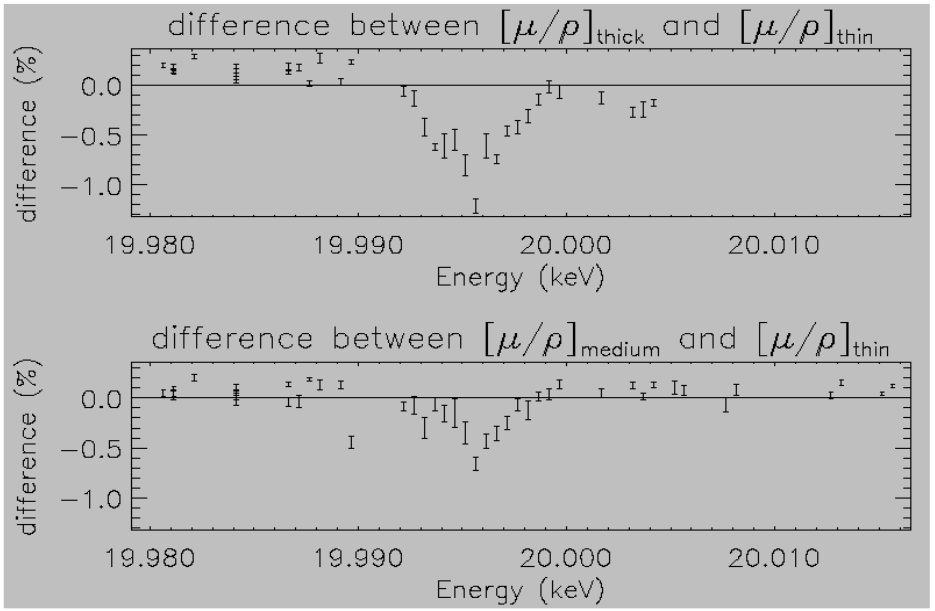

XAFS Theory: XANES and EXAFS Spectra

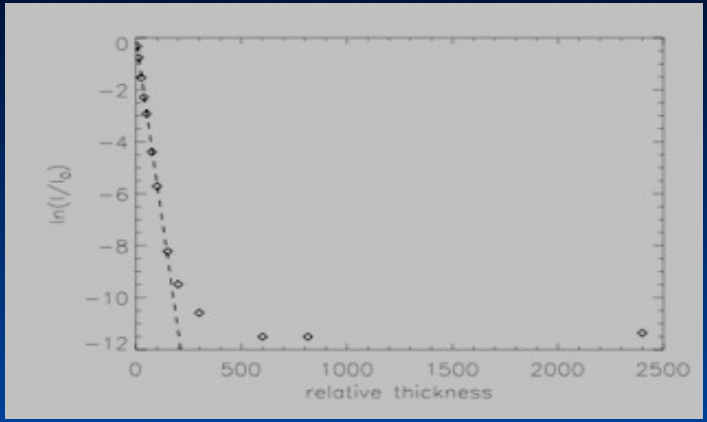

Barnea, Z., Chantler, C. T., Glover, J. L., Grigg, M. W., Islam, M. T., de Jonge, M. D., Rae, N. A. & Tran, C. Q. (2011). *J. Appl. Cryst.* **44**, 281–6

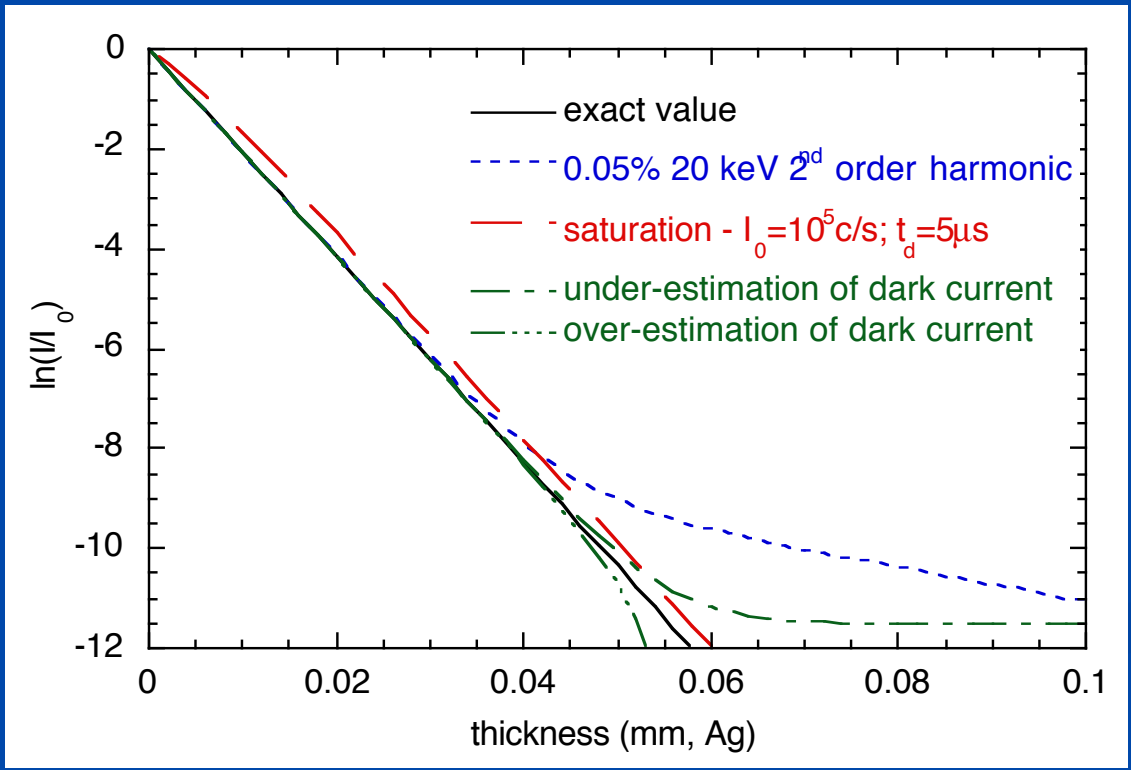

The linearity of the data indicated by the dashed line shows

(i) the excellent linearity of the detection system &

(ii) no significant harmonic photons over a large attenuation range $0>\ln(I/I_0)>-9$.

ideal measurements

$$\ln\frac{I}{I_0} = -\mu t$$

I, I_0: attenuated & incident intensities, respectively

μ: linear attenuation coeff. t: sample thickness

effect of harmonics

$$\ln\left(\frac{I}{I_0}\right) = \ln\left[(1-x)e^{-\mu_f t} + xe^{-\mu_h t}\right]$$

ction of harmonic

μ_f, μ_h: attenuation coeffs at fund. & harm. energies

effect of saturation

$$\ln\left(\frac{I}{I_0}\right) = \ln\left(\frac{\frac{I_T}{1+I_T t_d}}{\frac{I_{0,T}}{1+I_{0,T} t_d}}\right)$$

I_T, $I_{0,T}$: true count rates of attenuated & incident beams

t_D: dead time

dark current correction

$$\ln\left(\frac{I}{I_0}\right) = \ln\left(\frac{I - I_{off}}{I_0 - I_{0,off}}\right)$$

I_{off}, $I_{0,off}$: dark current correction for detectors

XAFS Theory: XANES and EXAFS Spectra

Quantitative Investigation Of Current XAFS Analysis Techniques

Results - Standard Analysis [FEFF8.2]

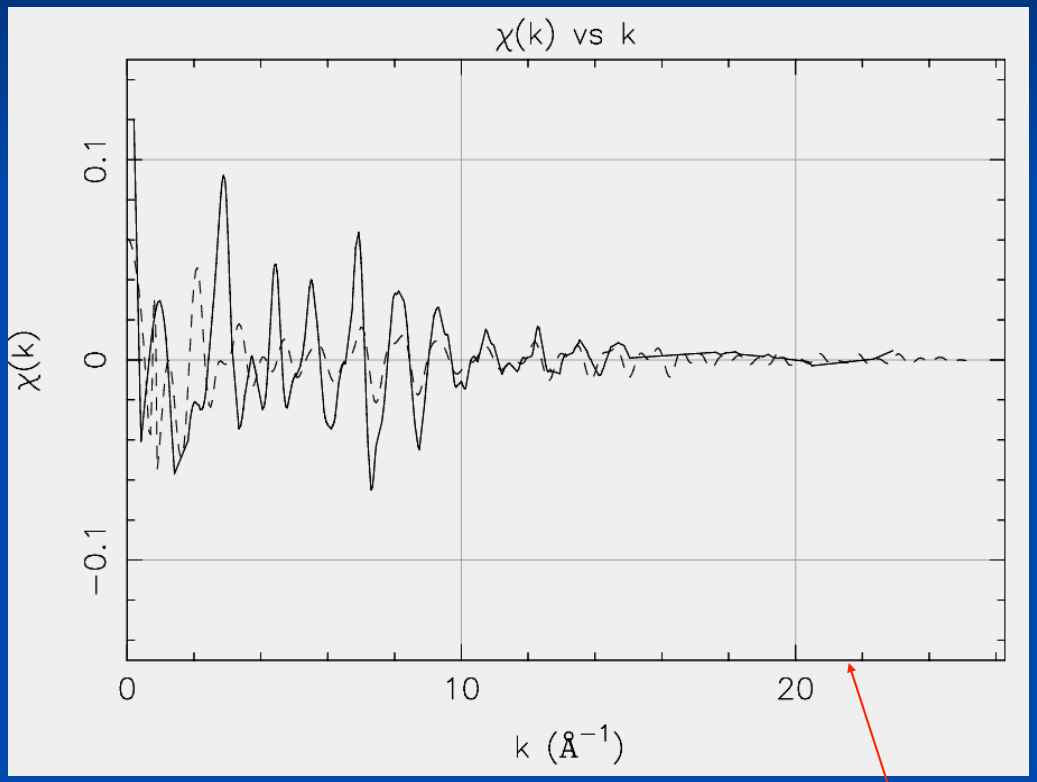

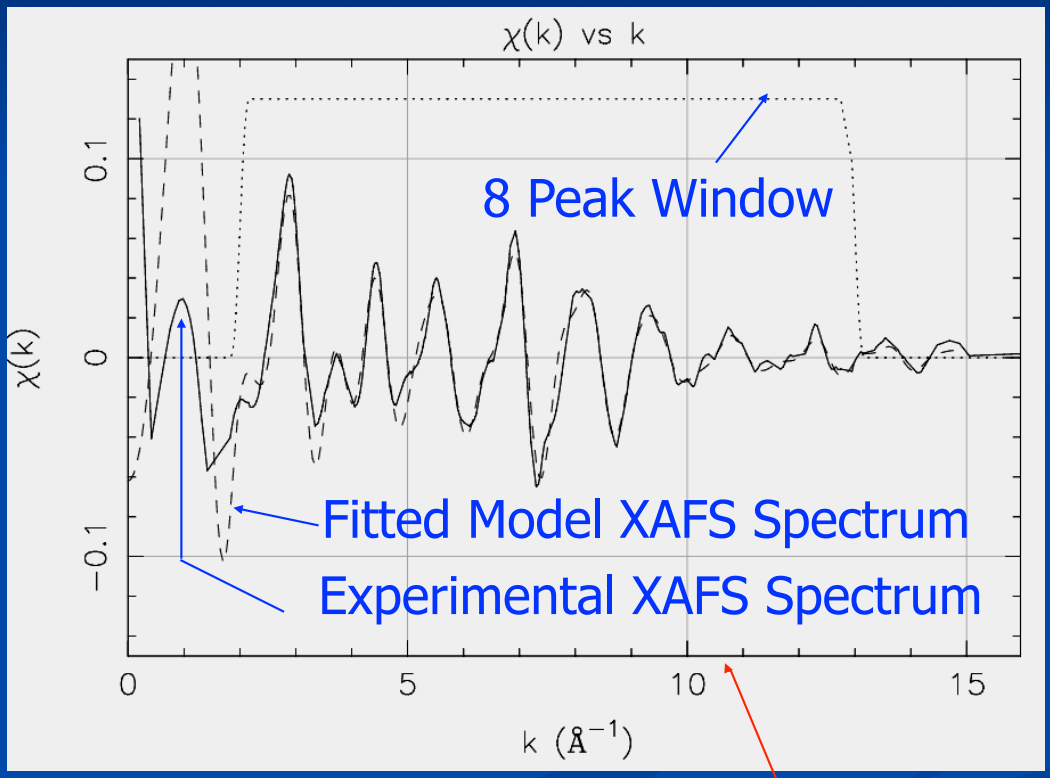

Smale, LF, Chantler, CT, de Jonge, MD, Barnea, Z & Tran, CQ (2006). Rad. Phys. Chem. **75**, 1559–1563

Un-Windowed Fit of "Reduced Parameter Set"

χ_r^2 = **2500-3000**

8 Peak Windowed Fit of "Reduced Parameter Set"

χ_r^2 = **130**

XAFS Theory: XANES and EXAFS Spectra

Standard XAFS expectations

Accuracy of XAS measurements depend on the data quality (e.g. it is recommended to optimise S/N ratio, kmax and harmonics rejection, to chose appropriate detectors, etc.)

XAFS, EXAFS and **XANES:**

Be careful of the calibration of the E scale;Measure error bar for accurate comparison of XANES or XAFS spectra

Conventional EXAFS:

Distances 0.02Å This value could increase or decrease depending on quality data or other factors (errors in E0 of order 10 eV or more which can result in bond length errors of order 0.02Å or more); Coordination number 20-25%; Scattering Atom ΔZ~1 (Z=6-17) ΔZ~3 (Z=20-35)

High-accuracy XERT:

- BONDING: Mo, Au: Glover, Chantler 0.1% e.g. 0.002 Å
- Atomic ABSORPTION: *absolute* 1 x 10^{-4} Meas.Sci.Tech.18(2007)2916; J Phys.B43(2010) 085001
- LATTICE SPACING: on same 'real systems' from crystallography: 0.1% e.g. 0.002 Å
- quality of XAFS data and intrinsic information content can be outstanding, even comparing lattice spacing determinations for single crystals
- Coordination [under analysis]; scattering atom and ionisation state [under analyis]
- ***its ability to determine bonding and dynamical modes can be unsurpassed, especially for non-crystalline solids or solutions***

XAFS Theory: XANES and EXAFS Spectra

X-ray Extended Range Technique: Determine [μ/ρ] accurately & quantify systematics

X-Ray Bandwidth
PRA69, 2004

Harmonic components
X-Ray Spect 32, 2003

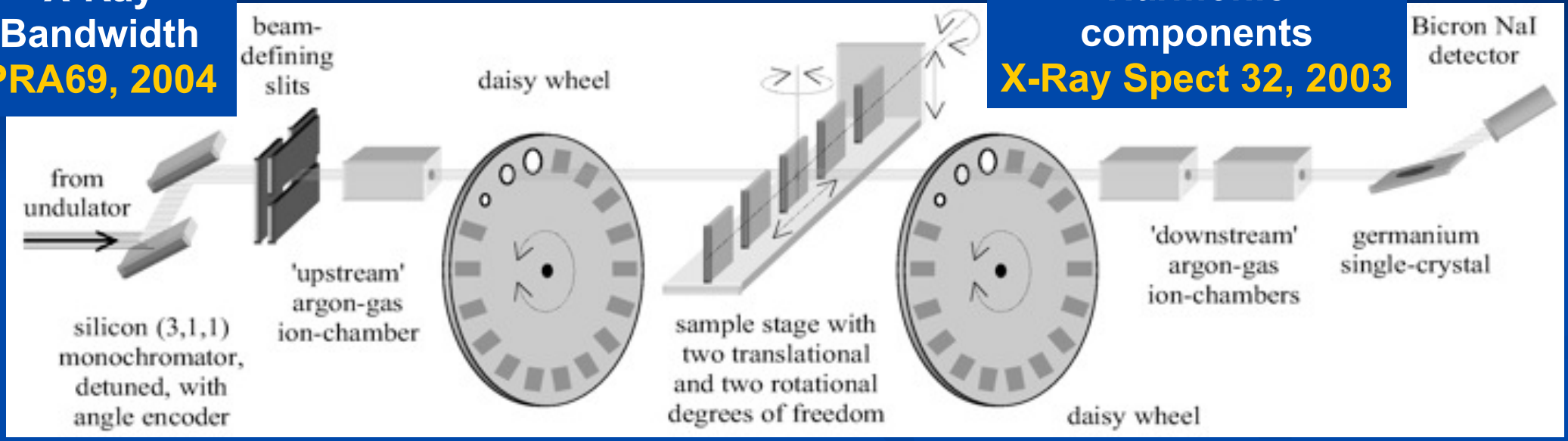

Optimisation of statistical level
X-Ray Spect 29, 2000

Sample thickness
Meas.Sci.&Technol.15, 2004
RSI 75, 2004

Fluorescence & scattering contributions
Rad.Phys.& Chem. 61, 2001
J.Phys.B37, 2004

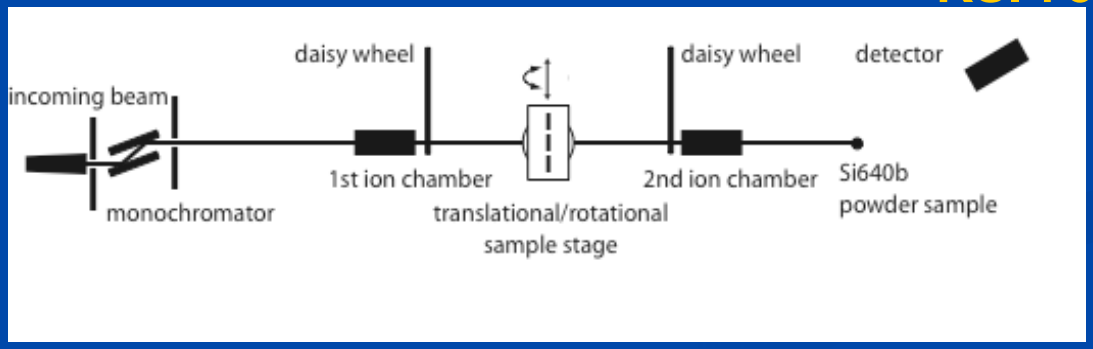

C. T. Chantler, Rad. Phys. Chem. 79 (2010) 117-123

4. Past, Present & Future: What is XERT? Experiment:

- Independently calibrate monochromated energy
  - Avoid 3-10 eV or 30 -100 eV errors or offsets
- Energy is stepped commensurate with structure
  - Finer grid near edges
- Multiple thickness foils for each energy
- Measurements of multiple apertures for each foil
- For each foil-aperture: sample, blank, dark current
- Repeat each measurement e.g. 10 times
- Measure harmonic contamination (daisy wheels)
- Detailed materials characterisation / profiling

XAFS Theory: XANES and EXAFS Spectra

3. How XAFS works - Realisation

B: Fluorescence [Chantler et al. JSR 2012]

For fluorescence, to first order: $I_{f0} = f\, I_0\, (1 - \exp\{-[\mu/\rho][\rho t_p]\})$; I_0 : number of fluorescence photons, t_p: path length through the sample, f : fluorescence yield for the probability of producing a fluorescent photon (a K-α photon if the experiment is around the K-shell, or a L-shell photon if the experiment is around the L-shell etc.) after the process of photoabsorption and photoionisation (we should label $[\mu/\rho]$ with the subscript *pe* for the photoelectric effect only, and an asterisk indicating that only the component absorbed in the active centre producing a fluorescent photon is relevant - i.e. as $[\mu/\rho]^*_{pe}$). To first order, these fluorescent photons are emitted isotropically. Then

$$I_f = \frac{\frac{f I_0 \Omega [\mu/\rho]^*_{pe}}{4\pi \cos\theta_{inc}}}{\frac{[\mu/\rho]}{\cos\theta_{inc}} + \frac{[\mu_f/\rho]}{\cos\theta_{out}}} \left(A - \exp\left(- \frac{\left[\frac{\mu}{\rho}\right][\rho t]}{\cos\theta_{inc}} - \frac{\left[\frac{\mu_f}{\rho}\right][\rho t]}{\cos\theta_{out}} \right) \right)$$

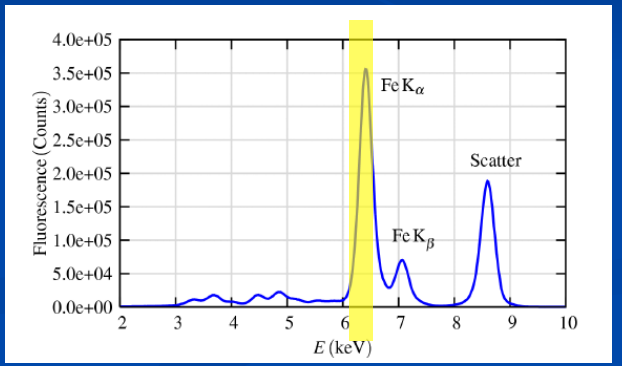

t is the depth of penetration into the material, W is the solid angle subtended by the detector channel, θ_{inc} is the angle of incidence of the incident X-ray (relative to the normal), θ_{out} is the angle of emission of the fluorescent X-ray (relative to the normal), $[\mu_f/\rho]$ is the mass attenuation coefficient of the material for the *fluorescent* photon energy; the integration constant A may be (loosely) estimated as $A = 1$. The number of fluorescent X-rays detected (in the region of interest) should include losses due to air path *air*, detector windows *w* etc. and detector quantum efficiencies overall e as

N.b. I_f= F(ROI)

$$\frac{I_{f_{detected}}}{I_{0monitored}} = \frac{I_f}{I_0} \left(\frac{\epsilon_{det}(E)}{\epsilon_{mon}(E)} \right) \exp\left(- \frac{\left[\frac{\mu_f}{\rho}\right]_{air}[\rho t_{air}]}{\cos\theta_{air}} - \frac{\left[\frac{\mu_f}{\rho}\right]_{w}[\rho t_w]}{\cos\theta_w} \right)$$

$t_{air}/\cos\theta_{air}$ is the path-length from the sample (surface) to the front face of the detector (window) and $t_w/\cos\theta_w$ is the path-length through a detector window of thickness t_w. Note the energy dependence of the relative efficiencies of the detectors.

XAFS Theory: XANES and EXAFS Spectra

3. How XAFS works - Realisation

B: Fluorescence

$$I_f = \frac{\frac{fI_0\Omega[\mu/\rho]^*_{pe}}{4\pi\cos\theta_{inc}}}{\frac{[\mu/\rho]}{\cos\theta_{inc}} + \frac{[\mu_f/\rho]}{\cos\theta_{out}}} \left(A - \exp\left(-\frac{\left[\frac{\mu}{\rho}\right][\rho t]}{\cos\theta_{inc}} - \frac{\left[\frac{\mu_f}{\rho}\right][\rho t]}{\cos\theta_{out}} \right) \right)$$

$$\frac{I_{f_{detected}}}{I_{0monitored}} = \frac{I_f}{I_0} \left(\frac{\epsilon_{det}(E)}{\epsilon_{mon}(E)} \right) \exp\left(-\frac{\left[\frac{\mu_f}{\rho}\right]_{air}[\rho t_{air}]}{\cos\theta_{air}} - \frac{\left[\frac{\mu_f}{\rho}\right]_{w}[\rho t_w]}{\cos\theta_w} \right)$$

For normal fluorescence XAFS geometries, the multi-element detector is placed at 90^0 to the incident beam, with the fluorescent sample, solid or solution, placed at an angle of 45^0 to the incident beam in order to minimise self-absorption. A particular detector channel will correspond to an emission angle θ_{out} which varies depending upon how close the sample stage is to the detector and its orientation etc. Similarly, the air path for the fluorescent X-ray to the detector, and the angle for the window attenuation, may then be given by $\theta_{w\,h} \simeq \theta_{air\,h} \simeq \theta_{out\,h} - 45^0$

XAFS Theory: XANES and EXAFS Spectra

3. How XAFS works - Realisation

B: Fluorescence

$$I_f = \frac{\frac{fI_0\Omega[\mu/\rho]^*_{pe}}{4\pi\cos\theta_{inc}}}{\frac{[\mu/\rho]}{\cos\theta_{inc}} + \frac{[\mu_f/\rho]}{\cos\theta_{out}}}\left(A - \exp\left(-\frac{\left[\frac{\mu}{\rho}\right][\rho t]}{\cos\theta_{inc}} - \frac{\left[\frac{\mu_f}{\rho}\right][\rho t]}{\cos\theta_{out}}\right)\right)$$

$$\frac{I_{f_{detected}}}{I_{0monitored}} = \frac{I_f}{I_0}\left(\frac{\epsilon_{det}(E)}{\epsilon_{mon}(E)}\right)\exp\left(-\frac{\left[\frac{\mu_f}{\rho}\right]_{air}[\rho t_{air}]}{\cos\theta_{air}} - \frac{\left[\frac{\mu_f}{\rho}\right]_{w}[\rho t_w]}{\cos\theta_w}\right)$$

1) While the equation is a little complex, several components are fixed by geometry. If they are known, then the information content can be recovered effectively.

2) Absorption yields a straightforward relation from the log (I/I_0); this is not true for fluorescence.

3) If L is the distance from sample surface to detector, then $W \simeq D/L^2$ where D is the area of the detector element.

4) θ_{out} varies across the detector & between detector channels. If detector channel centres are separated by a distance C and some central detector point is at 45^0 to the sample surface, then the angle of emission in the plane of incidence is $\theta_{out\,h} = 45^0 + \tan^{-1}(nC/L)$ where n is the number of channel elements from the central point. Due to misalignment, we should generalise this to $\theta_{outh} = \theta_0 + \tan^{-1}(nC/L)$. Different detector channels with different path-lengths will have strongly different self-absorption correction factors. Channels on the downstream side of the detector have approximately a single angle & a single self-absorption correction; those on the other side (upstream) have a much smaller self-absorption correction. Self-absorption is strongly energy-dependent especially due to $[\mu/\rho](E)$.

5) The pattern of the data expected from different channels can be fitted and corrected for self-absorption to provide a more robust data set with greater information content.

6) In many fluorescent geometries, square channel arrays are deliberately quite close to the sample stage to improve scattered fluorescent signals. Then the solid angle to a particular detector channel is important and we must use $\cos\theta_{out} = \cos\theta_{out\,h}\cos\theta_{out\,v}$ where v is the vertical angle, which is zero in the plane of incidence. Then $\cos\theta_{out\,v} = \tan^{-1}(mC/L)$ where m is the number of channel elements from the plane of incidence in the vertical axis.

7) Main parameters are θ_0 and L, allowing reduction of the whole equation to a consistent dataset with maximal information content.

XAFS Theory: XANES and EXAFS Spectra

3. How XAFS works - Realisation

B: Fluorescence

$$I_f = \frac{\frac{fI_0\Omega[\mu/\rho]^*_{pe}}{4\pi\cos\theta_{inc}}}{\frac{[\mu/\rho]}{\cos\theta_{inc}} + \frac{[\mu_f/\rho]}{\cos\theta_{out}}}\left(A - \exp\left(-\frac{\left[\frac{\mu}{\rho}\right][\rho t]}{\cos\theta_{inc}} - \frac{\left[\frac{\mu_f}{\rho}\right][\rho t]}{\cos\theta_{out}}\right)\right)$$

$$\frac{I_{f_{detected}}}{I_{0monitored}} = \frac{I_f}{I_0}\left(\frac{\epsilon_{det}(E)}{\epsilon_{mon}(E)}\right)\exp\left(-\frac{\left[\frac{\mu_f}{\rho}\right]_{air}[\rho t_{air}]}{\cos\theta_{air}} - \frac{\left[\frac{\mu_f}{\rho}\right]_{w}[\rho t_w]}{\cos\theta_w}\right)$$

8) There are two particularly useful limits for fluorescence measurements. In the *thin sample limit* where $[\mu/\rho]\,\varrho t \ll 1$, the $1 - e^x$ term expands by Taylor series expansion, cancelling the denominator (and the self-absorption correction) so that

$$\frac{I_{f_{detected}}}{I_{0monitored}} = \frac{ft\Omega[\mu/\rho]^*_{pe}}{4\pi\cos\theta_{inc}}\frac{\epsilon_{det}(E)}{\epsilon_{mon}(E)}e^{-\frac{\left[\frac{\mu_f}{\rho}\right]_{air}[\rho t_{air}]+\left[\frac{\mu_f}{\rho}\right]_{w}[\rho t_w]}{\cos(\theta_{out\,h}-45^0)\cos\theta_{out\,v}}}$$

and to first order the observed intensity ratios are proportional to the photoelectric coefficient and the XAFS structure may be cleanly extracted. This *thin sample limit* is invalid whenever a dispersion between detector elements is observed - i.e. almost always.

9) The second convenient limit is the *thick dilute sample limit* where $[\mu/\rho]\,\varrho t \gg 1$ but $[\mu/\rho]_{pe} \ll [\mu/\rho]$ the exponential goes to zero yielding

$$\frac{I_{f_{detected}}}{I_{0monitored}} = \frac{\frac{f\Omega[\mu/\rho]^*_{pe}}{4\pi\cos\theta_{inc}}}{\frac{[\mu/\rho]}{\cos\theta_{inc}} + \frac{[\mu_f/\rho]}{\cos\theta_{out}}}\frac{\epsilon_{det}(E)}{\epsilon_{mon}(E)}e^{-\frac{\left[\frac{\mu_f}{\rho}\right]_{air}[\rho t_{air}]+\left[\frac{\mu_f}{\rho}\right]_{w}[\rho t_w]}{\cos(\theta_{out\,h}-45^0)\cos\theta_{out\,v}}}$$

Iff the energy dependence of the denominator is small (dominated by scattering coefficients or background absorption), then the angular self-absorption can be modelled and the corrected intensity ratio provides the photoelectric absorption coefficients for theoretical modelling using XAFS analysis. However, for most samples, the thin limit is not obeyed. Similarly, for most of the X-ray regime $[\mu/\rho]_{pe}$ is dominant and is not dominated by the scattering coefficients. For a typical metallic XAFS investigation, the concentration must be very low for $[\mu/\rho]^*_{pe}$ of the active fluorescent centre in the sample to be dominated by background absorption $[\mu/\rho]_{pe}$. Then of course the signal and statistical precision are also very low.

XAFS Theory: XANES and EXAFS Spectra

3. How XAFS works - Realisation

B: Fluorescence

$$I_f = \frac{\frac{fI_0\Omega[\mu/\rho]^*_{pe}}{4\pi\cos\theta_{inc}}}{\frac{[\mu/\rho]}{\cos\theta_{inc}} + \frac{[\mu_f/\rho]}{\cos\theta_{out}}}\left(A - \exp\left(-\frac{\left[\frac{\mu}{\rho}\right][\rho t]}{\cos\theta_{inc}} - \frac{\left[\frac{\mu_f}{\rho}\right][\rho t]}{\cos\theta_{out}}\right)\right)$$

$$\frac{I_{f_{detected}}}{I_{0monitored}} = \frac{I_f}{I_0}\left(\frac{\epsilon_{det}(E)}{\epsilon_{mon}(E)}\right)\exp\left(-\frac{\left[\frac{\mu_f}{\rho}\right]_{air}[\rho t_{air}]}{\cos\theta_{air}} - \frac{\left[\frac{\mu_f}{\rho}\right]_{w}[\rho t_w]}{\cos\theta_w}\right)$$

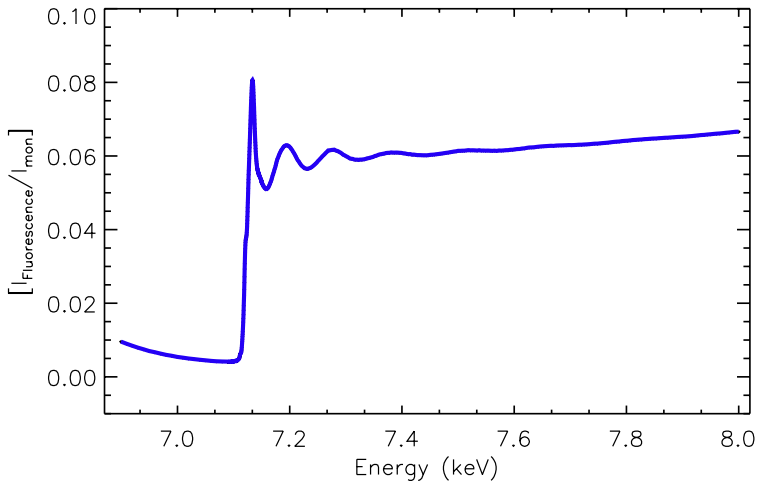

10mM Ferrocene
Standard Fluorescence XAFS
Nobel Prize - sandwich compounds

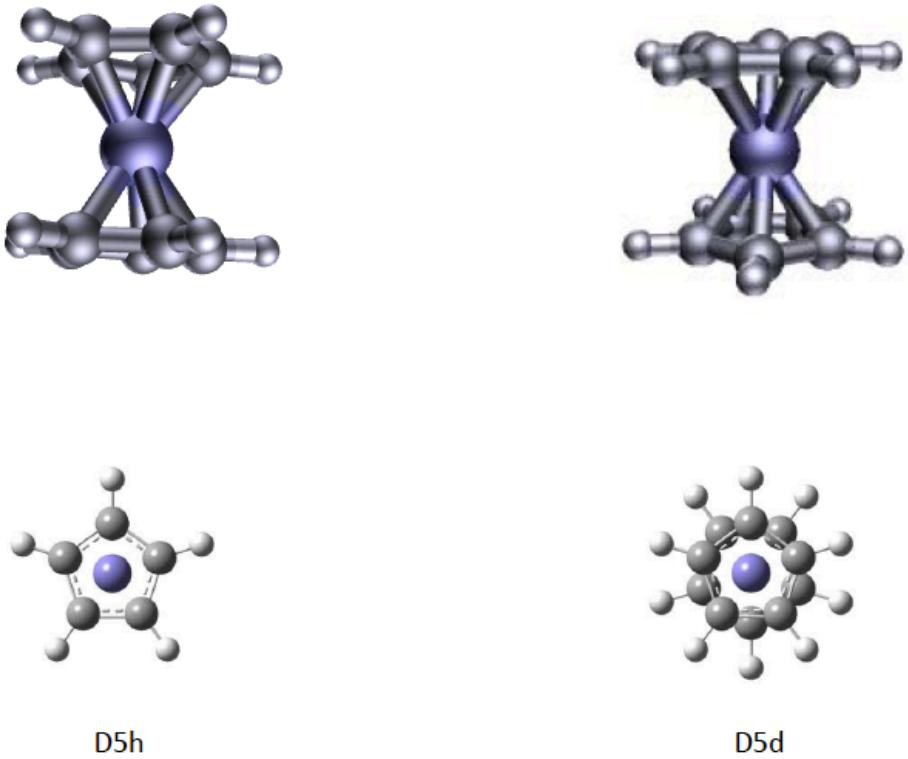

Chantler et al., J Synch Rad 2012

XAFS Theory: XANES and EXAFS Spectra

3. How XAFS works - Realisation

B: Fluorescence

$$I_f = \frac{\frac{fI_0\Omega[\mu/\rho]^*_{pe}}{4\pi\cos\theta_{inc}}}{\frac{[\mu/\rho]}{\cos\theta_{inc}} + \frac{[\mu_f/\rho]}{\cos\theta_{out}}}\left(A - \exp\left(-\frac{\left[\frac{\mu}{\rho}\right][\rho t]}{\cos\theta_{inc}} - \frac{\left[\frac{\mu_f}{\rho}\right][\rho t]}{\cos\theta_{out}}\right)\right)$$

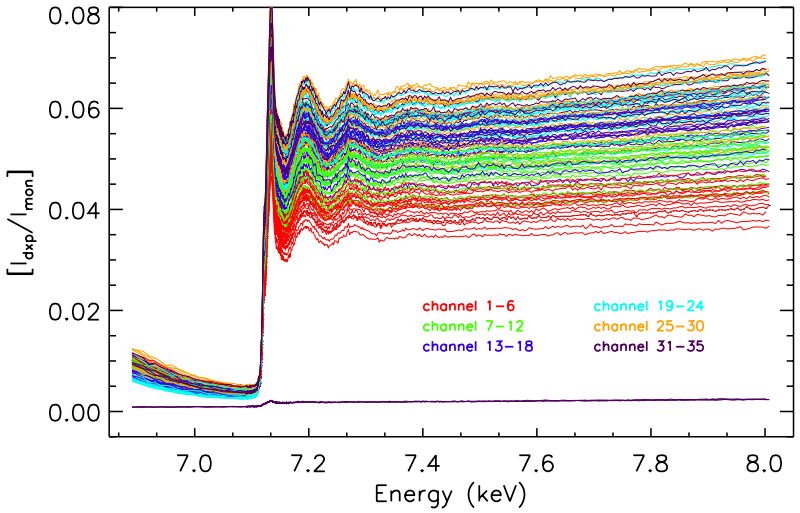

10mM Ferrocene
3 scans, 35 pixels per scan
Fluorescence XAFS

$$\frac{I_{f_{detected}}}{I_{0monitored}} = \frac{I_f}{I_0}\left(\frac{\epsilon_{det}(E)}{\epsilon_{mon}(E)}\right)\exp\left(-\frac{\left[\frac{\mu_f}{\rho}\right]_{air}[\rho t_{air}]}{\cos\theta_{air}} - \frac{\left[\frac{\mu_f}{\rho}\right]_{w}[\rho t_w]}{\cos\theta_w}\right)$$

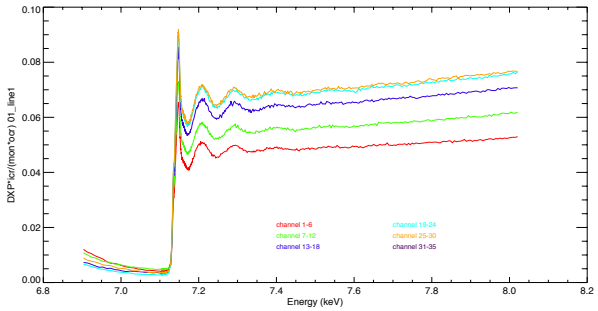

Single column dispersion

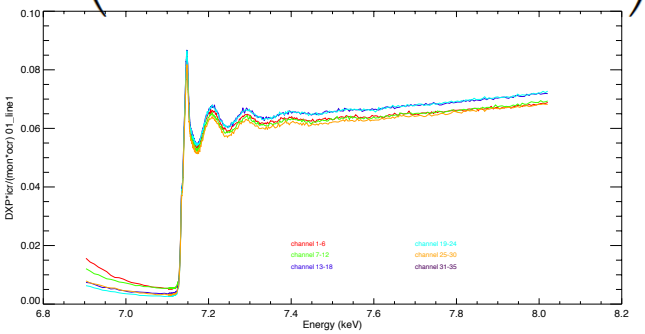

Corrected for self-absorption

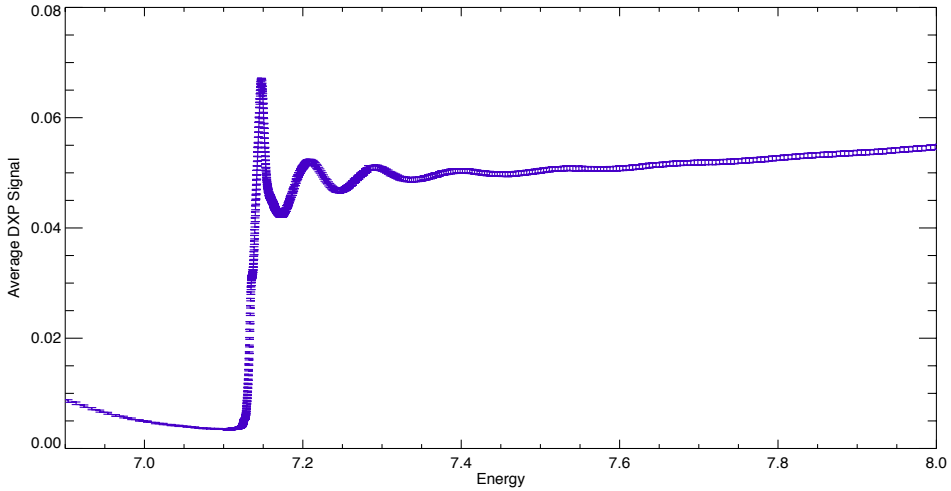

Corrected XAFS Spectrum WITH ERROR BARS PROPAGATED

XAFS Theory: XANES and EXAFS Spectra

3. How XAFS works - Realisation

B: Fluorescence

$$I_f = \frac{\frac{fI_0\Omega[\mu/\rho]^*_{pe}}{4\pi\cos\theta_{inc}}}{\frac{[\mu/\rho]}{\cos\theta_{inc}} + \frac{[\mu_f/\rho]}{\cos\theta_{out}}} \left(A - \exp\left(-\frac{\left[\frac{\mu}{\rho}\right][\rho t]}{\cos\theta_{inc}} - \frac{\left[\frac{\mu_f}{\rho}\right][\rho t]}{\cos\theta_{out}} \right) \right)$$

$$\frac{I_{f_{detected}}}{I_{0monitored}} = \frac{I_f}{I_0} \left(\frac{\epsilon_{det}(E)}{\epsilon_{mon}(E)} \right) \exp\left(-\frac{\left[\frac{\mu_f}{\rho}\right]_{air}[\rho t_{air}]}{\cos\theta_{air}} - \frac{\left[\frac{\mu_f}{\rho}\right]_{w}[\rho t_w]}{\cos\theta_w} \right)$$

10mM Ferrocene
XAFS signal and fit
standard window

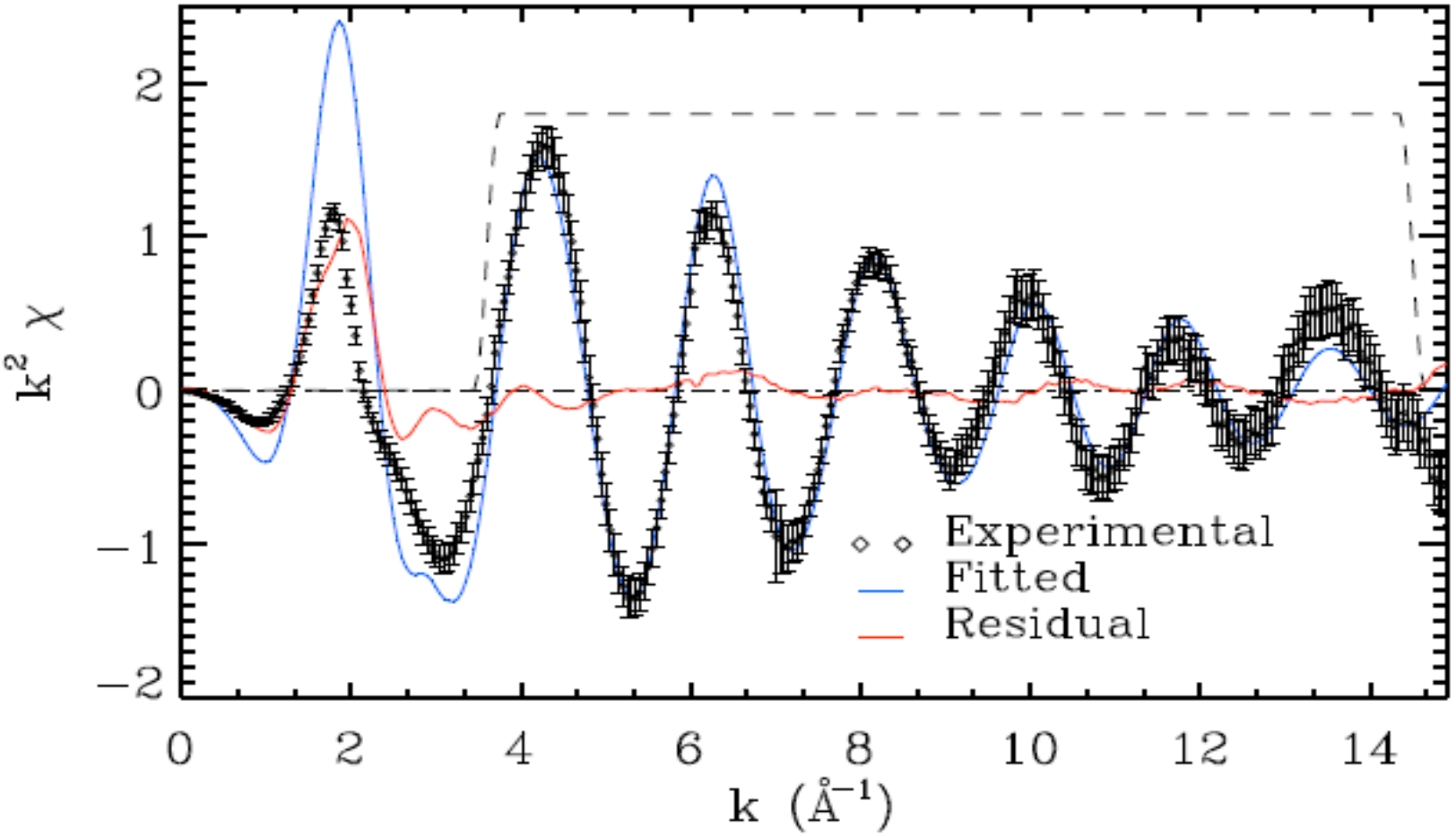

3. How XAFS works
B: Fluorescence

Conformation	Eclipsed
Fitted Parameters	
χ^2_r	0.089
ΔE_0 offset (eV)	-1.72±0.94
$1+\alpha$ scaling of lattice	1.0036±0.0037
σ^2 thermal parameter	0.0049±0.0013
S_0^2 amplitude reduction	1.069±0.086
Fixed Values	
Fe x,y,z,Å	0,0,0
C1(x,y,z)	1.6555,1.2007,0.0000
C2(x,y,z)	-1.6555,1.2007,0.0000
C3(x,y,z)	1.6555,-0.9714,0.7058
C4(x,y,z)	-1.6555,-0.9714,0.7058
C5(x,y,z)	1.6555,-0.9714,-0.7058
C6(x,y,z)	-1.6555,-0.9714,-0.7058
C7(x,y,z)	1.6555,0.3710,1.1420
C8(x,y,z)	-1.6555,0.3710,1.1420
C9(x,y,z)	1.6555,0.3710,-1.1420
C10(x,y,z)	-1.6555,0.3710,-1.1420
Derived Parameters including α scale uncertainty	
Fe-C_5,Å	1.6555(1.0036±0.0037)
Fe-C1,Å	2.045(1.0036±0.0037)
C-C,Å	1.4116(1.0036±0.0037)
Fe-C_5,Å	1.6615±0.0061
Fe-C1,Å	2.0524±0.0076
C-C,Å	1.4167±0.0052

Table 1: Fitted parameters

XAFS Theory: XANES and EXAFS Spectra
3. How XAFS works
B: Fluorescence

bond T lattice	**XAFS Eclipsed** 10K -	**e-scattering**[a]	**Neutron**[b] 173K	**Xray**[c] 98K Orthorhombic	**Xray**[d] 101K Triclinic	**Xray**[e] 173K Monoclinic	MP2[f]	CCSD/T[f]	This Study[g] Theory
Fe-C1,Å	2.0524±0.0076	2.064±0.003	±0.003-0.005	2.056,2.059±0.005	2.046,2.052±0.007	2.033-	1.910	2.056	2.065
range,Å	2.0524±0.0076	-	[2.005-2.050]	[2.051-2.062]	[2.041-2.052]	[2.017-2.048]			
C-C,Å	1.4167±0.0052	1.440±0.002	±0.005-0.009	1.429,1.431±0.006	1.426,1.433±0.007	1.395-	1.441	1.433	1.428
range,Å	1.4167±0.0052	-	[1.349-1.468]	[1.421-1.437]	[1.423-1.429]	[1.346-1.441]			
Fe-C_5,Å	1.6615±0.0061	1.660±0.003	-	1.658±0.006	1.646±0.007	1.651-	1.464	1.655	1.670

[a] (Haaland & Nilsson, 1968),[b] (Takusagawa & Koetzle, 1979),[c] (Seiler & Dunitz, 1982),[d] (Seiler & Dunitz, 1979*b*),[e] (Seiler & Dunitz, 1979*a*),
[f] (Coriani *et al*., 2006),[g] the B3LYP/m6-31G model.

Table 2: Comparison of experimental bond lengths and theoretical predictions

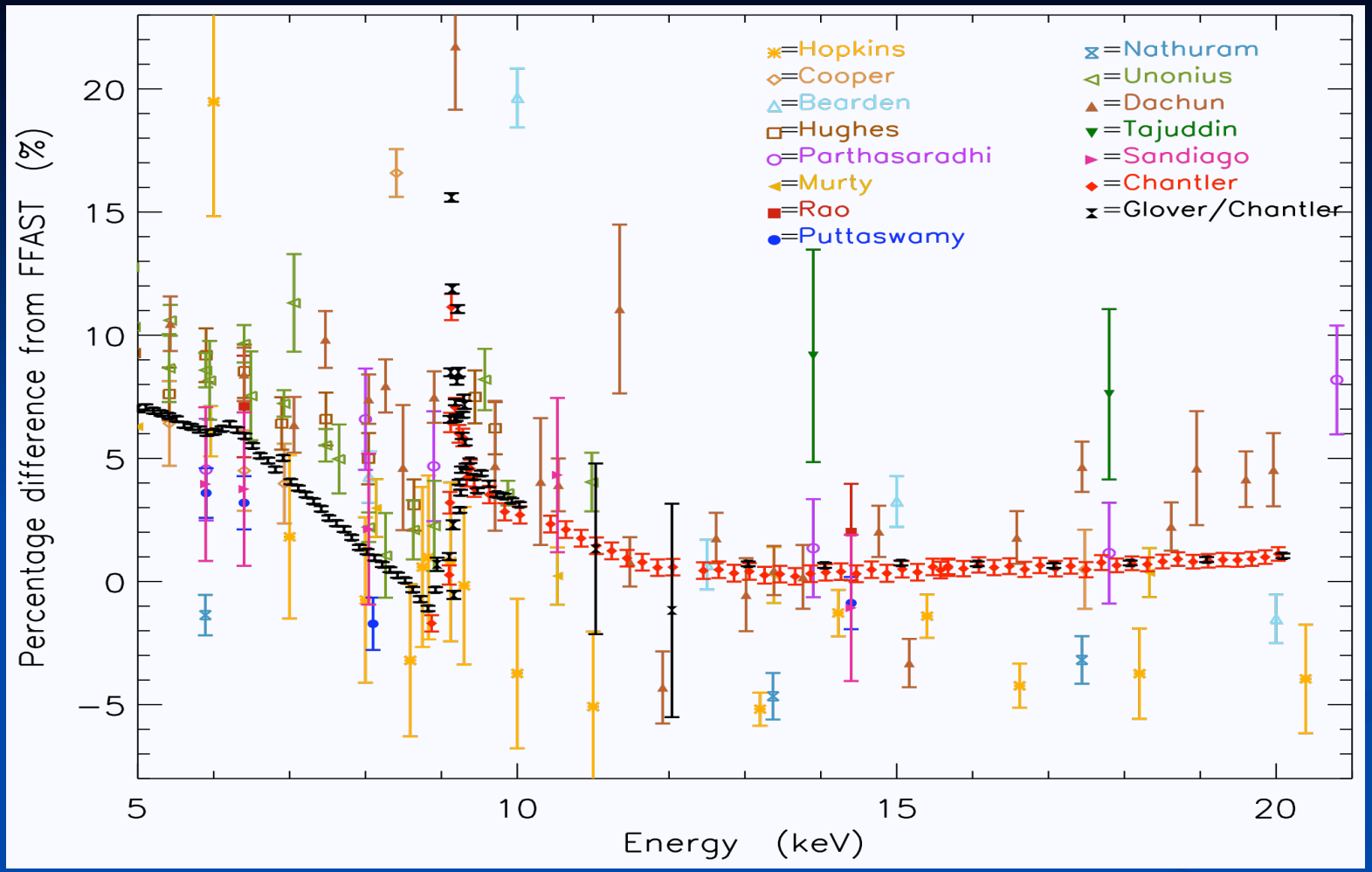

Copper

J. L. Glover, C. T .Chantler, Z. Barnea, N. A. Rae, C. Q. Tran, D. C. Creagh, D. Paterson, B. B. Dhal, 'High-accuracy measurements of the X-ray mass-attenuation coefficient and imaginary component of the form factor of copper,' Phys. Rev. A78 (2008) 052902

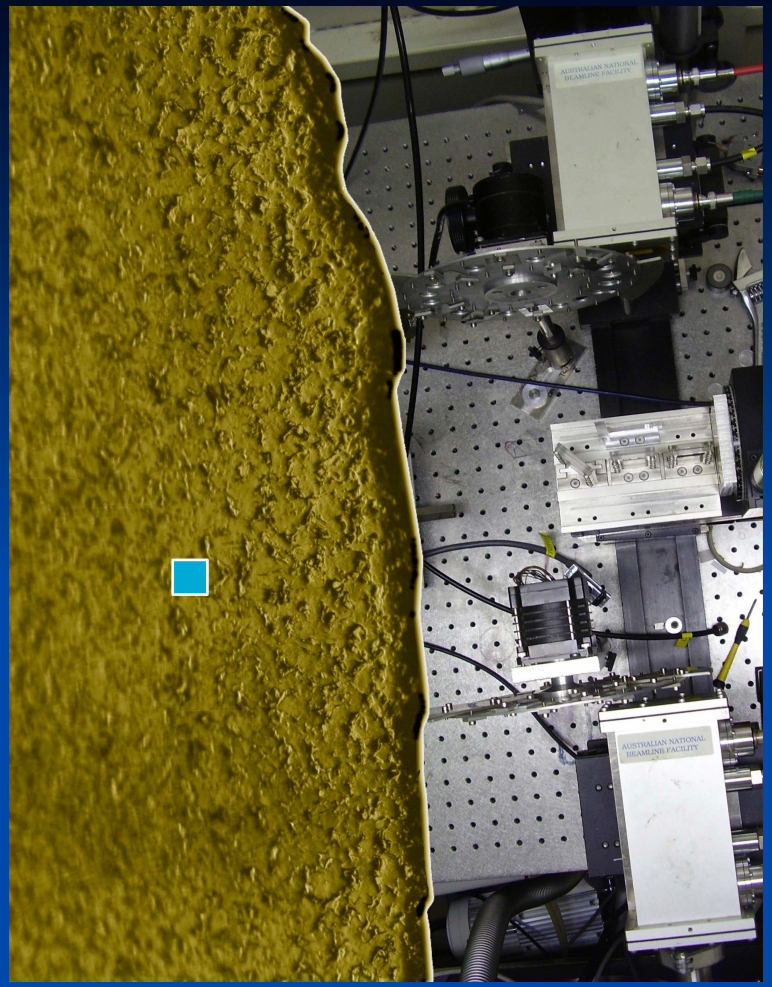

4. Past, Present & Future: Measurement of Nano-roughness

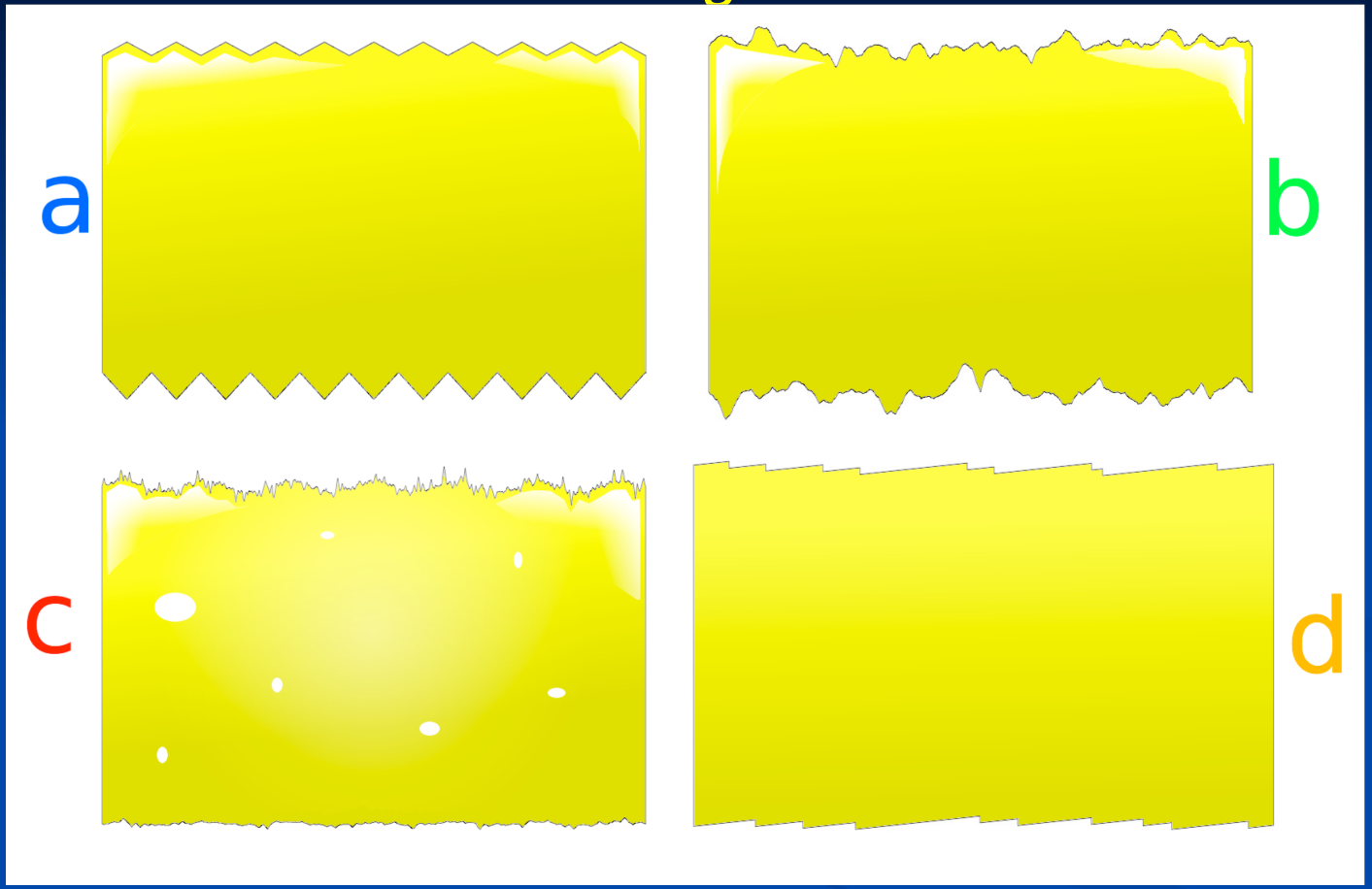

J. L. Glover, C. T. Chantler, M. D. de Jonge, 'Nano-roughness in gold revealed from X-ray signature,' Phys. Lett. A373 (2009) 1177-1180

4. Past, Present & Future: Application to fluorescence measurements, dilute samples, organometallics, catalysts…

epoxidation catalysts in the Ni-catalysed polymerisation of isocyanides:

Activated complex,
$C_{31}H_{53}Cl_2N_5NiO_8$
tri(tert-pentyl isocyanide)
[benzylamino(tertpentylamino)
carbene] nickel(II) perchlorate

[Glover et al. AIP Proc. CP882/
XAFS13 (2007) 625]

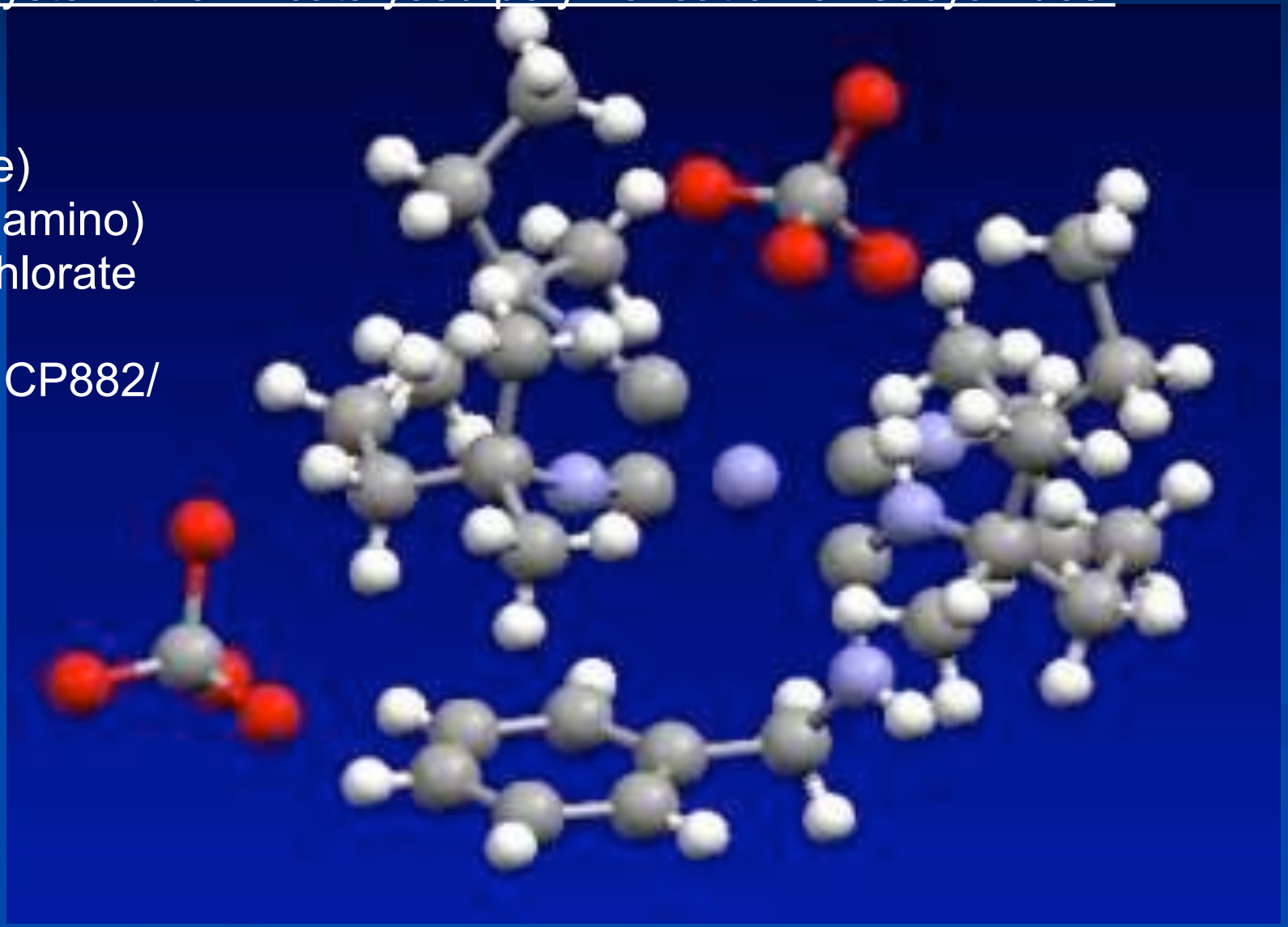

4. Past, Present & Future: Application to fluorescence measurements, dilute samples, organometallics, catalysts…

Activated complex, $C_{31}H_{53}Cl_2N_5NiO_8$
tri(tert-pentyl isocyanide)
[benzylamino(tertpentylamino)
carbene] nickel(II) perchlorate
[Glover et al. AIP Proc. CP882/
XAFS13 (2007) 625]

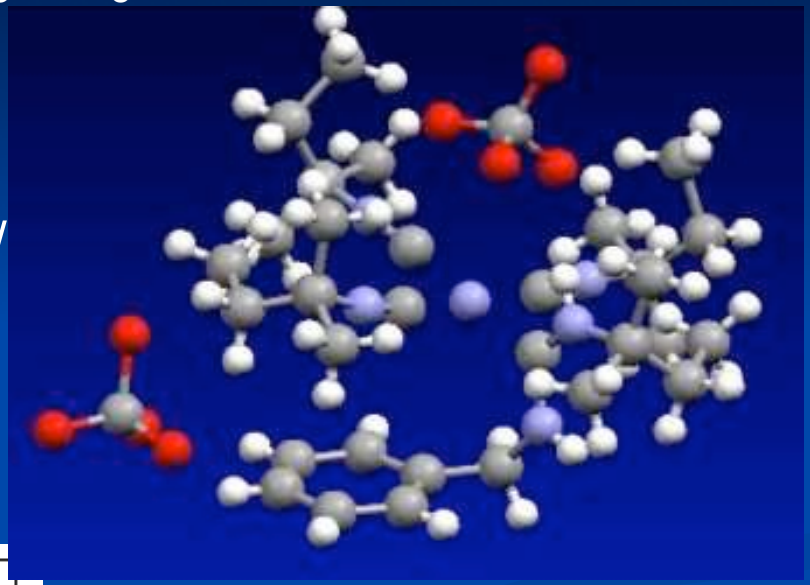

Muffin-Tin Potential:
Poor approx. for
near edge structure

FDMNES:
good for
near edge structure

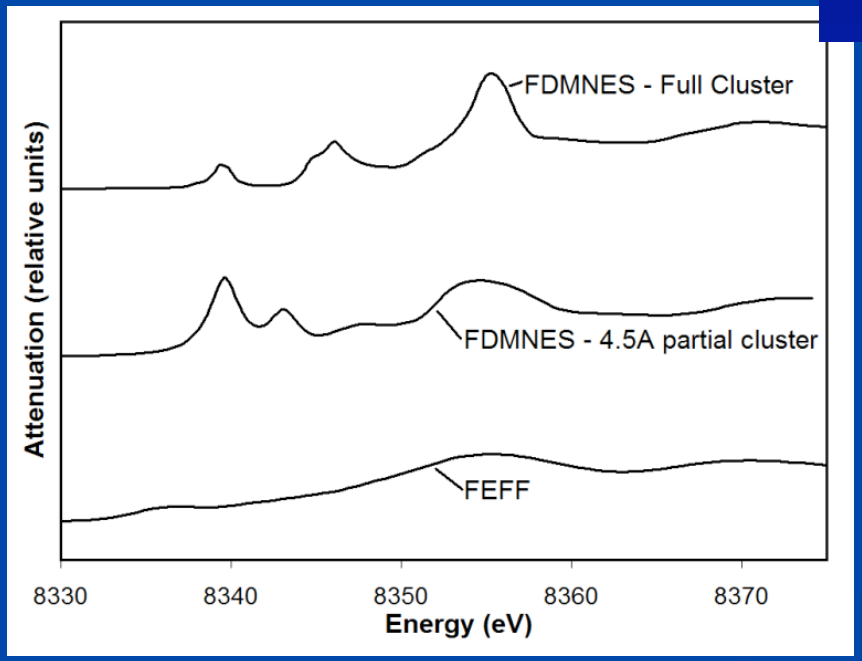

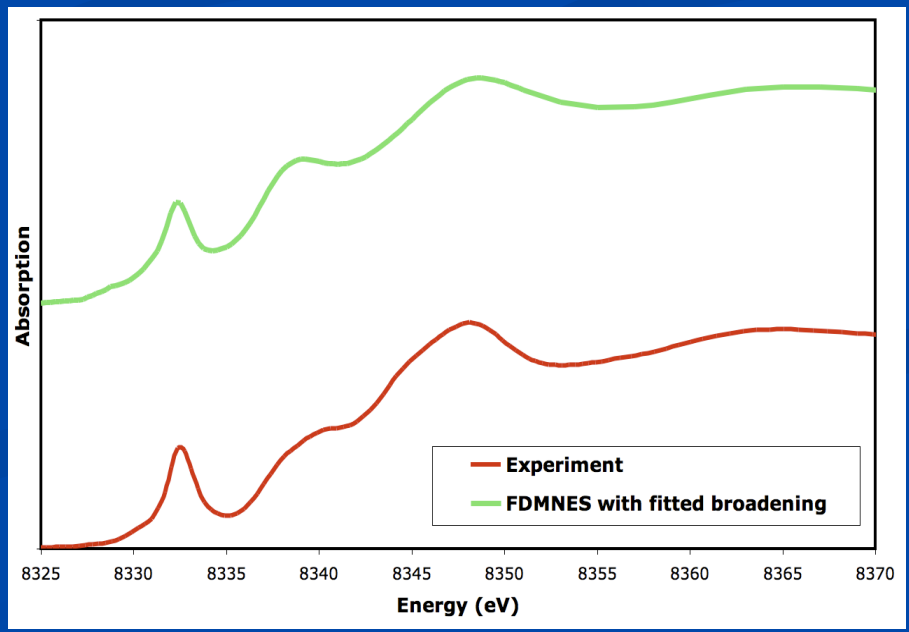

Key Challenges for the Future?

- 1. XAFS using **fluorescence** (& energy dispersive detection) – treatment of self-absorption & statistics; **phases** with temperature
- 2. **dilute non-crystalline systems**: glasses, polymers, composites, solutions – maximum (sufficient?) information content cf noise level
- 3. development of **routine** experimental setup, analysis & processing for conventional users
- 4. **data uncertainties** & **propagation of errors**
- 5. development of DHF & **condensed matter theory** – preferably for XAFS & XANES

New synchrotron techniques & applications

FINITE DIFFERENCE STRUCTURE COMPUTATIONS FOR XANES - AND XAFS

- J. D. BOURKE, C. T. CHANTLER, C. WITTE, 'Finite Difference Method Calculations of X-ray Absorption Fine Structure for Copper,' Physics Letters A, 360 (2007), 702-706
- J. D. Bourke, C. T. Chantler, 'Finite difference method calculations of long-range X-ray absorption fine structure for copper over k ~ 20 A^{-1},' NIM A619 (2010) 33-36
- Y Joly: FDMNES

DEVELOPMENTS OF FEFF, IFFEFIT etc.:

- J. J. Kas, J. J. Rehr, J. L. Glover, C. T. Chantler, Comparison of Theoretical and Experimental Cu and Mo K-edge XAS, NIM A619 (2010) 28-32
- L. F. SMALE, C. T. CHANTLER, M. D. DE JONGE, Z. BARNEA, C.Q. TRAN, `Analysis of X-ray Absorption Fine Structure using Absolute X-ray Mass Attenuation Coefficients: Application to Molybdenum,' Radiation Physics & Chemistry 75 (2006) 1559-1563

Solid State Structure - Copper

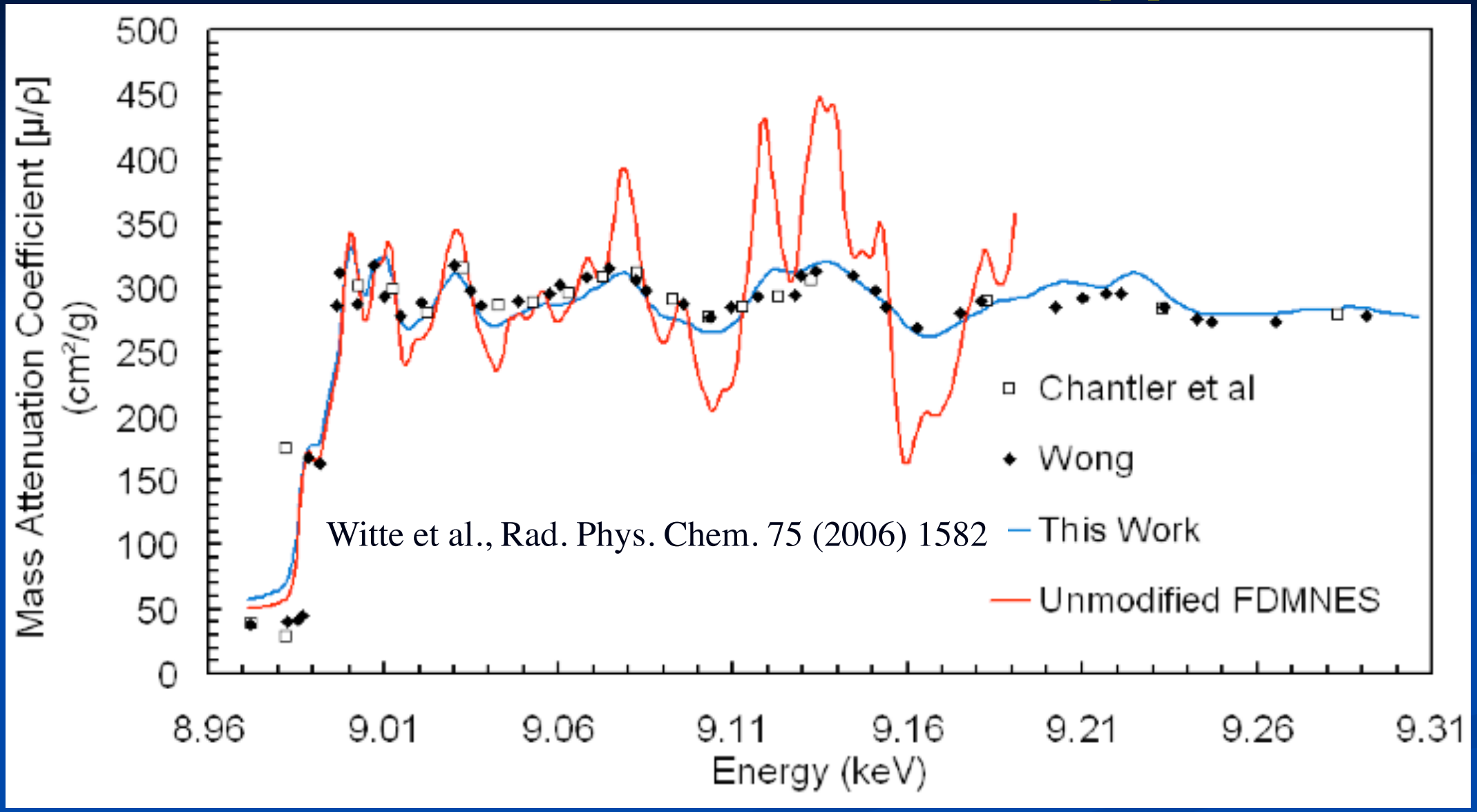

NO fitting parameter: **accurate** experiment and **accurate** theory **CAN** agree!

New synchrotron techniques & applications

INELASTIC MEAN FREE PATHS from XAFS

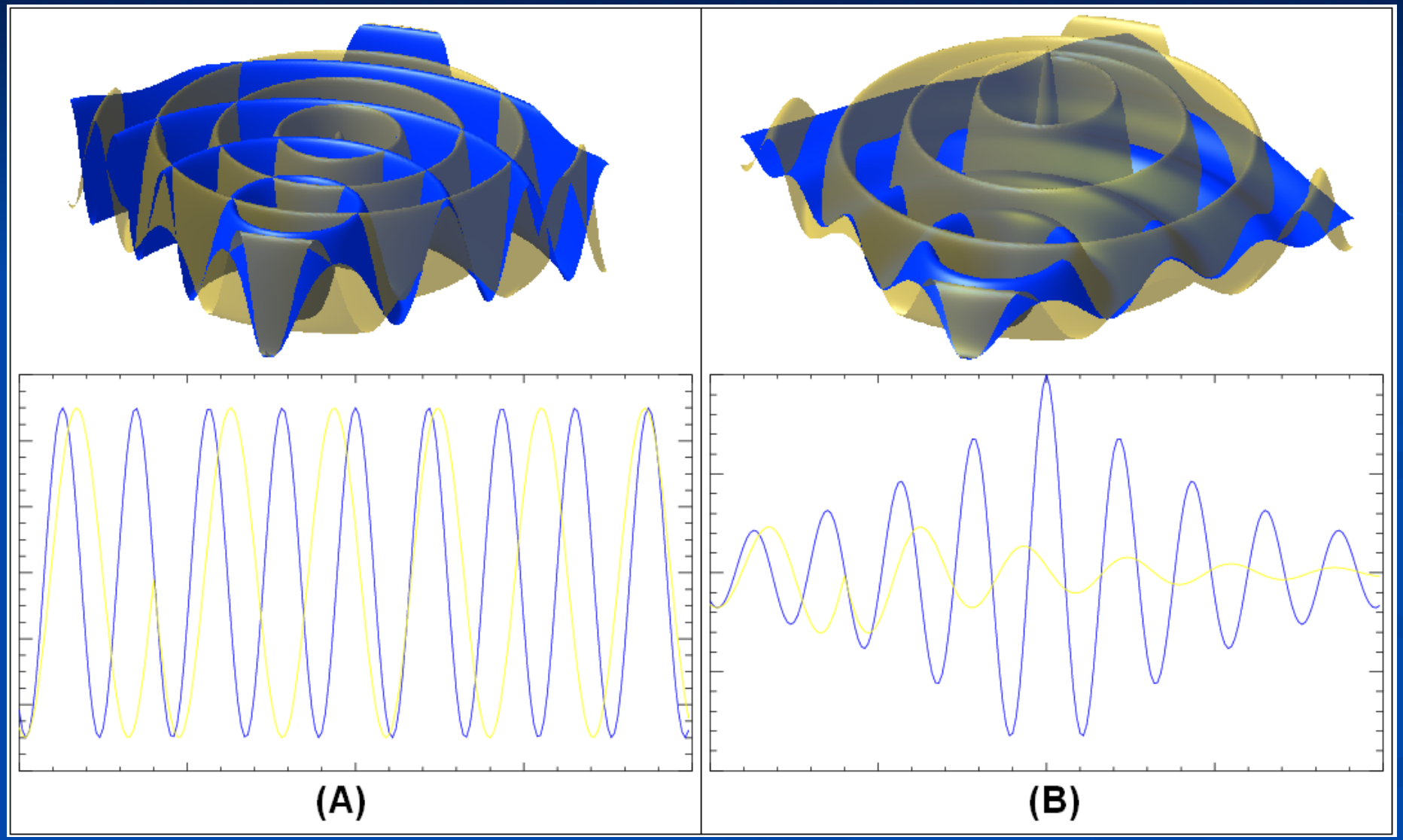

New synchrotron techniques & applications

INELASTIC MEAN FREE PATHS from XAFS

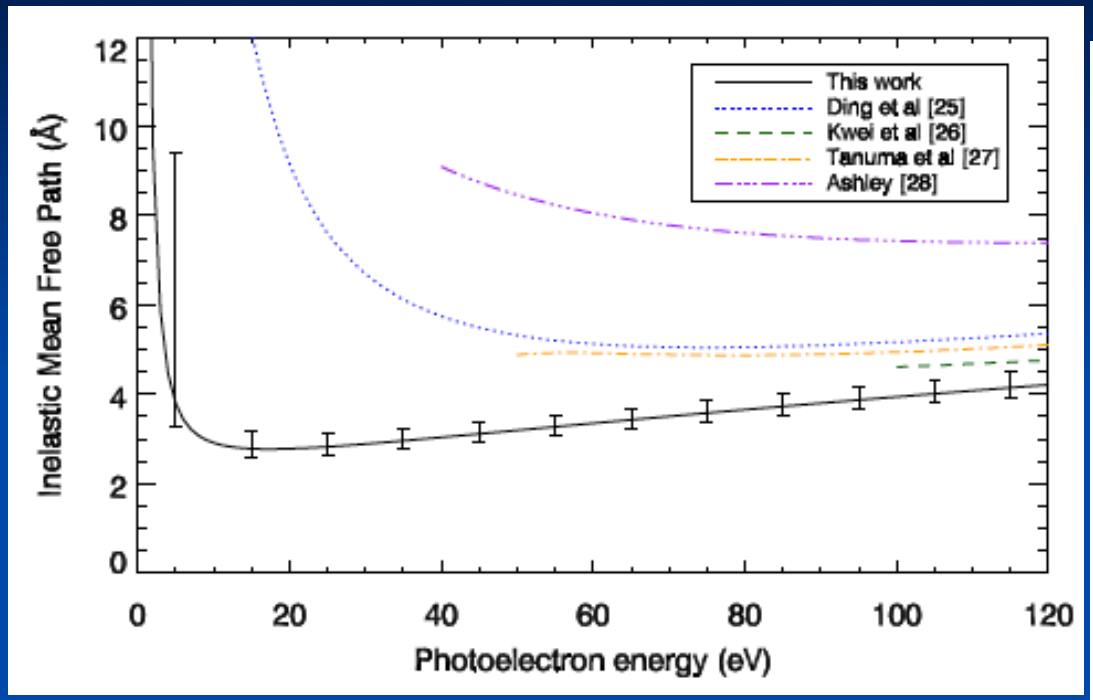

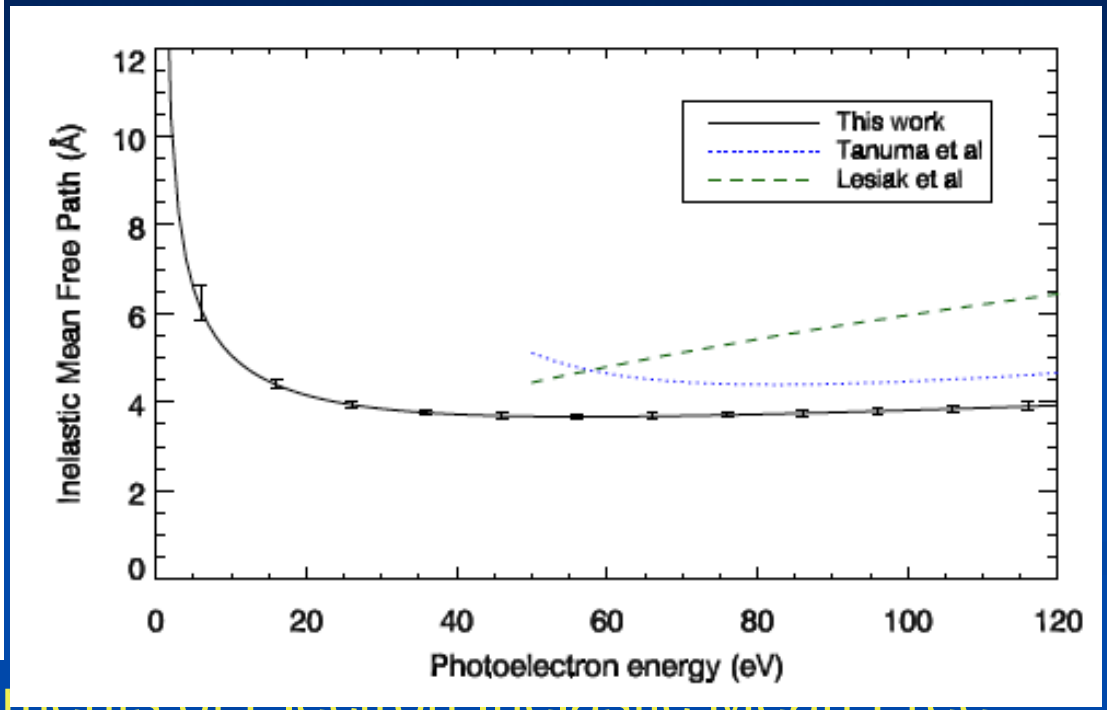

- J. D. Bourke, C .T. Chantler, Measurements of Electron Inelastic Mean Free Paths in Materials, Phys. Rev. Letters 104 (2010) 206601-1-4
- C .T. Chantler, J. D. Bourke, X-ray Spectroscopic Measurement of the Photoelectron Inelastic Mean Free Paths in Molybdenum, Journal of Physical Chemistry Letters 1 (2010) 2422-2427
- MS76 Sunday & many other presentations at this congress.